PONTIFÍCIA UNIVERSIDADE CATÓLICA DO RIO GRANDE DO SUL
FACULDADE DE BIOCIÊNCIAS
PROGRAMA DE PÓS-GRADUAÇÃO EM BIOLOGIA CELULAR E MOLECULAR

ANNE DRUMOND VILLELA

**ESTUDOS BIOQUÍMICOS E NOCAUTE GÊNICO DA ENZIMA URACIL FOSFORRIBOSIL TRANSFERASE DE *Mycobacterium tuberculosis* COMO ALVO PARA O DESENVOLVIMENTO DE CEPAS ATENUADAS**

Porto Alegre
2011

ANNE DRUMOND VILLELA

# ESTUDOS BIOQUÍMICOS E NOCAUTE GÊNICO DA ENZIMA URACIL FOSFORRIBOSIL TRANSFERASE DE *Mycobacterium tuberculosis* COMO ALVO PARA O DESENVOLVIMENTO DE CEPAS ATENUADAS

Tese apresentada como requisito para a obtenção do grau de Doutor pelo Programa de Pós-Graduação em Biologia Celular e Molecular da Faculdade de Biociências da Pontifícia Universidade Católica do Rio Grande do Sul.

Orientador: Dr. Diógenes Santiago Santos
Co-orientador: Dr. Luiz Augusto Basso

Porto Alegre
2011

ANNE DRUMOND VILLELA

**ESTUDOS BIOQUÍMICOS E NOCAUTE GÊNICO DA ENZIMA URACIL FOSFORRIBOSIL TRANSFERASE DE *Mycobacterium tuberculosis* COMO ALVO PARA O DESENVOLVIMENTO DE CEPAS ATENUADAS**

Tese apresentada como requisito para a obtenção do grau de Doutor pelo Programa de Pós-Graduação em Biologia Celular e Molecular da Faculdade de Biociências da Pontifícia Universidade Católica do Rio Grande do Sul.

BANCA EXAMINADORA:

Prof. Dr. Luiz Hildebrando Pereira Silva – IPEPATRO / FIOCRUZ

Prof. Dr. Luiz Roberto Ribeiro Castello-Branco – FIOCRUZ

Profª. Dra. Nadja Schroder – PUCRS

Porto Alegre
2011

**Agradecimentos**

Agradeço aos meus orientadores Prof. Dr. Diógenes Santiago Santos e Prof. Dr. Luiz Augusto Basso pela oportunidade, ensinamentos e apoio dispensado na realização deste trabalho.

À Dra. Mary Jackson pela ajuda, apoio, atenção e ensinamentos durante o período de doutorado sanduíche na Colorado State University, Fort Collins, EUA. Aos colegas do laboratório da Dra. Mary Jackson, em especial à Ha Pham e ao Vinícius Calado, pela ajuda, apoio, ensinamentos e amizade que foram fundamentais durante o período de doutorado sanduíche.

Ao Rodrigo Ducati e ao Leonardo Rosado pela ajuda no planejamento dos experimentos e na análise dos resultados. Aos colegas e amigos do CPBMF e da Quatro G pelo carinho, amizade, ajuda, apoio, ensinamentos e força nos momentos mais difíceis que foram de fundamental importância para a realização deste trabalho.

Ao Programa de Pós-Graduação em Biologia Celular e Molecular da PUCRS.

Ao CNPq pela bolsa fornecida durante o doutorado e a CAPES pela bolsa fornecida durante o período de doutorado sanduíche.

Agradeço, enfim, a todos que de alguma forma, contribuíram não só para a realização deste trabalho, como também para a minha formação pessoal e profissional. Muito obrigada a todos!

# Resumo

A tuberculose (TB) é uma doença infecciosa causada principalmente pelo *Mycobacterium tuberculosis,* o qual atualmente infecta um terço da população mundial. Apesar da disponibilidade da vacina Bacille Calmette-Guérin e da eficaz quimioterapia de curta duração, o aumento na incidência global da TB está relacionado à co-infecção com o HIV e ao surgimento de cepas multi, extensivamente e agora totalmente resistente a drogas. Além disto, a capacidade do *M. tuberculosis* de permanecer viável dentro do hospedeiro infectado por longo período em uma infecção assintomática é um problema adicional para o controle da TB. As rotas de biossíntese de nucleotídeos fornecem alvos moleculares promissores para o desenvolvimento de novas vacinas e estratégias terapêuticas para controlar a incidência global de TB no mundo. A uracil fosforribosil transferase (UPRT) catalisa a conversão de uracil e 5'-fosforribosil-$\alpha$-1'-pirofosfato (PRPP) a uridina 5'-monofosfato (UMP) e pirofosfato (PP$_i$). A UPRT tem um papel importante na rota de salvamento das pirimidinas já que seu produto (UMP) é o precursor comum de todos os nucleotídeos pirimídicos. Este trabalho apresenta a clonagem, expressão recombinante em *E. coli*, e a purificação da UPRT de *M. tuberculosis* codificada pelo gene *upp* (*Mt*UPRT). Adicionalmente, foram realizadas análises de espectrometria de massas e sequenciamento N-terminal que confirmaram a identidade da *Mt*UPRT homogênea. A massa molecular da *Mt*UPRT nativa seguiu um modelo de associação monômero-tetrâmero por ultracentrifugação analítica. Esta enzima não mostrou uma regulação pronunciada por GTP já que este nucleotídeo não afetou os parâmetros cinéticos da enzima, e a sua ligação não foi detectada por calorimetria de titulação isotérmica (ITC). A velocidade inicial e os estudos de ITC sugeriram que a catálise procede através de um mecanismo ordenado sequencial, no qual o PRPP liga primeiramente, seguido pela ligação de uracil, e PP$_i$ é o primeiro produto a ser liberado, seguido pelo UMP. ITC também mostrou que a ligação de PRPP e UMP são processos termodinamicamente favoráveis. O perfil de pH indicou que grupamentos com os valores de p*K* próximos de 5,7 e 8,1 são importantes para a atividade catalítica e um grupamento com valor de p*K* próximo a 9,45 está envolvido na ligação do PRPP. Dados de cinética no estado pré-estacionário sugeriram que a liberação de produto não é a etapa limitante da reação catalisada pela *Mt*UPRT. Estudos de fluorescência demonstraram a existência de duas formas da enzima em solução, das quais apenas uma pode ligar ao PRPP. O nocaute do gene *upp* demonstrou que este gene não é essencial para o *M. tuberculosis* H37Rv nas condições empregadas no experimento e a ausência do gene *upp* não afetou o crescimento micobacteriano. A UPRT mostrou ser expressa tanto em altas como em baixas concentrações de oxigênio. A *Mt*UPRT foi inibida por um metabólito ativo do *isoxyl*, que não parece inibir as enzimas RNA polimerase, adenina fosforribosil transferase e hipoxantina-guanina fosforribosil transferase. A concentração inibitória mínima de *isoxyl* para as cepas de *M. tuberculosis* mutante para o gene *upp*, complementada e tipo selvagem foi de 12,8 μg/mL, o que significa que a ausência do gene *upp* não afetou a sensibilidade do *M. tuberculosis* ao *isoxyl*. Assim, estes dados podem ser úteis para um melhor entendimento sobre a via de biossíntese de nucleotídeos em *M. tuberculosis* e podem servir como base para o desenvolvimento de estratégias terapêuticas e preventivas eficientes para diminuir a incidência global deste patógeno.

# Abstract

Tuberculosis (TB) is an infectious disease mainly caused by *Mycobacterium tuberculosis,* which currently infects one-third of the world's population. Despite the availability of the Bacille Calmette-Guérin vaccine and effective short-course chemotherapy, the increasing global burden of TB has been linked to the co-infection with HIV, the emergence of multi, extensively and now totally drug-resistant strains. Furthermore, the capacity of *M. tuberculosis* to remain viable within infected hosts in a long-term asymptomatic infection is an additional problem for the control of TB. Nucleotides biosynthesis pathways provide promising molecular targets for the development of new vaccines and therapeutic strategies to control the global incidence of TB. Uracil phosphoribosyltransferase (UPRT) catalyzes the conversion of uracil and 5'-phosphoribosyl-$\alpha$-1'-pyrophosphate (PRPP) to uridine 5'-monophosphate (UMP) and pyrophosphate ($PP_i$). UPRT plays an important role in the pyrimidine salvage pathway since its product (UMP) is a common precursor of all pyrimidine nucleotides. This work presents cloning, recombinant expression in *Escherichia coli*, and purification of the *upp*-encoded *M. tuberculosis* UPRT (*Mt*UPRT). Mass spectrometry analysis and N-terminal amino acid sequencing confirmed the identity of homogeneous *Mt*UPRT. The molecular mass of the native *Mt*UPRT was shown to follow a monomer-tetramer association model by analytical ultracentrifugation. This enzyme did not show a pronounced regulation by GTP as this nucleotide did not affect enzyme kinetic parameters, and its binding was not detected by isothermal titration calorimetry (ITC). Initial velocity and ITC studies suggested that catalysis proceeds through a sequential ordered mechanism, in which PRPP binds first, followed by uracil binding, and $PP_i$ is the first product to be released, followed by UMP. ITC also showed that PRPP and UMP binding are thermodynamically favorable processes. The pH-rate profiles indicated that groups with p$K$ values of 5.7 and 8.1 are important for catalytic activity and a group with a p$K$ value of 9.45 is involved in PRPP binding. Pre-steady-state kinetic data suggested that product release is not the rate-limiting step of the reaction catalyzed by *Mt*UPRT. Kinetic fluorescence studies demonstrated two forms of enzyme in solution of which only one can bind to PRPP. Knockout of the *upp* gene showed that this gene is not essential for *M. tuberculosis* H37Rv in the employed experimental conditions and the absence of *upp* gene did not affect the mycobacterium growth. UPRT is expressed in both high and low oxygen conditions of *M. tuberculosis* H37Ra growth. *Mt*UPRT is inhibited by an active metabolite of isoxyl, which does not seem to inhibit RNA polymerase, adenine phosphoribosyltransferase and hypoxanthine-guanine phosphoribosyltransferase. Minimum inhibitory concentration of isoxyl for *M. tuberculosis* mutant for *upp* gene, complemented and wild type strains was 12.8 $\mu$g/mL, meaning that the absence of the *upp* gene did not affect *M. tuberculosis* sensitivity to isoxyl. Altogether, these data may be useful for a better understanding about the nucleotide biosynthesis pathway in *M. tuberculosis* and as a framework on which to base efforts towards the development of efficient prophylactic and therapeutic strategies to decrease the global incidence of this pathogen.

## Lista de Abreviaturas e Siglas

**ADC**: complexo contendo albumina, dextrose e catalase

**AIDS**: síndrome da imunodeficiência adquirida

**AMPc**: adenosina monofosfato cíclico

**APRT**: adenina fosforribosil transferase

**ATP**: adenosina trifosfato

**AUC**: ultracentrifugação analítica

**BCG**: Bacille Calmette-Guérin

**Can**: canamicina

**Can$^R$**: resistência à canamicina

**CDA**: citidina deaminase

**CDC**: *Centers for Disease Control and Prevention*

**CDP**: citidina 5'-difosfato

**CMP**: citidina 5'-monofosfato

**CTP**: citidina 5'-trifosfato

**DCO**: *Double cross-over*

**dCTP**: 2'-desoxicitidina 5'-trifosfato

**DMSO**: dimetilsulfóxido

**DOTS**: *Directly Observed Treatment Short Course Strategy*

**dTDP**: 2'-desoxitimidina 5'-difosfato

**dTMP**: 2'-desoxitimidina 5'-monofosfato

**dTTP**: 2'-desoxitimidina 5'-trifosfato

**dUMP**: 2'-desoxiuridina 5`-monofosfato

**dUTP**: 2'-desoxiuridina 5'-trifosfato

**dUTPase**: desoxiuridina trifosfatase

**GMPc**: guanosina monofosfato cíclico

**GTP**: guanosina trifosfato

**HGPRT**: hipoxantina guanina fosforribosil transferase

**HIV**: vírus da imunodeficiência humana

**ITC**: calorimetria de titulação isotérmica

**LC/MS**: cromatográfica líquida acoplada a espectrometria de massas

**MIC**: concentração inibitória mínima

**NDP**: nucleosídeo difosfato

**OADC**: complexo contendo ácido oleico, albumina, dextrose e catalase

**OMP**: orotidina 5'-monofosfato

**OMS**: Organização Mundial da Saúde

**OPRT**: orotato fosforribosil transferase

**PCR**: reação em cadeia da polimerase

**PDB**: *Protein Data Bank*

**PP$_i$**: pirofosfato

**PRPP**: 5-fosforribosil-$\alpha$-1-pirofosfato

**PyNP**: pirimidina nucleosídeo fosforilase

**SCO**: *Single cross-over*

**TB**: tuberculose

**TB-MDR**: tuberculose resistente a múltiplas drogas

**TB-TDR**: tuberculose totalmente resistente a drogas

**TB-XDR**: tuberculose extensivamente resistente a drogas

**UDP**: uridina 5'-difosfato

**UMP**: uridina 5'-monofosfato

**UPRT**: uracil fosforribosil transferase

**UTP**: uridina 5'-trifosfato

**Δ*upp*::Can**: gene *upp* interrompido pelo cassete contendo o gene que confere resistência à canamicina

# SUMÁRIO

# Capítulo 1

# INTRODUÇÃO

## 1. Tuberculose

A tuberculose humana (TB) é uma doença infecto-contagiosa causada principalmente pelo *Mycobacterium tuberculosis.* A TB é considerada a segunda principal causa de mortalidade devido a uma doença infecciosa no mundo, depois do vírus da imunodeficiência humana (HIV) que causou cerca de 1,8 milhões de mortes no ano de 2008 (1). No ano de 2010, estimativas da Organização Mundial da Saúde (OMS) indicaram a ocorrência de 8,5 – 9,2 milhões de novos casos de TB, com aproximadamente 1,5 milhões de mortes (1). A maior parte do número estimado de casos em 2010 ocorreu na Ásia (59 %) e na África (26%), e proporções menores de casos ocorreram na Região Mediterrânea Oriental (7 %), na Região Européia (5 %) e na Região das Américas (3 %) (**Figura 1**) (1). Aproximadamente 80 % do total de casos de TB no mundo ocorrem em apenas 22 países, incluindo o Brasil que ocupa o 15° lugar entre os países com maior número de casos de TB.
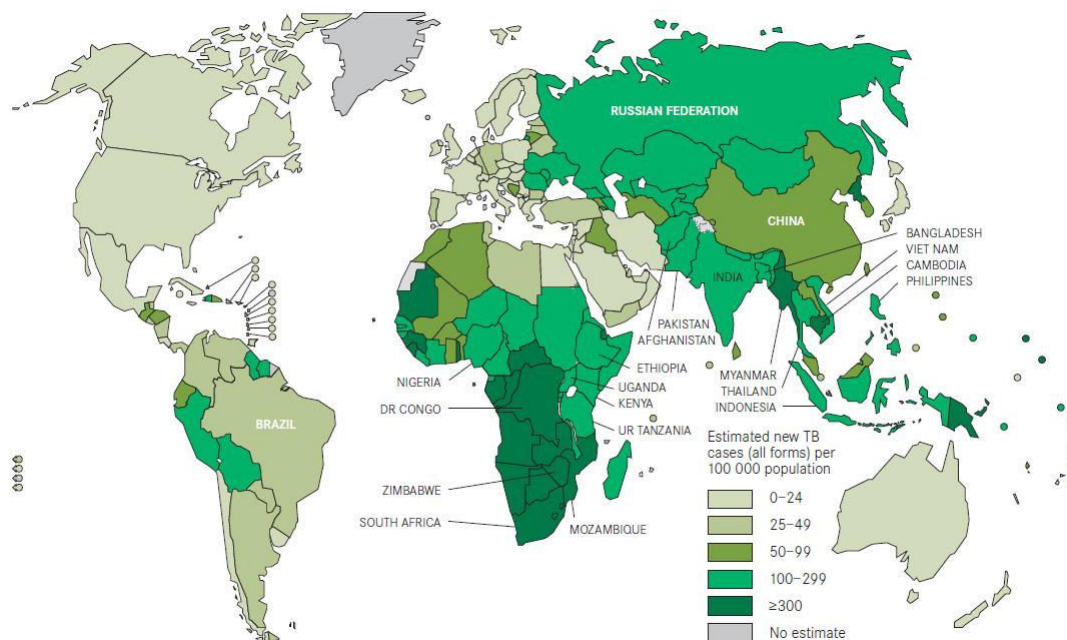
**Figura 1.** Estimativa da ocorrência de novos casos de TB em 2010 no mundo (1).

## 1.1 Infecção

A TB é transmitida principalmente pela inalação de aerossóis contendo o *M. tuberculosis,* gerados de uma pessoa infectada (2). No pulmão, o bacilo é internalizado por fagocitose pelos macrófagos alveolares, iniciando a resposta inata. As células dendríticas iniciam a resposta adaptativa mediada por células T que ativam os macrófagos através da liberação de citocinas, resultando na: eliminação da bactéria, estabelecimento da TB latente ou da doença ativa (**Figura 2**) (2). A eliminação completa do *M. tuberculosis* do organismo é difícil de ser atingida, uma vez que dentro do fagossoma, o *M. tuberculosis* secreta proteínas que previnem a fusão do fagossoma com o lisossoma, impedindo assim a sua destruição (3). Além disto, o bacilo da TB possui uma espessa parede celular que fornece resistência contra os mecanismos

3

microbicidas dos macrófagos (4). Deste modo, o bacilo é capaz de sobreviver dentro dos macrófagos, controlado pelo sistema imunológico do hospedeiro, dentro de uma estrutura chamada de granuloma (a principal característica da TB latente) (**Figura 2**). A biologia do granuloma é parcialmente compreendida; acredita-se que o granuloma contenha no seu centro macrófagos não ativados, rodeados por macrófagos infectados contendo o *M. tuberculosis* envolvidos por células do sistema imunológico, como linfócitos T (3). Assim, a estrutura do granuloma representa um balanço entre o sistema imunológico do hospedeiro e o patógeno.

Entretanto, se a resposta das células T for insuficiente para controlar a infecção inicial, sintomas clínicos se desenvolvem dentro de 1 ano na forma de infecção progressiva primária (TB ativa) (**Figura 2**). A infecção primária ocorre dentro de 1 ou 2 anos depois da infecção inicial, envolvendo a replicação do *M. tuberculosis*, a colonização dos linfonodos locais e eventual disseminação da infecção para locais mais distantes (4, 5). A TB pós-primária é desenvolvida mais tarde, e pode ser causada tanto pela reativação de bacilos remanescentes da infecção inicial como pela impossibilidade de controlar uma infecção subseqüente (**Figura 2**). A TB pós-primária gera extensivo dano pulmonar, além de facilitar a transmissão bacilar por aerossóis (4, 5).
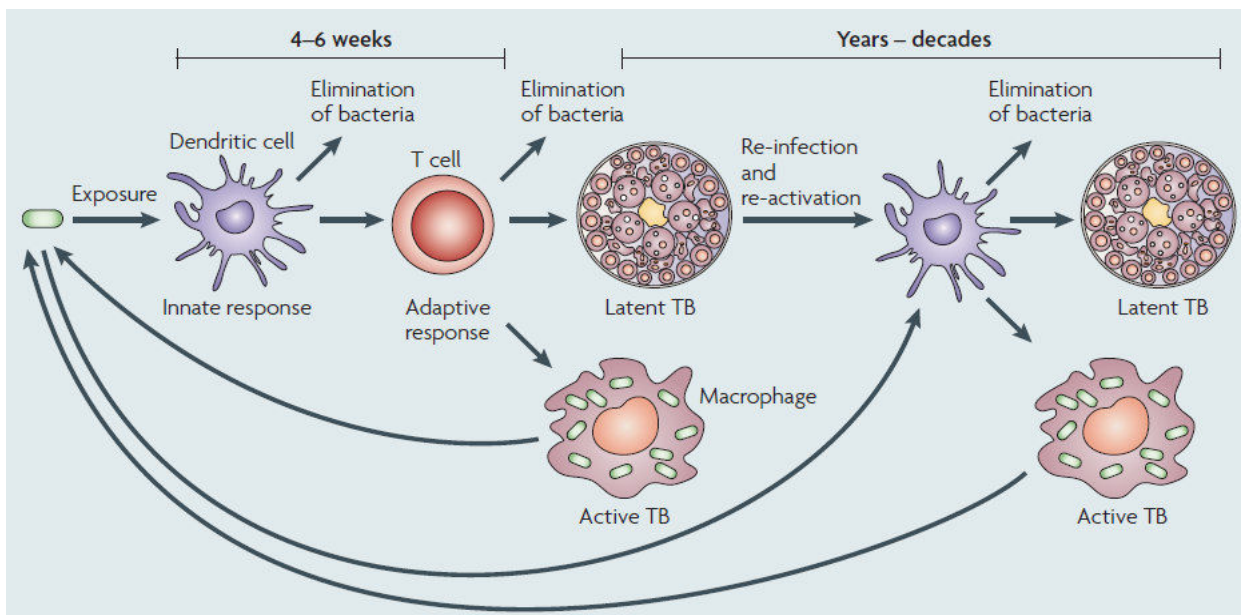
**Figura 2.** Resposta do hospedeiro à exposição ao *M. tuberculosis*. O bacilo é internalizado por fagocitose pelos macrófagos alveolares, iniciando a resposta inata. As células dendríticas iniciam a resposta adaptativa mediada por células T que ativam os macrófagos através da liberação de citocinas, o que pode resultar na: eliminação da bactéria, TB latente ou TB ativa. A TB latente pode evoluir para a forma ativa da doença após anos ou décadas (2).

## 1.2 Latência

O *M. tuberculosis* pode permanecer dentro do granuloma por muito tempo sem que o hospedeiro apresente os sintomas da doença, enquanto o seu sistema imunológico for capaz de manter seus macrófagos ativados e suas células T funcionais (3). A resposta imune do hospedeiro contra o *M. tuberculosis* é altamente efetiva no controle da replicação bacteriana, impedindo a progressão da doença e limitando-a ao local inicial da infecção. Esta condição é chamada de TB latente, que é a forma não contagiosa da doença, onde a bactéria permanece inativa, período durante o qual a pessoa infectada não apresenta TB clínica aparente. Isto é o que ocorre com a maioria dos indivíduos saudáveis que são infectados com o *M. tuberculosis*, devido à capacidade do bacilo em estabelecer e manter a latência, pois a completa eliminação

do patógeno é lenta e geralmente difícil de ser atingida. O bacilo pode permanecer neste estado "dormente" por meses, anos ou até décadas. O mecanismo de latência do bacilo causador da TB no hospedeiro ainda é desconhecido. Acredita-se que aproximadamente dois bilhões de indivíduos (um terço da população mundial) possuam a TB na forma latente (6, 7). No entanto, entre 5-10% dos indivíduos que estão infectados com a TB latente desenvolvem a forma ativa da doença (4). O desenvolvimento da forma ativa da TB geralmente ocorre quando o sistema imunológico do hospedeiro está debilitado. Quando, por exemplo, a função das células T está comprometida, o crescimento descontrolado do bacilo dentro dos macrófagos causa a disseminação do *M. tuberculosis* pelo rompimento do granuloma (2, 3).

### 1.3 Co-infecção com HIV

Indivíduos co-infectados com HIV e TB têm entre 21 e 34 vezes mais chances de desenvolver a TB ativa comparados com aqueles que são HIV-negativos, representando o principal risco para a progressão da TB latente para a forma ativa (8, 9). A co-infecção de indivíduos com TB e HIV afeta aproximadamente 11 milhões de indivíduos no mundo e resultou na morte de cerca de 200.000 pessoas no ano de 2005 (10). Mundialmente, uma em cada dez das quase 9 milhões de pessoas que desenvolvem TB a cada ano é HIV-positivas, o que equivale a 1,1 milhões de novos casos de TB entre os indivíduos portadores de HIV no ano de 2010 (1). Dos novos casos de co-infecção com TB e HIV no ano de 2010, 82 % concentraram-se na região africana, o que representa 900.000 (39 %) dos 2,3 milhões de pessoas que

desenvolveram TB e eram HIV-positivas, resultando em aproximadamente 0,35 milhões de mortes no mundo (1). No Brasil, a percentagem de pacientes tuberculosos co-infectados com HIV foi de 23% em 2010 (1).

A OMS fornece recomendações, desde 2004, quanto às intervenções necessárias para prevenir, diagnosticar e tratar a TB em pacientes portadores de HIV. As intervenções recomendadas incluem o tratamento com antirretroviral e com cotrimoxazol (sulfametoxazol e trimetroprima) para prevenir a pneumonia em pacientes co-infectados, intensificação na busca de pacientes infectados com TB entre os pacientes portadores de HIV, tratamento preventivo com isoniazida para indivíduos portadores de HIV que não possuem TB ativa, e controle da infecção em centros de saúde (1).

### 1.4 Tratamento e cepas resistentes

O tratamento padrão de "curta duração" da TB, recomendado pela OMS (DOTS – *directly observed treatment short course strategy*), consiste na combinação de potentes agentes bactericidas como a isoniazida, rifampicina, pirazinamida e etambutol por dois meses, seguido do tratamento com isoniazida e rifampicina por mais quatro meses (9). Estes medicamentos de primeira linha utilizados no tratamento da TB foram desenvolvidos há aproximadamente 50 anos atrás. No entanto, estes agentes bactericidas são altamente eficientes no tratamento de novos casos de TB suscetível a drogas, com taxas de cura de aproximadamente 90 % em pacientes HIV-negativos. Dos 22 países com maior número de casos de TB, 15 alcançaram 85 % de sucesso no

tratamento da TB, e dos 7 países que reportaram a menor taxa de sucesso no tratamento estão incluídos Brasil (72 %), Etiópia (84 %), Nigéria (83 %), Federação Russa (55 %), África do Sul (77 %), Uganda (67 %) e Zimbabwe (78 %). As baixas taxas de sucesso no tratamento da TB no Brasil e Uganda refletem a alta proporção de pacientes para os quais o resultado do tratamento não foi avaliado (11 % e 16 % respectivamente) (1).

Em 2009, aproximadamente 7% dos novos casos mundiais de TB foram devido à infecção com TB resistente a múltiplas drogas (TB-MDR), sendo que a taxa de sucesso no tratamento dos casos confirmados de TB-MDR foi de 60% (1). A TB-MDR ocorre quando uma cepa de *M. tuberculosis* é resistente a isoniazida e a rifampicina, duas das mais potentes drogas de primeira linha. O CDC (*Centers for Disease Control and Prevention*) dos Estados Unidos relatou que dos 17.690 isolados clínicos de *M. tuberculosis* no período de 2000 a 2004, 20% eram de cepas MDR e 2% eram de cepas extensivamente resistentes a drogas (TB-XDR) (11). Cepas XDR foram definidas como resistentes à isoniazida e rifampicina (TB-MDR) e também a fluoroquinolonas e a pelo menos uma das três drogas injetáveis de segunda linha que são usualmente utilizadas no tratamento de TB-MDR (capreomicina, canamicina e amicacina) (10). Portanto, o tratamento da TB-MDR e da TB-XDR consiste em drogas de segunda linha, que são mais caras, mais tóxicas, menos eficazes, apresentam mais efeitos adversos e são utilizadas por mais tempo (pelo menos 20 meses de tratamento) do que as drogas de primeira linha (10). As taxas de mortalidade entre pacientes infectados com HIV e TB-MDR frequentemente excede 80% e o período entre o diagnóstico e a morte geralmente varia de 4 a 16 semanas (9).

Em 2009, cepas de *M. tuberculosis* totalmente resistentes a drogas (TB-TDR) foram isoladas e demonstraram resistência *in vitro* a todas as drogas de primeira e segunda linha testadas (12). Nestas cepas, 30% da população total de *M. tuberculosis* se transformou em formas adaptadas, produzindo bacilos com formas arredondadas ou ovais (15 – 20%), ou tendo uma parede celular extremamente espessa (5 – 7%) (12). Essas características não foram encontradas nas cepas suscetíveis a drogas ou na TB-MDR, e assim podem estar relacionadas à resistência a drogas.

Agentes quimioterápicos mais eficazes e menos tóxicos são necessários para simplificar e reduzir a duração do tratamento atual, melhorando as possibilidades de tratamento para a TB-MDR e TB-XDR e possibilitando o tratamento da TB-TDR. Além disso, há a necessidade de um tratamento mais eficaz para a TB latente, impedindo que a doença evolua para a forma ativa, uma vez que o tratamento preventivo atual consiste em 6 a 9 meses com isoniazida. O desenvolvimento de novas drogas para tratar a TB que não interfiram com os antirretrovirais também é de grande interesse, para que possam ser utilizadas em pacientes co-infectados com HIV. Além de novos agentes quimioterápicos, o desenvolvimento de novas vacinas seria de fundamental importância na redução da incidência global da TB.

## 1.5 Desenvolvimento de vacinas

O desenvolvimento de novas estratégias terapêuticas profiláticas é necessário para diminuir a incidência global da TB uma vez que a vacina utilizada atualmente contra esta doença, *Mycobacterium bovis* Bacille Calmette-Guérin (BCG), fornece uma

proteção eficiente contra a TB em recém-nascidos, mas não previne o estabelecimento da TB latente ou a reativação da TB pulmonar em adultos (13). Além disso, embora a BCG tenha sido administrada em mais de 3 bilhões de pessoas, demonstrando satisfatória segurança, ocorreram alguns casos de disseminação de BCG em crianças vacinadas que desenvolveram a síndrome da imunodeficiência adquirida (AIDS) (14).

As principais estratégias atuais para o desenvolvimento de melhores vacinas contra a TB podem ser divididas em duas abordagens. A primeira abordagem visa substituir a BCG por uma vacina mais eficaz, como a produção de uma cepa micobacteriana atenuada obtida através da geração de mutantes de *M. tuberculosis* por deleção gênica. A segunda abordagem consiste no melhoramento da BCG, introduzindo antígenos importantes do *M. tuberculosis* ou alterando a BCG para que ela seja mais eficiente na indução de respostas imunológicas semelhantes às geradas pelo *M. tuberculosis* visando prolongar a imunidade e fornecer proteção à população adulta (13, 15). Algumas vacinas candidatas incluindo ambas as abordagens mencionadas acima estão em estudos pré-clínicos e outras em estudos clínicos (15, 16, 17, 18). Alguns aspectos importantes sobre uma vacina candidata contra TB devem ser levados em consideração. Em primeiro lugar, devido a estabilidade, a genética do mutante e a possibilidade de reversão para a cepa selvagem de *M. tuberculosis* é obrigatório que qualquer vacina viva para uso humano tenha pelo menos duas deleções genômicas independentes. Em segundo lugar, a cepa atenuada deve ser absolutamente segura em indivíduos imunocomprometidos, uma vez que os indivíduos portadores de HIV seriam uma população alvo importante (15).

Os avanços significativos nas ferramentas genéticas para manipulação de *M. tuberculosis* na última década (19, 20) e a disponibilidade do seqüenciamento completo do genoma da cepa de *M. tuberculosis* H37Rv (21) têm possibilitado o estudo e validação de alvos moleculares para o desenvolvimento de novas estratégias terapêuticas contra a TB. O conhecimento de características estruturais e funcionais das enzimas envolvidas em rotas metabólicas é uma etapa importante em direção ao desenvolvimento de novas estratégias profiláticas e terapêuticas seletivas contra a TB.

## 2.    Biossíntese de Nucleotídeos

Nucleotídeos são ésteres de fosfato de pentoses que possuem uma base nitrogenada ligada covalentemente ao C1' do açúcar. Nos ribonucleotídeos, as unidades monoméricas do RNA, a pentose é uma D-ribose, enquanto que nos desoxirribonucleotídeos, as unidades monoméricas do DNA, a pentose é uma 2'-desoxi-D-ribose. O grupo fosfato pode ligar ao C5' da pentose para formar um nucleotídeo 5' ou ao C3' para formar um nucleotídeo 3'. Nos nucleotídeos e nucleosídeos encontrados naturalmente, a base nitrogenada liga ao C1' da pentose, chamada de ligação glicosídica. Existem duas famílias de bases nitrogenadas: as purinas que possuem um anel de seis átomos fusionado a um anel de cinco átomos e as pirimidinas que possuem um anel de seis átomos. As principais purinas que compõem os ácidos nucléicos são os resíduos de adenina e guanina enquanto que as principais pirimidinas são citosina, uracil e timina (22, 23).

Os nucleotídeos têm funções essenciais em muitos processos bioquímicos. Eles são os precursores dos ácidos nucleicos, moléculas essenciais na replicação do genoma e na transcrição da informação genética em RNA.  Os nucleotídeos adenosina trifosfato (ATP) e guanosina trifosfato (GTP) são moléculas fundamentais que servem como fonte de energia em processos biológicos. Além disso, o ATP funciona como doador do grupo fosforil transferido pelas proteínas quinases. Derivados de nucleotídeos como UDP-glicose, participam de processos biossintéticos como a formação de glicogênio. Os nucleotídeos também são componentes essenciais nas rotas de transdução de sinais, como os nucleotídeos cíclicos que são os segundo

mensageiros adenosina monofosfato cíclico (AMPc) e guanosina monofosfato cíclico (GMPc) que transmitem sinais tanto dentro das células como entre as células (24).

As rotas biossintéticas para as moléculas de purina e pirimidina constroem a base para todos os demais passos do metabolismo de nucleotídeos e rotas relacionadas. Há duas principais rotas para a síntese de nucleotídeos de purinas e pirimidinas: a síntese *de novo* e a rota de salvamento. Na rota *de novo*, a síntese de nucleotídeos inicia a partir de precursores simples, enquanto na rota de salvamento, os nucleosídeos e bases livres são diretamente utilizados na síntese de ribonucleotídeos e desoxirribonucleotídeos (25). A síntese *de novo* de nucleotídeos requer mais energia do que a rota de salvamento (26). Assim, as rotas biossintéticas de nucleotídeos são tremendamente importantes como pontos de intervenção para agentes terapêuticos. Muitas das drogas mais utilizadas no tratamento do câncer atuam inibindo a biossíntese de nucleotídeos, como é o caso do Raltitrexed (ZD1694, Tomudex) e do 5-fluorouracil, inibidores da timidilato sintase (27). Além disso, as enzimas envolvidas na rota de salvamento de nucleotídeos púricos e pirimídicos são alvos atrativos para o desenvolvimento de agentes quimioterápicos para o tratamento de doenças infecciosas (28, 29).

## 2.1 Síntese *de novo* de pirimidinas

A rota biossintética *de novo* de pirimidinas resulta na formação do produto final 2'-desoxitimidina 5'-trifosfato (dTTP) e dos intermediários obrigatórios uridina 5'-trifosfato (UTP), citidina 5'-trifosfato (CTP) e 2'-desoxicitidina 5'-trifosfato (dCTP) (30). A

primeira reação química desta rota biossintética é catalisada pela carbamoil fosfato sintase (genes *carA,* Rv1383 e *carB,* Rv1384) utilizando ATP, glutamina e carbonato como substratos e formando carbamoil fosfato (**Figura 3**) (31). A etapa seguinte é catalisada pela aspartato transcarbamilase (gene *pyrB*, Rv1380) utilizando aspartato e carbamoil fosfato para sintetizar carbamoil aspartato e liberar fosfato inorgânico. A terceira reação da via é uma condensação intramolecular catalisada pela diidroorotase (gene *pyrC*, Rv1381) que resulta na formação de diidroorotato. A quarta reação é catalisada pela diidroorotato desidrogenase (gene *pyrD*, Rv2139) formando orotato. A enzima orotato fosforribosil transferase (OPRT) (gene *pyrE*, Rv0382c) catalisa a conversão do grupo fosforribosil do 5-fosforribosil-$\alpha$-1-pirofosfato (PRPP) para a base pirimídica do orotato formando orotidina 5'-monofosfato (OMP) a qual é descarboxilada, em uma reação catalisada pela enzima OMP descarboxilase (gene *pyrF*, Rv1385), formando uridina 5'-monofosfato (UMP), o primeiro nucleotídeo pirimídico (**Figura 3**). UMP é fosforilado a uridina 5'-difosfato (UDP) e, posteriormente, a UTP pela ação sequencial das enzimas UMP quinase (gene *pyrH,* Rv2883c) e nucleosídeo difosfato (NDP) quinase (gene *ndkA,* Rv2445c). A transferência do grupo amino da glutamina para o UTP pela CTP sintase (gene *pyrG,* Rv1699) leva a síntese de CTP (26). Na maioria dos organismos eucariotos, as três primeiras enzimas envolvidas na síntese *de novo* estão localizadas em um único polipeptídeo, assim como as atividades de OPRT e OMP descarboxilases são encontradas na proteína bifuncional UMP sintase (32). Comparadas com as proteínas monofuncionais bacterianas, as proteínas eucarióticas tem uma organização funcional mais complexa e um controle mais sofisticado, a rota é

submetida a diversos mecanismos regulatórios incluindo inibição e ativação alostérica, fosforilação e alterações na localização intracelular (32).

O parasita *Toxoplasma gondii* mostrou ter uma dependência estrita pela via de síntese *de novo* de pirimidinas, uma vez que o nocaute do gene que codifica para a primeira enzima da rota, a carbamoil fosfato sintase II, resultou em uma cepa auxotrófica para uracil e completamente avirulenta (33).
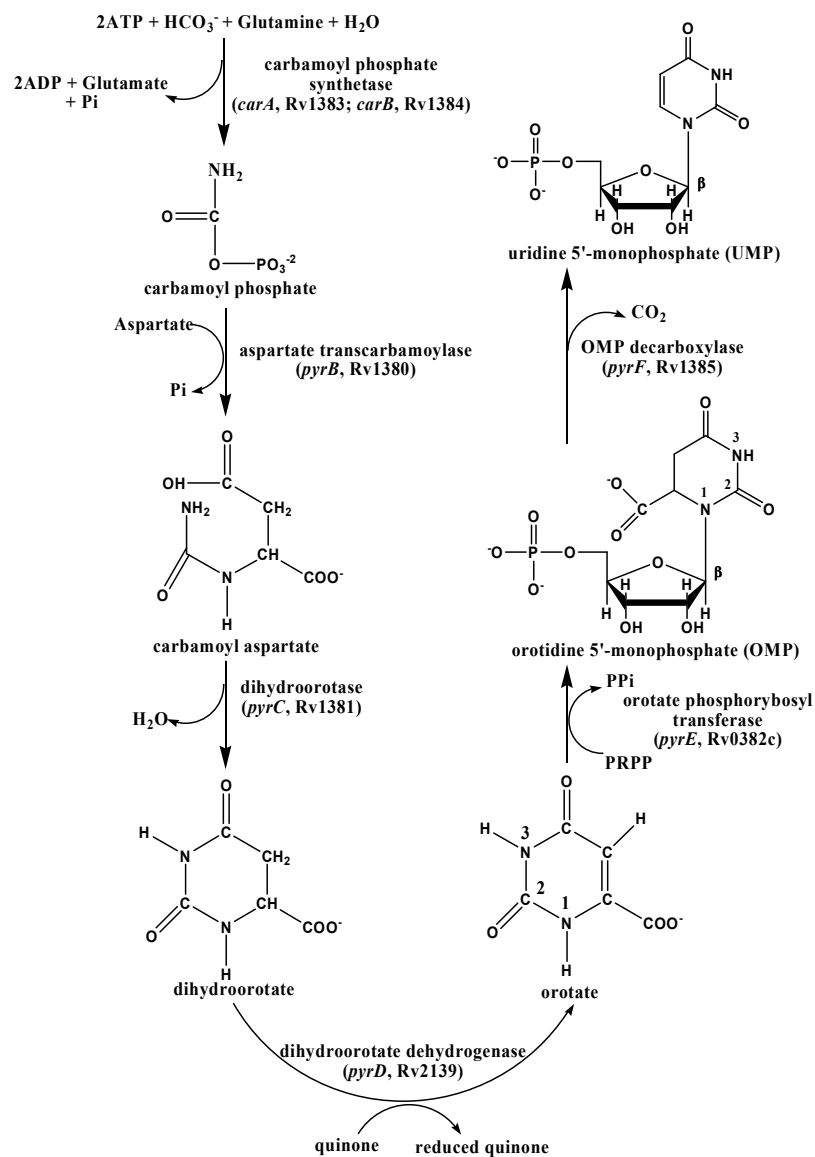


**Figura 3.** Rota de síntese *de novo* de pirimidinas.

## 2.2　Rota de Salvamento de pirimidinas

A rota de salvamento das pirimidinas tem como função a reutilização de bases e nucleosídeos livres tanto exógenos quanto os produzidos no meio intracelular a partir da reciclagem de nucleotídeos. Os nucleosídeos são predominantemente metabolizados a bases livres antes de serem utilizados na síntese de nucleotídeos. Quantidades significativas de ribonucleotídeos são degradadas durante o crescimento normal, e a reutilização dessas bases e nucleosídeos livres requer enzimas da rota de salvamento. Além disso, a rota de salvamento tem o papel de manter disponíveis as pentoses dos nucleosídeos exógenos como fonte de carbono e energia e os grupamentos amino dos compostos de citosina disponíveis como fonte de nitrogênio (30). A reciclagem de bases pirimídicas pela rota de salvamento é preferencialmente utilizada, pois demanda menos energia do que a síntese *de novo* (26).

Algumas enzimas da rota de salvamento foram identificadas por homologia de sequência no genoma do *M. tuberculosis* (21): dCTP deaminase (gene *dcd*, Rv0321), que catalisa a conversão de dCTP a 2'-desoxiuridina 5'-trifosfato (dUTP); desoxiuridina trifosfatase (dUTPase) (gene *dut*, Rv2697c), que converte dUTP a 2'-desoxiuridina 5`-monofosfato (dUMP); timidilato sintase (gene *thyA*, Rv2764c), que converte dUMP a 2'-desoxitimidina 5'-monofosfato (dTMP); a dTMP kinase (gene *tmk*, Rv3247c) catalisa a conversão de dTMP a 2'-desoxitimidina 5'-difosfato (dTDP) seguida pela NDP quinase (gene *ndkA*, Rv2445c), que converte dTDP a dTTP (**Figura 4**). Outros genes que codificam enzimas da rota de salvamento das pirimidinas incluem: citidina deaminase

(CDA) (gene *cdd*, Rv3315c) converte citidina ou desoxicitidina a uridina ou desoxiuridina, respectivamente; pirimidina nucleosídeo fosforilase (PyNP) (gene *deoA*, Rv3314c) que recicla o nucleosídeo timidina ou uridina a desoxiribose-1-fosfato e timina ou uracil; a enzima uracil fosforribosil transferase (UPRT) (gene *upp*, Rv3309c) catalisa a conversão de uracil e PRPP a UMP e pirofosfato ($PP_i$); citidina 5'-monofosfato (CMP) quinase (gene *cmk*, Rv1712) e UMP quinase (gene *pyrH*, Rv2883c), que catalisam a conversão reversível do grupamento γ-fosforil do nucleosídeo trifosfato para a CMP e UMP, respectivamente, para gerar citidina 5'-difosfato (CDP) e UDP, respectivamente (**Figura 4**). A uridina fosforilase, uridina quinase e timidina quinase estão descritas como membros da rota de salvamento de *Escherichia coli* e *Salmonella typhimurium* (34). Entretanto, nenhuma homologia foi encontrada no genoma do *M. tuberculosis* para os genes que codificam as seguintes enzimas: uridina nucleosidase, uridina fosforilase, uridina quinase, uridina monofosfatase, 2'-desoxicitidina 5`-monofosfato deaminase e timidina quinase (21).
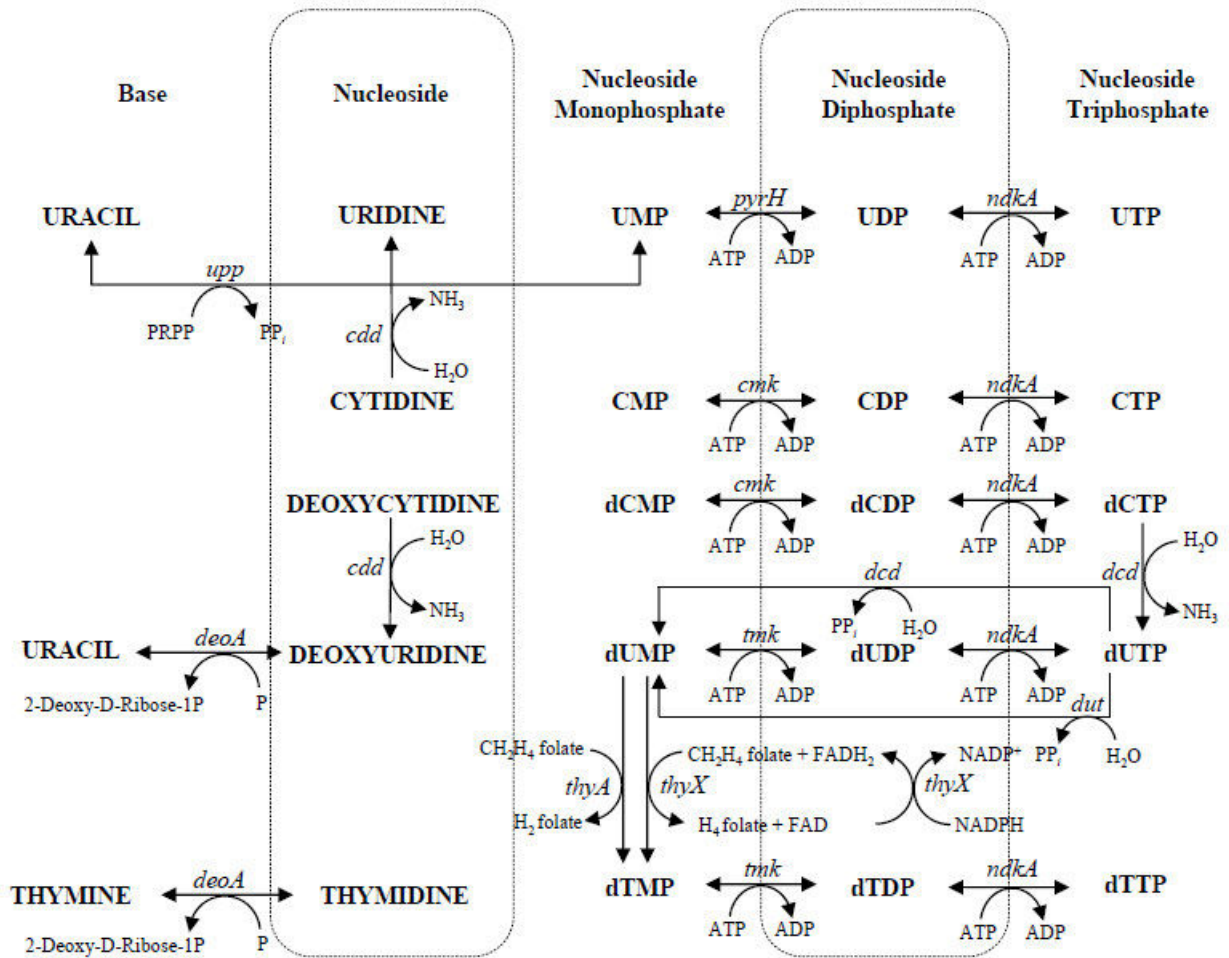
**Figura 4.** Rota de salvamento de pirimidinas. Enzimas envolvidas na rota: dCTP deaminase (*dcd*), dUTPase (*dut*), timidilato sintase (*thyA*), dTMP quinase (*tmk*), NDP quinase (*ndkA*), UPRT (*upp*), UMP quinase (*pyrH*), CMP quinase (*cmk*), CDA (*cdd*), e PyNP (*deoA*) (29).

## 3. Uracil Fosforribosil Transferase de *M. tuberculosis*

A UPRT, também conhecida como UMP pirofosforilase e UMP difosforilase (codificada pelo gene *upp*, 624 pb, Rv3309c, EC 2.4.2.9, 207 aa, 21.866,1 Da, e PI = 4,73) catalisa a conversão de uracil e PRPP em UMP e $PP_i$ (**Figura 5**). A UPRT é uma enzima chave da rota de salvamento de pirimidinas, já que o produto desta reação (UMP) é o precursor dos outros nucleotídeos pirimídicos. A uridina nucleosidase e a uridina fosforilase, que catalisam a conversão de uracil para uridina, não foram encontradas por homologia de sequência no genoma do *M. tuberculosis* (21). Além disso, a uridina quinase e a uridina monofosfatase, que convertem a uridina a UMP, também não foram identificadas no genoma do *M. tuberculosis* (21). Assim, a UPRT parece ter um papel importante na rota de salvamento das pirimidinas, já que ela é a única enzima que converte bases pirimídicas pré-formadas em nucleotídeos.
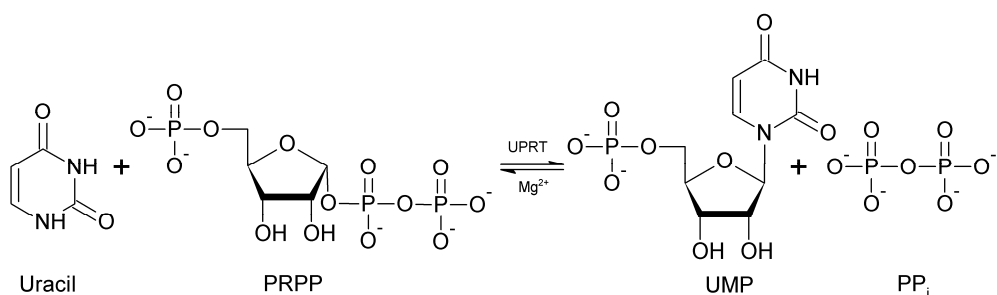


**Figura 5.** Reação química catalisada pela UPRT.

Em *M. tuberculosis* H37Rv, dois genes foram identificados por homologia de sequência por possuírem provável atividade de UPRT (EC 2.4.2.9): *upp* (Rv3309c) e *pyrR* (Rv1379) (21). Apesar das proteínas *pyrR* serem evolutivamente relacionadas com as UPRTs como demonstrado por similaridades de sequência e estrutural, *pyrR* de *M. tuberculosis* mostrou ter atividade catalítica fraca de UPRT (35). Assim, a maior parte

de atividade de UPRT e salvamento de uracil em *M. tuberculosis* dependem do gene *upp*.

A UPRT é um membro da família das fosforribosil transferases tipo I, que apresentam um dobramento característico. Este dobramento consiste em uma região central que compreende 5 folhas β paralelas e pelo menos 3 hélices α com uma alça flexível e um subdomínio conhecido por "capa" (36, 37). A "capa" contém os resíduos requeridos para a ligação da nucleobase (uracil para UPRTs) e é também formada por resíduos da porção C-terminal (36). O sítio ativo está localizado entre a capa e a região central, abrigando o motivo de ligação ao PRPP, e os resíduos catalíticos da alça flexível cobrem o sítio ativo, protegendo o estado de transição da hidrólise (36, 38).

As estruturas tridimensionais das UPRTs de algumas espécies foram determinadas e encontram-se depositadas no *Protein Data Bank* (PDB), incluindo as enzimas do *Thermus termophilus* (código de depósito no PDB: 1V9S, a ser publicado), *Bacillus caldolyticus* (código de depósito no PDB: 1I5E) (36), *Thermotoga maritime* (código de depósito no PDB: 1O5O, a ser publicado), *Escherichia coli* (código de depósito no PDB: 2EHJ, a ser publicado), *Aquifex aeolicus* (código de depósito no PDB: 2E55, a ser publicado), *S. solfataricus* (código de depósito no PDB: 1XTT) (39), e *Toxoplasma gondii* (código de depósito no PDB: 1UPU) (40). As sequências de aminoácidos das UPRTs destas espécies foram alinhadas com a sequência da enzima de *M. tuberculosis* (**Figura 6**) e foi encontrada identidade total entre 47 % e 35 %, o que confirma que todas estas enzimas pertencem à família das fosforribosil transferases do tipo I. As regiões destacadas em vermelho na **Figura 6** são regiões altamente conservadas entre as UPRTs que são importantes para o reconhecimento do substrato

e catálise. A identidade encontrada entre as sequências de aminoácidos das UPRTs de outras espécies com a de *M. tuberculosis* sugere uma possível semelhança tanto nas posições dos sítios catalíticos e de ligação, quanto na estrutura secundária da UPRT de *M. tuberculosis*. Assim, analisando e comparando mais detalhadamente a estrutura e a sequência de aminoácidos da UPRT do *B. caldolyticus* com a enzima do *M. tuberculosis*, que apresentam uma identidade de 45 %, pode-se observar que a sequência de aminoácidos da UPRT de *M. tuberculosis* possui os resíduos Asp131-Ser139, identificados na UPRT de *B. caldolyticus* por ser a sequência consenso do motivo de ligação de PRPP e ligação à ribose-5'-fosfato do UMP (36). Este motivo de ligação de PRPP está presente em todas as fosforribosil transferases do tipo I (36, 37). O segmento Tyr193-Ala201, presente nas sequências de aminoácidos da UPRT de *B. caldolyticus* e de *M. tuberculosis*, liga ao uracil do UMP, e é especifico para as UPRTs (36).

As UPRTs de algumas espécies são alostericamente ativadas por GTP, como as enzimas de *T. gondii* (41), *Giardia intestinalis* (42), *E. coli* (43), e *S. solfataricus* (38, 39). Além disso, a enzima de *S. solfataricus* mostrou ser alostericamente inibida por CTP (38, 39).
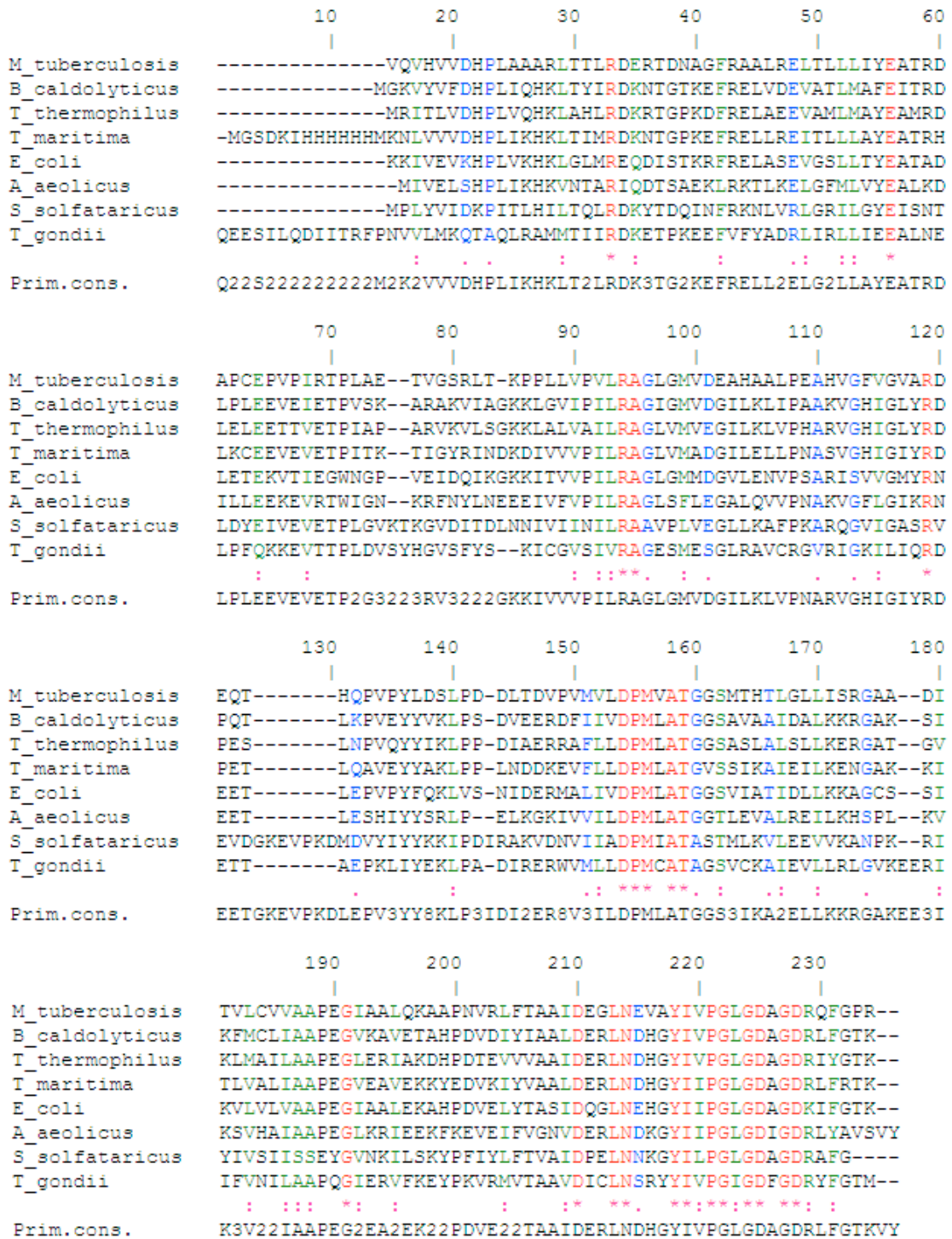
**Figura 6.** Alinhamento da sequência de aminoácidos da UPRT de *M. tuberculosis* e seus homólogos que apresentam estrutura depositada no PDB. As sequências estão indicadas pela espécie: UPRT de *B. caldolyticus* (código de depósito no PDB: 1I5E); UPRT de *T. termophilus* (código de depósito no PDB: 1V9S); UPRT de *T. maritima* (código de depósito no PDB: 1O5O); UPRT de *E. coli* (código de depósito no PDB: 2EHJ); UPRT de *A. aeolicus* (código de depósito

no PDB: 2E55); UPRT de *S. solfataricus* (código de depósito no PDB: 1XTT) e UPRT de *T. gondii* (código de depósito no PDB: 1UPU).

Em *T. gondii*, o nocaute do gene *upp* não afetou o crescimento e mostrou não ser essencial para a viabilidade do parasita, mas a habilidade do parasita de incorporar uracil foi completamente abolida (44). O gene *upp* de *M. tuberculosis* foi predito como gene não essencial pela mutagênese mediada por transposon e baseada em Himar-1 na cepa H37Rv (45).

Diferentemente das enzimas da síntese *de novo* de UMP, as UPRTs foram caracterizadas apenas em organismos menos complexos. Esta enzima foi parcialmente caracterizada em eubactéria, archaea, eucariotos menores e também foi encontrada em plantas (36). Recentemente, com base na comparação de sequência de aminoácidos foi proposta uma fase de leitura aberta que codifica a UPRT em humanos (46). No entanto, a clonagem a partir de uma biblioteca de cDNA humano, a expressão e purificação da proteína resultou em uma cadeia polipeptídica que não apresentou atividade catalítica (46). A demonstração definitiva de que uma determinada cadeia polipeptídica possui atividade de UPRT deve necessariamente demonstrar o consumo do substrato (uracil ou PRPP) e/ou produção do produto (UMP), isto é, que a cadeia polipeptídica catalisa a reação química. Portanto, ainda não há evidência experimental da presença da UPRT em humanos.

# HIPÓTESE DO TRABALHO

As vias de biossíntese de nucleotídeos de pirimidina são alvos atrativos para o desenho racional de drogas contra a TB pois é composta por enzimas consideravelmente diferentes daquelas presentes em humanos. As enzimas da rota de salvamento de pirimidinas talvez tenham um papel importante na latência do *M. tuberculosis*, já que o bacilo possivelmente necessite reciclar bases e/ou nucleosídeos para sobreviver no ambiente hostil imposto pelo hospedeiro. Assim, as enzimas dessa rota podem ser alvos importantes para o desenvolvimento de novas vacinas. Entre as enzimas da rota de salvamento que foram identificadas em *M. tuberculosis*, a enzima uracil fosforribosil transferase, predita como sendo não essencial para a viabilidade da micobactéria, é um alvo molecular atrativo para o desenvolvimento de cepas atenuadas.

# OBJETIVOS GERAIS

Caracterizar a enzima UPRT de *M. tuberculosis* codificada pelo gene *upp*, validar seu papel biológico e determinar a sua relevância na rota de salvamento das pirimidinas e no metabolismo do *M. tuberculosis*, visando à obtenção de cepas atenuadas.

# OBJETIVOS ESPECÍFICOS

1. Amplificar e clonar o gene *upp* de *M. tuberculosis*; expressar, purificar e caracterizar a proteína recombinante UPRT de *M. tuberculosis.*

2. Determinar as constantes cinéticas aparentes e verdadeiras da reação catalisada pela enzima, as constantes termodinâmicas envolvidas na ligação de substratos e produtos e estabelecer o mecanismo cinético.

3. Analisar a importância da enzima UPRT na rota de salvamento das pirimidinas e no metabolismo do *M. tuberculosis* através de nocaute do gene *upp* e da análise da expressão da proteína em diferentes condições de crescimento da micobactéria.

Os capítulos estão organizados da seguinte forma:

No **Capítulo 2** consta um artigo de revisão sobre as enzimas envolvidas na rota de salvamento das pirimidinas em *M. tuberculosis*.

O **Capítulo 3** consiste em um artigo científico onde são apresentados os seguintes resultados: a amplificação do gene *upp* a partir do DNA genômico de *M. tuberculosis* H37Rv, clonagem em pET23a(+), expressão na cepa *E. coli* BL21(DE3), purificação utilizando cromatografia líquida de rápida performance, confirmação da identidade da proteína homogênea por espectrometria de massas e sequenciamento N-terminal (**Objetivo Específico 1**); teste de atividade da enzima UPRT, determinação da massa molecular da proteína por ultracentrifugação analítica, determinação dos parâmetros termodinâmicos para a ligação de substratos e produtos á enzima livre utilizando calorimetria de titulação isotérmica, determinação das constantes cinéticas aparentes e verdadeiras da reação catalisada pela enzima, determinação do mecanismo cinético e do perfil de pH (**Objetivo Específico 2**).

No **Capítulo 4** são apresentados os resultados obtidos na construção da cepa de *M. tuberculosis* H37Rv mutante para o gene *upp* através de nocaute gênico utilizando o vetor suicida pPR27*xylE*, construção da cepa de *M. tuberculosis* H37Rv mutante para o gene *upp* e complementada com uma cópia extra do gene *upp,* curva de crescimento das cepas *M. tuberculosis* H37Rv mutante para o gene *upp,* complementada e tipo selvagem; análise da expressão da UPRT em diferentes condições de crescimento de *M. tuberculosis* H37Ra; os resultados do metabólito ativo do *isoxyl* como inibidor da *Mt*UPRT, a análise da incorporação de bases e nucleosídeos marcados com trítio em culturas de *M. tuberculosis* H37Ra, o ensaio de atividade da *Mt*UPRT e a reação de ativação do *isoxyl* para análise da inibição da enzima UPRT *in vitro* utilizando espectrofotômetro, a determinação da concentração inibitória mínima de *isoxyl* para as cepas de *M. tuberculosis* mutante para o gene *upp*, complementada e tipo selvagem

(**Objetivo específico 3**). Estes experimentos foram realizados durante o doutorado sanduíche no laboratório coordenado pela Dra. Mary Jackson, que está localizado na Colorado State University em Fort Collins, Estados Unidos da América.

No **Capítulo 5** são apresentadas as considerações finais.

# Capítulo 2

Pyrimidine Salvage Pathway in
*Mycobacterium tuberculosis*

A.D. Villela, Z. A. Sánchez-Quitian, R.G. Ducati,
D.S. Santos, L.A. Basso

# Pyrimidine Salvage Pathway in *Mycobacterium tuberculosis*[†]

A.D. Villela[1,2], Z.A. Sánchez-Quitian[1,2], R.G. Ducati[1], D.S. Santos*[,1,2] and L.A. Basso*[,1,2]

[1]*Instituto Nacional de Ciência e Tecnologia em Tuberculose (INCT-TB), Centro de Pesquisas em Biologia Molecular e Funcional (CPBMF), Pontifícia Universidade Católica do Rio Grande do Sul, Porto Alegre, RS, Brazil;* [2]*Programa de Pós-Graduação em Biologia Celular e Molecular, Faculdade de Biociências, Pontifícia Universidade Católica do Rio Grande do Sul, Porto Alegre, RS, Brazil*

**Abstract:** The causative agent of tuberculosis (TB), *Mycobacterium tuberculosis*, infects one-third of the world population. TB remains the leading cause of mortality due to a single bacterial pathogen. The worldwide increase in incidence of *M. tuberculosis* has been attributed to the high proliferation rates of multi and extensively drug-resistant strains, and to co-infection with the human immunodeficiency virus. There is thus a continuous requirement for studies on mycobacterial metabolism to identify promising targets for the development of new agents to combat TB. Singular characteristics of this pathogen, such as functional and structural features of enzymes involved in fundamental metabolic pathways, can be evaluated to identify possible targets for drug development. Enzymes involved in the pyrimidine salvage pathway might be attractive targets for rational drug design against TB, since this pathway is vital for all bacterial cells, and is composed of enzymes considerably different from those present in humans. Moreover, the enzymes of the pyrimidine salvage pathway might have an important role in the mycobacterial latent state, since *M. tuberculosis* has to recycle bases and/or nucleosides to survive in the hostile environment imposed by the host. The present review describes the enzymes of *M. tuberculosis* pyrimidine salvage pathway as attractive targets for the development of new antimycobacterial agents. Enzyme functional and structural data have been included to provide a broader knowledge on which to base the search for compounds with selective biological activity.

**Keywords:** Enzyme functional features, enzyme structural features, *Mycobacterium tuberculosis*, pyrimidine salvage pathway, rational drug design, tuberculosis.

## 1. INTRODUCTION

The causative agent of tuberculosis (TB), *Mycobacterium tuberculosis* (MTB), infects one-third of the world population. The World Health Organization (WHO) estimates that approximately 10 million new TB cases occurred in 2008, resulting in 2 million deaths worldwide [1]. TB remains the major cause of mortality in the world caused by a single infectious agent. This is especially true in developing countries, considering that the highest levels of TB deaths in the world occur in these nations [2].

Progression of TB infection may proceed either through microbial immediate elimination or latency conditioning; whereas host immunological failure facilitates the development of active disease [3]. The term "dormancy" has been coined for the latent state of TB, and strongly associated with the *in vitro* model of MTB growth under laboratorial limiting oxygen conditions [4], in which the bacillus remains quiescent within infected macrophages, and may reflect a metabolic shutdown, as a result of the action of a cell-mediated immune response capable of containing, but not eradicate, the infection [3]. Rougly 10% of individuals with latent TB infection might, after years, or even decades, develop the active disease [5], owing to failure of the host immune defense system to maintain MTB in check, leading to progressive disease and active transmission of the pathogen [6]. The probability to develop active TB is significantly increased by 10% annually in human immunodeficiency virus (HIV) infected individuals [7].

The ability of MTB to persist in the human host for long periods in a latent state makes TB control even more difficult, since the direct identification of latent TB infection is not possible. The diagnostic procedure used to identify individuals infected with MTB is the tuberculin skin test, which was designed to identify an adaptive immune response against a pathogen. However, it cannot distinguish if the infection is latent or active. The prophylatic vaccine currently in use, *Mycobacterium bovis* bacille Calmette-Guérin (BCG), which was introduced more than 60 years ago, is the most widely used vaccine in the world. Although BCG vaccination confers protection against TB in certain populations, mainly the severe disease manifestation in children [8], it has modest protective effect against the adult form of the disease, and does not prevent the establishment of latent TB or reactivation of the pulmonary disease in adult life [9, 10]. Latent TB infection represents a large reservoir of the TB bacilli, from which most cases of active disease arise; as previously mentioned, it represents a major obstacle in achieving worldwide control of TB [7]. Accordingly, TB was declared a global emergency by the WHO a decade ago.

The TB bacilli can become resistant to the drugs currently used in the Directly Observed Treatment Short-course, which comprises isoniazid, rifampicin, pyrazinamide, and ethambutol for two months, and isoniazid and rifampicin for an additional period of four months. Although chemotherapeutic agents are currently available to treat TB, drug resistance has become a dramatic problem. Inappropriate treatment regimens and patient noncompliance in completing the therapies are associated with the emergence of multi-drug resistant TB (MDR-TB), defined as strains of *M. tuberculosis* resistant to at least two first-line drugs (isoniazid and rifampicin), which are the most powerful anti-TB drugs employed in the standard treatment of TB. In addition, the emergence of extensively drug-resistant (XDR) TB cases, defined as cases in persons with TB whose isolates are MDR as well as resistant to any one of the fluoroquinolones and to at least one of the three injectable second-line drugs [11], highlighted TB as a global threat to public health in 2006, especially in high HIV-prevalence countries [1, 12]. Accordingly, there is an urgent need for more effective and less toxic drugs to be introduced in TB treatment, which would act on different mycobacterial targets with respect to the current anti-TB drugs in order to provide an efficient alternative treatment for TB, including MDR-TB and XDR-TB infections. Moreover, there is a critical need for the development of vaccines to prevent initial infection, and of new drugs to reduce progression from latent infection to active disease.
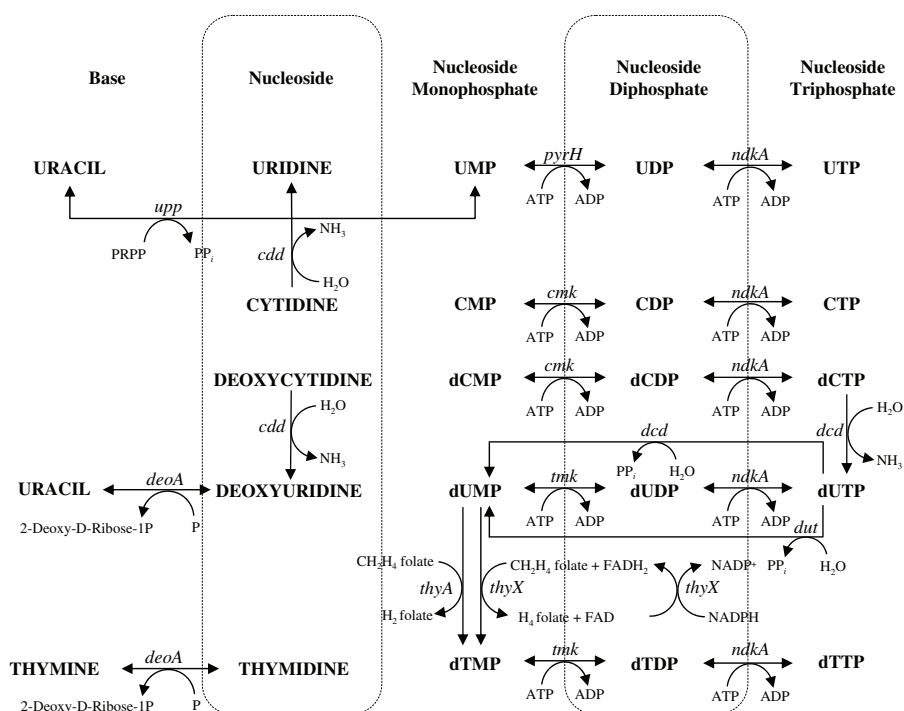
**Fig. (1).** Overview of the pyrimidine salvage pathway in MTB. Enzymes involved in the pathway: dCTP deaminase *(dcd)*, dUTPase *(dut)*, thymidylate synthase *(thyA)*, dTMP kinase *(tmk)*, NDK *(ndkA)*, UPRTase *(upp)*, UMP kinase *(pyrH)*, CMP kinase *(cmk)*, CDA *(cdd)*, and PyNP *(deoA)*.

The complete genome sequencing of MTB H37Rv [13], the best-characterized MTB strain, has improved research towards the understanding of the MTB biology and the validation of molecular targets to be explored for the rational design of drugs to treat TB. Singular features of this pathogen, such as enzymes of fundamental metabolic pathways can be evaluated as possible targets for drug development [14]. For instance, it has been shown that, although bovine and human purine nucleoside phosphorylase enzymes share 87% sequence identity and have conserved active site residues, inhibitors with differential specificity could be designed [15]. Thus, the knowledge of functional and structural features of the enzymes involved in metabolic pathways is an important step towards target-based development of selective chemotherapeutic agents to treat TB. Enzymes involved in the pyrimidine salvage pathway might be attractive targets for rational drug design against TB, since they may have an important role in the latent state of the TB bacillus and possess structural and functional features different from those of humans.

## 2. PYRIMIDINE SALVAGE PATHWAY

Enzymes responsible for pyrimidine biosynthesis have important roles in cellular metabolism, as they provide pyrimidine nucleosides that are essential components of many biomolecules [16]. There are two major pathways for pyrimidine nucleotide synthesis: *de novo* and salvage. Genes encoding the six enzymes involved in the *de novo* pyrimidine ribonucleotide synthesis have been identified in the MTB genome [13]. Since the *de novo* synthesis requires energy, cells use the salvage pathway to reutilize pyrimidine bases and nucleosides derived from preformed nucleotides [17]. Pyrimidine salvage pathways are vital for all bacterial cells, and may differ among species [18]. It was shown that the pyrimidine salvage pathway of *Pseudomonas* genus organisms possesses different enzymes. For instance, *Pseudomonas aeruginosa* possesses both cytosine deaminase and nonspecific ribonucleoside hydrolase enzymes, and does not have cytidine deaminase, uridine phosphorylase, and uridine/cytidine hydrolase, while *Pseudomonas mendocina* possesses cytidine deaminase, cytosine deaminase, and uridine

phosphorylase enzymes, and does not have nonspecific ribonucleoside hydrolase and uridine/cytidine hydrolase [18]. The pyrimidine salvage pathways of *Escherichia coli* and *Salmonella typhimurium* serve three physiological functions: the incorporation of exogenous free bases and nucleosides; the synthesis of pentose moieties from exogenous nucleosides to be used as carbon and energy sources as well as the amino groups of cytosine compounds available as a nitrogen source; and the reutilization of free bases and nucleosides produced intracellularly from nucleotide turnover [19].

Enzymes of the pyrimidine salvage pathway might stand as attractive targets for cancer and infectious disease treatments, since pyrimidine analogues were found to be toxic for cell growth. There are three general features that most known pyrimidine analogues follow: first, the analogue must be converted to the nucleotide level in order to express toxicity; second, nucleotide analogue toxicity can be achieved either by inhibition of one or more enzymes of the pathway or can lead to the incorporation of the analogue into either DNA or RNA after its conversion to triphosphate; third, the understanding of conversions of natural bases and nucleosides is very important since some analogues become inhibitory only after being metabolized [20]. For instance, 5-fluorouracil (5-FU), a major pyrimidine antagonist that has been used for more than 40 years in cancer chemotherapies, has to be metabolized to display its inhibitory effect [16].

A number of enzymes of the pyrimidine salvage pathway have been identified by sequence homology in the MTB genome [13]: deoxycytidine triphosphate (dCTP) deaminase, which converts dCTP to deoxyuridine triphosphate (dUTP); deoxyuridine triphosphatase (dUTPase), which converts dUTP to deoxyuridine 5'-monophosphate (dUMP); thymidylate synthase, which takes dUMP to deoxythymidine monophosphate (dTMP); and makes deoxythymidine diphosphate (dTDP) by dTMP kinase enzyme activity followed by nucleoside diphosphate kinase, which converts dTDP to deoxythymidine triphosphate (dTTP) (Fig. **1**). Additional genes encoding enzymes in the pyrimidine salvage pathway include cytidine deaminase, that converts cytidine or deoxycytidine to uridine or deoxyuridine, respectively; pyrimidine nucleoside phos-
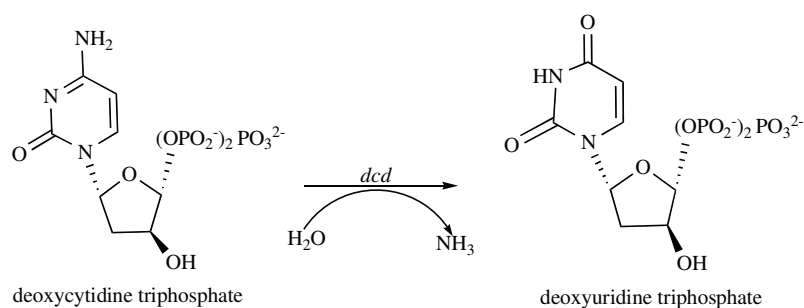
**Fig. (2).** Chemical reaction catalyzed by dCTP deaminase (*dcd*). The enzyme catalyzes the deamination of dCTP to form dUTP.
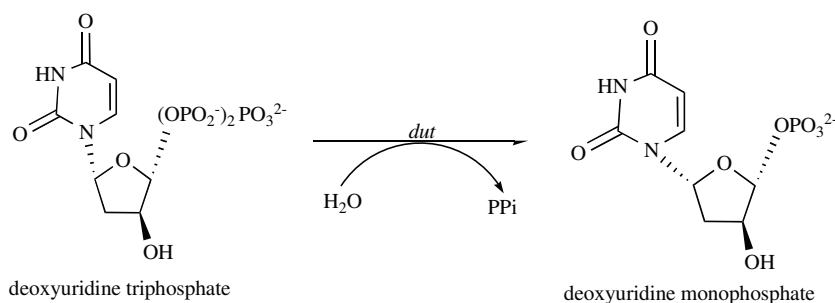


**Fig. (3).** Chemical reaction catalyzed by dUTPase (*dut*). The enzyme catalyzes the triphosphate hydrolysis reaction producing dUMP.

phorylase that rescues the nucleoside back to deoxyribose-1-phosphate (dRP) and thymine or uracil, the free base; uracil phosphorybosyltransferase, which catalyzes the conversion of uracil and 5'-phosphoribosyl-α-1'-pyrophosphate (PRPP) to uridine 5'-monophosphate (UMP) and pyrophosphate (PP$_i$); and cytidine monophosphate (CMP) kinase and uridine monophosphate (UMP) kinase, which catalyze the reversible γ-phosphoryl transfer from a nucleoside triphosphate to CMP and UMP, respectively, to generate cytidine diphosphate (CDP) and uridine diphosphate (UDP), respectively (Fig. **1**). Uridine phosphorylase, uridine kinase, and thymidine kinase are described as members of the *E. coli* and *S. typhimurium* salvage pathway [20]. However, no homology was found in MTB genome for uridine nucleosidase, uridine phosphorylase, uridine kinase, uridine monophosphatase, dCMP deaminase, and thymidine kinase encoding genes [13]. The enzymes involved in the MTB salvage pathway (Fig. **1**) will be described subsequently, focusing mainly on functional and structural features of each enzyme aiming towards target-based development of chemotherapeutic agents to treat TB.

## 2.1. Deoxycytidine Triphosphate Deaminase

dCTP deaminase (encoded by *dcd* gene, 573 bp, MTB Rv0321, EC 3.5.4.13, 190 aa, 20,837.5 Da, and isoelectric point (PI) = 6.35) catalyzes the conversion of dCTP to dUTP (Fig. **2**). Recombinant dCTP deaminase from MTB was expressed in *E. coli*, and purified and characterized both functionally and structurally [21]. The enzyme proved to be bifunctional, catalyzing the deamination of dCTP to produce dUTP (dCTP deaminase activity) and hydrolysis of dUTP to dUMP and diphosphate (dUTPase activity; Fig. **3**) [21]. This bifunctional activity had also been demonstrated previously for the archaean *Methanocaldococcus jannaschii* enzyme [22, 23]. The characterization of the bifunctional dCTP deaminase:dUTPase from MTB was the first to be confirmed outside the archaea kingdom [21]. Although the dCTP deaminase:dUTPase from MTB and *M. jannaschii* are bifunctional, amino acid residues from the MTB enzyme are more similar to the monofunctional dCTP deaminase from *E. coli* than from *M. jannaschii* enzyme [21, 24]. The bifunctional enzyme catalyses both dUTP hydrolysis and dCTP deamination, where the product of the reaction, dUMP, is synthesized at the same rate as dCTP is deaminated to dUTP [21]. Thus, dUMP can

be formed from both dCTP and dUTP, since the bifunctional enzyme has also dUTPase activity [24]. A major function of dUTPase is to keep uracil out of the DNA, controlling the dUTP concentration in the nucleotide pool [25]. High amounts of dUTP can cause the utilization of uracil for DNA synthesis, which leads to cell death [26]. Then, the coupling of dCTP deaminase and dUTPase activities within the same active site excludes the possibility of dUTP to be used for DNA synthesis [26].

The crystal structure of dCTP deaminase:dUTPase from MTB was determined in the apo form (PDB access code: 2QLP) and in complex with dTTP (PDB access code: 2QXX), which is an inhibitor of this enzyme [21]. The bifunctional dCTP deaminase:dUTPase enzyme is homotrimeric, with three active sites, and each site is located in a pocket between two subunits [21]. Binding of dTTP into the active site of dCTP deaminase:dUTPase leads to an inactive conformation due to structural changes [21]. To accommodate the 5'-methyl group of the thymine moiety, a dramatic rearrangement in the position of residues 110-117 has to occur, which results in the displacement of a water molecule (Wat 59) from the active site [21]. In *M. tuberculosis* dCTP deaminase:dUTPase enzyme, Wat 59 makes a hydrogen bond with O2 of the α-phosphoryl group and is likely involved in stabilization of the transition state by withdrawing electrons from the α-phosphoryl leading to increased susceptibility to a nucleophilic attach [21]. In agreement with this proposal, displacement of Wat 59 by dTTP binding would inhibit dUTPase enzyme catalysis.

The monofunctional dCTP deaminase from *E. coli* was shown to be inhibited by dTTP through a similar mechanism to the bifunctional enzyme from MTB, which is a nonallosteric inhibition [27, 28]. However, the mechanism of dTTP inhibition for dCTP deaminase from *E. coli* is competitive, where an increase in substrate concentration affects dTTP inhibition [27], while MTB dCTP deaminase:dUTPase bifunctional enzyme possesses a noncompetitive mode of action [21]. Moreover a comparison of the active sites among the bifunctional dCTP deaminase from *M. jannaschii* and the monofunctional dCTP deaminase and dUTPase *E. coli* enzymes suggests a similar reaction mechanism and position of amino acid residues in the active site [24, 29]. The broader substrate specificity of bifunctional MTB dCTP deaminase:dUTPase enzyme may rep-
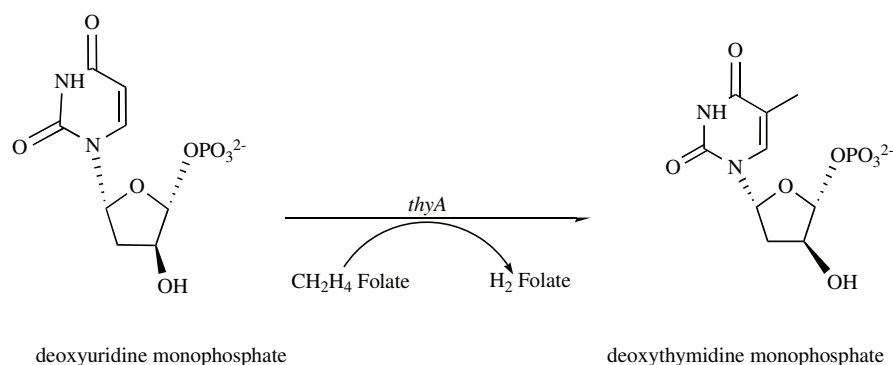
**Fig. (4).** Chemical reaction catalyzed by thymidylate synthase (*thyA*). The enzyme catalyzes the reductive methylation of dUMP by CH$_2$H$_4$folate to produce dTMP and H$_2$folate.

resent a flexible target for specific nucleotide analogs to be used as therapeutic agents against TB [30].

## 2.2. Deoxyuridine Triphosphatase

dUTPase, also known as dUTP pyrophosphatase, deoxyuridine 5'-triphosphate nucleotidohydrolase, dUTP diphosphatase, and deoxyuridine 5'-triphosphatase (encoded by *dut* gene, 465 bp, MTB Rv2697c, EC 3.6.1.23, 154 aa, 15,770.9 Da, and PI = 5.99), converts dUTP to dUMP (Fig. **3**). The reaction product is the immediate precursor of thymidine nucleotides. dUTPase is also important to decrease the intracellular concentration of dUTP [26], which can be incorporated into DNA, affecting the genome integrity, as the availability of dTTP is insufficient to prevent uracil integration during DNA synthesis [25]. Most DNA polymerases cannot distinguish between thymine and uracil, so the incorporation ratios of the nucleotides is defined by the relative level of the respective dNTPs (dUTP/dTTP) [26]. It was shown by Wang and Weiss that *E. coli dut* mutants, which should accumulate dUTP, incorporate large amounts of uracil into DNA, which is toxic [25]. The accumulation of dUTP leads to the incorporation of high levels of uracil into DNA, which is lethal, since under high dUTP/dTTP ratio thymine-replacing uracils will be reincorporated by repair enzymes. Moreover, this continuous uracil repair cycle leads to cell death, since the double-stranded DNA is subjected to degradation [26, 31, 32].

Moreover, dUTPase enzyme activity also has an important role, as dUTP is an obligatory precursor for thymidylate biosynthesis in *E. coli* [25]. The hydrolysis of dUTP catalyzed by either the bifunctional *dcd*-encoded dCTP deaminase:dUTPase enzyme or *dut*-encoded dUTPase enzyme in *M. tuberculosis* leads to dUMP formation, a precursor for thymidylate biosynthesis. Neither dCMP deaminase (that converts dCMP into dUMP) nor thymidine kinase (that catalyzes the conversion of thymidine into dTMP) enzymes were identified in the MTB genome [33]. Thereby, the obtainment of thymidylate has no alternative pathway but bifunctional dCTP deaminase:dUTPase and dUTPase enzymes followed by thymidylate synthase [26, 33]. Therefore, dUTPase is a promising drug target against tuberculosis.

Recombinant dUTPase from MTB was expressed in *E. coli*, and purified and characterized both functionally and structurally [32, 33]. The crystal structure of MTB dUTPase was determined in complex with magnesium ion and the non-hydrolysable substrate analog, α,β-imino dUTP (PDB access codes: 1SIX, 1SJN) [32, 33]. dUTPases are mostly homotrimeric enzymes with five conserved sequence motifs among MTB*, E. coli*, human, equine infectious anemia virus, and feline immunodeficiency virus enzymes [32]. The five motifs (from I to V) and all the three monomers of dUTPase form each enzyme active site and also interact with the ligand [32, 33]. For instance, the interactions between MTB dUTPase and α,β-imino dUTP involve motifs I, II, and IV from monomer 1 that

contribute to the triphosphate moiety binding; motif III from monomer 2 contributes to the nucleoside moiety binding; and motif V from monomer 3 is involved in a hydrogen bond between the phosphate moiety of the ligand and an arginine residue [32].

Owing to the importance of dUTPase biological role, the therapeutic use of its inhibitors has been proposed for cancer chemotherapy and as antiviral, antimalarial, and anti-TB agents [32, 34, 35]. However, the high degree of sequence and structure similarity between dUTPases from different sources is a concern, as the therapeutic use of inhibitors for the pathogen dUTPase to treat human diseases might also inhibit the human enzyme. For instance, the human dUTPase shares a 34% sequence identity with MTB enzyme [32]. The exploitation of structural differences between the human and the pathogen enzymes is essential to establish selectivity in drug design.

## 2.3. Thymidylate Synthase

Thymidylate synthase (encoded by *thyA* gene, 792 bp, MTB Rv2764c, EC 2.1.1.45, 263 aa, 29,820.8 Da, and PI = 5.54) catalyzes the reductive methylation of dUMP by 5,10-methylenetetrahydrofolate (CH$_2$H$_4$ folate) to produce dTMP and dihydrofolate (H$_2$ folate) (Fig. **4**). This enzyme participates both in pyrimidines' *de novo* and salvage pathways. Its inhibition causes not only the reduction of dTTP levels but also the accumulation of dUMP, which leads to dUTP synthesis by dUTPase [36]. The increase of dUTP concentration causes its incorporation into DNA and cell death, as described previously. This cytotoxic effect is usually decreased by thymidine kinase, which converts thymidine into dTMP, and helps increase dTTP levels [37]. However, thymidine kinase was not identified in the MTB genome by sequence homology, underscoring the essentiality of thymidylate synthase in this pathogen [38]. Thus, owing to its important role in DNA synthesis, thymidylate synthase is an attractive target for antiproliferative and infectious disease drug design.

The enzyme is widely used either clinically or experimentally as a target for anticancer drugs, such as Raltitrexed (ZD1694, Tomudex), Nolatrexed (AG337), Pemetrexed (LY231514), and 5-FU [37]. 5-FU is a prodrug that inhibits thymidylate synthase via the metabolite FdUMP. This enzyme is also a good target for drugs against infectious diseases [39]. However, the high conserved amino acid sequence among sources within the active site complicates the design of a selective inhibitor for the bacterial enzyme within the substrate binding site. So, the strategy to find an inhibitor to be used against infectious diseases should take advantage of the different features between the bacterial and the human enzymes [39, 40]. As described in a few works, analogues of phenolphthalein were shown to be a family of folate-independent inhibitors of thymidylate synthase from *Lactobacillus casei* [41, 42]. An analogue of phenolphthalein was found to inhibit only the *L. casei*
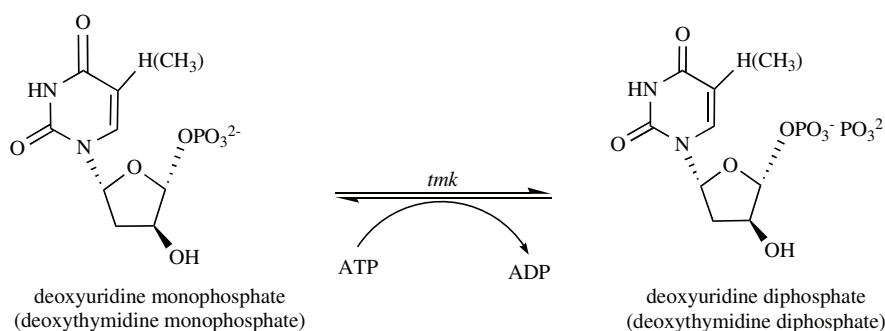
**Fig. (5).** Chemical reaction catalyzed by dTMP kinase (*tmk*). The enzyme catalyzes the phosphorylation of dTMP to form dTDP using ATP as the phosphoryl donor. MTB dTMP kinase uses both dUMP and dTMP as substrate.

enzyme due to inhibitor interactions with the enzyme residues Glu84, Trp85, Glu88, and the "small domain" (residues 90-139), which are not present in the human enzyme [39]. This inhibitor was shown to be 40-fold more selective for *L. casei* enzyme than compared to human thymidylate synthase and had 6-fold higher affinity than phenolphthalein [39]. Moreover, some phthalein derivatives from the lead compound phenolphthalein were found to have higher activity and specificity against thymidylate synthase from bacterial organisms, such as *L. casei*, *Pneumocystis carinii* or *Cryptococcus neoformans*, than to the human enzyme [40]. Accordingly, the discovery of specific inhibitors of MTB thymidylate synthase enzyme is in the realm of possibility. With that in mind, the *thyA* gene from MTB was cloned, expressed in *E. coli*, the recombinant protein purified, and its kinetic and inhibition properties determined [43]. Moreover, *thyA* was compared by its kinetics and ligand-preferences with the *thyX* gene, which encodes a flavin-dependent thymidylate synthase, another interesting target for drug design against TB, since *thyX* is absent in humans [43].

The folate analogue 1843U89 and the nucleotide analogue FdUMP were found to inhibit MTB thymidylate synthase [43]. FdUMP was shown to inhibit this enzyme with a $K_i$ of 2 nM, and 1843U89 inhibited the same enzyme with a $K_i$ of 18 nM [43]. Furthermore, thymidylate synthase from *Plasmodium falciparum* was also found to be inhibited by 1843U89 in a noncompetitive manner with a $K_i$ of 1 nM [44]. The mammalian enzyme was also shown to be inhibited by 1843U89 (known as OSI-7904) within a liposomal formulation in combination with cisplatin, which was evaluated in adults with advanced solid tumors and revealed a preliminary clinical activity against breast and gastric cancer [45]. The human thymidylate synthase is a well-established target for both FdUMP and 1843U89; as a result, these inhibitors are not selective agents for the treatment of TB. Novel inhibitors with selectivity against the enzyme from MTB could be found by employing a strategy similar to that used to find specific inhibitors to other bacterial enzymes, by focussing on the structural and functional differences between human and MTB enzymes.

**2.4. Nucleoside Monophosphate Kinases**

Nucleoside monophosphate kinases (NMP kinases) are key enzymes in the metabolism of ribo- and deoxyribonucleoside triphosphates, catalyzing the reversible γ-phosphoryl transfer from a nucleoside triphosphate (usually ATP) to a specific nucleoside monophosphate to generate nucleoside diphosphate and usually ADP [46]. The resulting nucleoside diphosphates are further phosphorylated (and eventually reduced) to produce nucleoside triphosphates, precursors of the major biological molecules: DNA, RNA, and phospholipids. NMP kinases are composed of three domains: the core, LID (that closes upon binding of the phosphate donor ATP), and NMP-binding (that closes the active site upon binding of the phosphate acceptor) domains [47]. In eukaryotes, phosphorylation

of UMP and CMP is carried out by a single enzyme (UMP-CMP kinase) that phosphorylates UMP and CMP with higher efficiency than dCMP [48, 49]. Conversely, bacteria possess two distinct enzymes, uridine monophosphate kinase (UMP kinase) and cytidine monophosphate kinase (CMP kinase), specific to either UMP or CMP, respectively [50]. Moreover, bacteria have a specific enzyme for dTMP, deoxythymidine monophosphate kinase (dTMP kinase), which also uses dUMP as substrate.

**2.4.1. Deoxythymidine Monophosphate Kinase**

dTMP kinase, also known as thymidylate kinase and thymidylic acid kinase (encoded by *tmk* gene, 645 bp, MTB Rv3247c, EC 2.7.4.9, 215 aa, 22,602.4 Da, and PI = 7.67), catalyzes the phosphorylation of dTMP to form dTDP using ATP as the phosphoryl donor (Fig. **5**). It also utilizes dUMP as substrate (Fig. **5**), but with lower affinity than dTMP [51]. dTMP kinase is involved in both *de novo* and salvage pathways of dTTP synthesis. The enzyme from *Saccharomyces cerevisiae* was shown to be essential for yeast DNA replication [52, 53], as maintenance of dTTP pools is crucial for DNA synthesis and cellular growth [54, 55].

Structure and catalytic properties of dTMP kinases are shown to be variable between different organisms. A structural model for dTMP kinase from MTB based on the solved three-dimensional structures of yeast and *E. coli* enzymes was proposed; it seems that the overall fold described is conserved among these organisms, but there are some differences at the level of primary and tertiary structures [56]. At the level of primary structure, a sequence comparison of dTMP kinase from MTB with *E. coli* and yeast enzymes shared 23% of sequence identity with both [56]. Moreover, a sequence comparison between dTMP kinase from MTB with the human enzyme revealed 22% sequence identity [57]. Although the primary structure of dTMP kinase from MTB showed a low sequence identity when compared with yeast, *E. coli* or human amino acid sequences, dTMP kinase residues involved in substrate binding and catalysis are mostly conserved [56].

dTMP kinases possess a similar structure to the NMP kinase enzymes, which contain a sequence motif called the P-loop and a region called LID, whose functions are to bind phosphates in the active site [58, 59]. The differences in the P-loop and LID sequences led to the characterization of two types of dTMP kinases based on its ability to phosphorylate azidothymidine monophosphate (AZT-MP), which is an intermediate from 3'-azido-3'-deoxythymidine (AZT), a prodrug used in the treatment of AIDS [58, 59]. Type I dTMP kinases, such as the human and yeast enzymes, have a basic residue in their P-loop sequence that interacts with the γ-phosphate from ATP and lack this residue in the LID region [59]. Type II dTMP kinases, such as *E. coli* enzyme, have a glycine residue in the P-loop and basic residues in the LID region that interact with ATP and stabilize the transition state [59]. On the other hand, MTB dTMP kinase has basic residues such as arginines in both P-loop and LID sequences, which suggests a "chimeric"
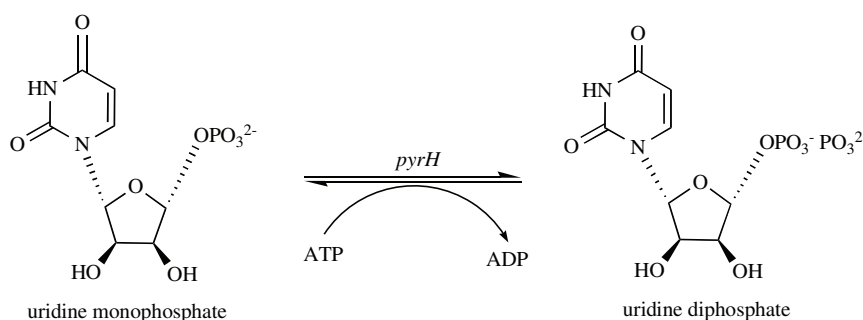
**Fig. (6).** Chemical reaction catalyzed by UMP kinase (*pyrH*). The enzyme catalyzes the phosphorylation of UMP to form UDP using ATP as the phosphoryl donor.

nature for the MTB enzyme when compared to *E. coli* and yeast enzymes [56]. Furthermore, AZT-MP acts as a substrate for both dTMP kinases from yeast and *E. coli*, but behaves as a competitive inhibitor of the MTB enzyme [56, 60]. dTMP kinase is, therefore, an attractive target for the development of specific drugs against TB based on subtle structural differences among similar proteins.

With that in mind, the three-dimensional structure of MTB dTMP kinase was determined in complex with the substrate dTMP at 1.94 Å resolution [54]. MTB dTMP kinase is a homodimer with 214 amino acids per monomer [56]. Structure determination enables analysis of the interactions between dTMP and the enzyme, providing information towards the development of novel inhibitors to be used as anti-TB agents. Thus, a series of nucleotides with modifications at the pyrimidine ring and/or at the sugar ring were analysed in order to find inhibitors and to establish a structure activity relationship [51, 57, 61]. Replacement of carbon-5 methyl group of the pyrimidine ring of dTMP by halogen atoms, such as fluorine, bromine, and iodine, turned out to be substrates for MTB dTMP kinase [57]. On the other hand, replacement of carbon-5 methyl group by bulky functional groups that significantly perturb the volume at this position behaved as inhibitors [61]. Moreover, the sugar-modified dTMP analogues, resultant of the introduction of 2'-chloro or replacement of 3'-OH by an azido group (AZT-MP), lead to inhibition of the enzyme with $K_i$ values of 19 μM and 10 μM, respectively [57]. The crystal structure of MTB dTMP kinase in complex with AZT-MP (PDB access code: 1W2H) indicates that the presence of the azido moiety prevents the binding of $Mg^{2+}$ ion, which is essential for catalysis [60]. Based on these findings, MTB inhibitors have been extensively studied. For instance, a bicyclic sugar nucleoside (compound 9) [62] was shown to be a good inhibitor of MTB dTMP kinase, with a $K_i$ value of 2.3 μM; it also displays inhibitory potency against the growth of MTB cultures [62]. In addition, a 5'-arylthiorea α-thymidine analogue (compound 15) [63] inhibited MTB dTMP kinase activity with a $K_i$ value of 0.6 μM and showed a selectivity index (versus human dTMP kinase) of 600 and low cytotoxicity [63]. An acyclic nucleoside analogue having a naphthosultam ring bound to a (*Z*)-butenyl spacer, which in turn is bound to N1 of the thymine base was shown to inhibit MTB dTMP kinase enzyme activity with a $K_i$ value of 0.27 μM [55], which was the most potent inhibitor of the MTB enzyme reported to date.

### 2.4.2. Uridine Monophosphate Kinase

UMP kinase, also known as uridylate kinase (encoded by *pyrH* gene, 786 bp, MTB Rv2883c, EC 2.7.4.-, 261 aa, 27,429.5 Da, and PI = 4.93), catalyzes the phosphorylation of UMP to form UDP using ATP as the phosphoryl donor (Fig. **6**). Bacterial UMP kinase does not display significant sequence similarity with the NMP kinase family, such as the eukaryotic UMP-CMP kinase enzyme [64]. Moreover, UMP kinases of eukaryotic origin are monomeric proteins that possess significant structural differences when compared with the overall fold of the prokaryotic UMP kinase mono-

mer [65]. Actually, UMP kinase demonstrated sequence similarity with aspartokinases (approximately 30% of sequence identity) and glutamate kinases or carbamate kinases (approximately 20% of sequence identity) [64, 66]; but the monomer fold of UMP kinase belongs to the carbamate kinase superfamily [66]. UMP kinases from prokaryotes such as *E. coli* [64], *Bacillus subtilis* [67], and *Sulfolobus solfataricus* [68] were shown to be hexamers and were inhibited by UTP, but only the *E. coli* and *B. subtilis* enzymes were shown to be allosterically activated by GTP. Superposition of the *E. coli* UMP kinase structure with that of archaeal UMP kinases demonstrates that a loop appears to interfere with GTP binding in archaeal enzymes, such as the one from *S. solfataricus* [69].

Some differences between UMP kinase from Gram-negative and Gram-positive organisms were observed. First, only UMP kinases from Gram-positive species, such as *Streptococcus pneumoniae*, exhibited cooperative kinetics with ATP as substrate [70, 71]. Second, in Gram-positive bacteria, inhibition of UTP is not sensitive to high concentrations of $Mg^{2+}$ or UMP, whereas the UTP inhibition in Gram-negative organisms is sensitive [70]. Third, in Gram-positive species, GTP and UTP were found to bind at the same binding site, while in Gram-negative organisms the GTP binding site is situated at an allosteric site, whereas the UTP binding site is situated at the active site or catalytic center [72]. However, the amino acid residues involved in substrate binding and catalysis were shown to be conserved among all bacterial UMP kinases [70].

UMP kinase from both Gram-negative species, such as *E. coli* [73], and Gram-positive species, such as *S. pneumoniae* [71], were shown to be essential for cell growth. Furthermore, the *pyrH* gene, encoding MTB UMP kinase was shown to be essential for infection or growth of the TB bacilli, which is an important finding to validate drug targets [74]. Thus, owing to the essentiality of *pyrH*, and the amino acid sequence and structural differences between the prokaryotic UMP kinase and the eukaryotic UMP-CMP kinase, the enzyme from MTB is a potential anti-TB drug target. Accordingly, we have recently cloned, expressed, purified, and kinetically characterized functional MTB UMP kinase (unpublished results).

### 2.4.3. Cytidine Monophosphate Kinase

CMP kinase, also known as cytidylate kinase (encoded by *cmk* gene, 693 bp, MTB Rv1712, EC 2.7.4.14, 230 aa, 24,145.2 Da, and PI = 4.83), catalyzes the phosphoryl transfer from ATP to dCMP or CMP (Fig. **7**). Although bacterial UMP kinase does not possess amino acid sequence and structural similarities with NMP kinase enzymes, residues involved in the binding of substrates and/or in catalysis of NMP kinase enzymes were found to be conserved among bacterial CMP kinases [75]. Moreover, a sequence comparison between CMP kinase and NMP kinase enzymes demonstrates conservation of the global fold found in adenylate kinases and in several CMP/UMP kinases [75].
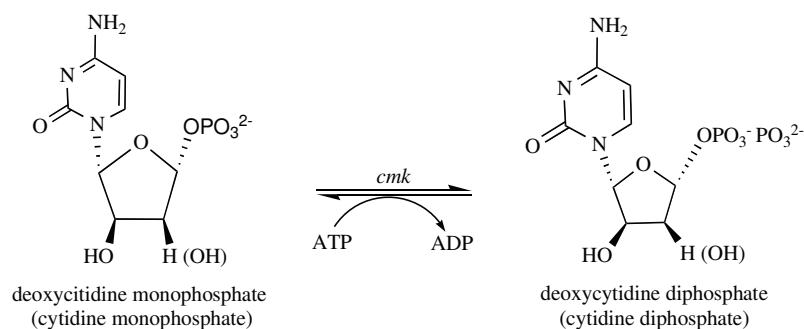
**Fig. (7).** Chemical reaction catalyzed by CMP kinase (*cmk*). The enzyme catalyzes the phosphorylation of CMP to form CDP using ATP as the phosphoryl donor. MTB CMP kinase uses both CMP and dCMP as subtrates.
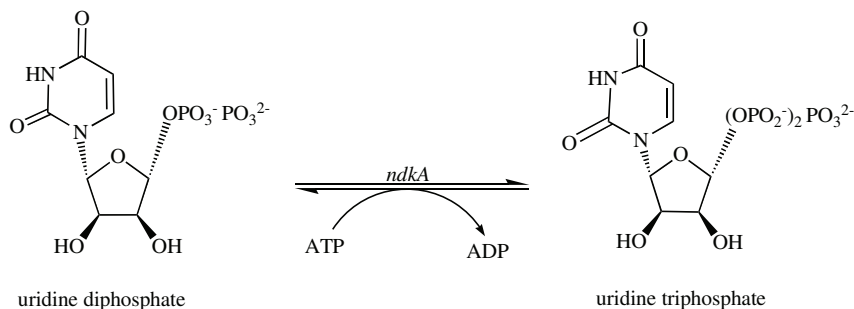


**Fig. (8).** Chemical reaction catalyzed by NDK (*ndkA*). The enzyme catalyzes the phosphorylation of nucleoside diphosphate to form nucleoside triphosphates using ATP as the phosphoryl donor. MTB NDK uses UDP, dUDP, CDP, dCDP, and dTDP as substrates.

The crystal structure of *E. coli* CMP kinase (PDB access code: 1CKE) resembles those of other NMP kinases sharing common features such as a central five-stranded β-sheet connected by α-helices, a fingerprint sequence of Glu-X-X-Gly-X-Gly-Lys (P-loop), and an anion hole in the central cavity for substrate binding [76]. Classically, NMP kinases are divided into short (including eukaryotic UMP-CMP kinases) and long forms. The latter group consists of adenylate kinases with an insertion of approximately 27 residues into the LID domain [50]. Bacterial CMP kinases represent a third distinct family of NMP kinases, as they possess a short LID domain but have an insertion of 40 amino acid residues in the NMP-binding domain [76]. These structural differences could be exploited in the development of novel inhibitors targeted specifically towards MTB CMP kinase enzyme.

CMP kinase has been shown to be essential for the growth of two Gram-positive bacteria: *B. subtilis* [77] and *Streptococcus pneumoniae* [78]. In addition, it has been proposed that CMP kinase is essential for *in vitro* growth of MTB, based on transposon site hybridization studies [79]. However, this approach is simply a screening tool and *cmk* gene replacement must be carried out to assign an essential role to its protein product. Accordingly, MTB CMP kinase was recently PCR amplified, cloned, expressed, and purified to homogeneity, and steady-state kinetic analysis showed that the enzyme preferentially phosphorylates CMP and dCMP and that UMP is a poor substrate [80]. Moreover, based on the tertiary structure of the MTB CMP kinase apoenzyme, predicted by molecular modeling using the crystallographic structure of *E. coli* CMP kinase as a template, it was suggested that the mode of action of the MTB enzyme may be similar to that of MTB shikimate kinase [81]. These structural and functional studies should aid in the design of chemical compounds capable of inhibiting MTB CMP kinase enzyme activity.

### 2.5. Nucleoside Diphosphate Kinase

Nucleoside diphosphate kinase (NDK), also known as NDP kinase and nucleoside-2-P kinase (encoded by *ndkA* gene, 411 bp,

MTB Rv2445c, EC 2.7.4.6, 136 aa, 14,475.4 Da, and PI = 5.18) catalyzes the phosphorylation of nucleoside diphosphate to form nucleoside triphosphate, using usually ATP as the phosphoryl donor (Fig. **8**). Besides the phosphotransferase activity of MTB NDK, it also possesses divalent cation-dependent autophosphorylation for which His117 was found to be essential and conserved between species [82, 83]. On the other hand, each His residue at positions 49, 53, and 117 were shown to have phosphotransferase activity independently [82]. NDK has a low specificity for the utilization of either purine or pyrimidine ribonucleoside or deoxyribonucleoside diphosphates as substrates [84]. Thus, it is involved in the production of dNTPs/NTPs, which are important for DNA/RNA synthesis, cell division, macromolecular metabolism, and growth [85]. Moreover, MTB NDK has been reported to be involved in several regulatory processes, such as mycobacterial survival within the macrophage [86] and establishment of MTB infection, as it may help in the dissemination of the bacilli and evasion of the host immune system [82].

The crystal structure of the NDK from MTB (PDB access code: 1K44) was determined at 2.6 Å resolution [87]. It was shown that the MTB and the human B NDK enzymes share 45% of sequence identity over the 135 common residues [87]. Furthermore, the subunit fold of MTB NDK was very similar to the human NDK B, the product of the *nm23-H2* gene [88], which is based on the αβ sandwich or ferredoxin fold [87, 89]. Ferredoxin fold has three specific features: a surface α-helix hairpin and the Knp loop, which are involved in the nucleotide binding, and the C-terminal extension, which is involved in the quaternary structure [89, 90]. However, C-terminal residues 138-152 of the human B NDK are absent in MTB enzyme [87, 91]. Although NDK enzymes have a similar fold and highly conserved amino acid sequence, some bacterial enzymes were found to be tetramers, such as *Myxococcus xanthus* [92, 93], whereas human [89] and MTB [87] enzymes formed hexamers. The amino acid residues of NDK active site and the subunit fold are identical between species and independent of the oligomeric state from bacteria to man [89]. Owing to the structural similarity between bacteria and human NDK enzymes, it may be
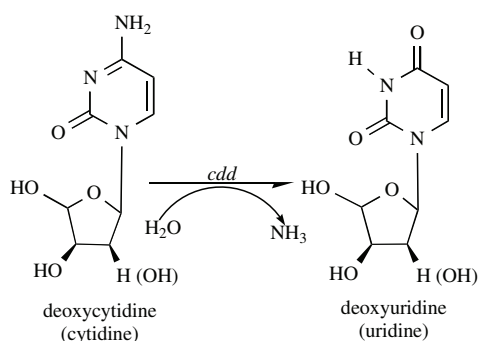
**Fig. (9).** Chemical reaction catalyzed by CDA (*cdd*). The enzyme catalyzes the hydrolytic deamination of cytidine and 2'-deoxycytidine to uridine and 2'-deoxyuridine, respectively.

very difficult to find NDK specific inhibitors for the bacterial enzyme.

### 2.6. Cytidine Deaminase

Cytidine deaminase (CDA), also known as cytidine aminohydrolase and cytidine nucleoside deaminase (encoded by *cdd* gene, 402 bp, MTB Rv3315c, EC 3.5.4.5, 133 aa, 14,071.1 Da, and PI = 6.08) belongs to a family of enzymes that catalyze the hydrolytic deamination of cytidine and 2′-deoxycytidine to uridine and 2′-deoxyuridine, respectively (Fig. **9**) [94]. Biochemical and structural studies of CDA from different organisms have led to the understanding of the enzyme reaction mechanism. CDA contains a zinc atom on the active site which possesses important functions. The active-site zinc ion, which is essential for catalysis, is coordinated to an active-site water/hydroxide nucleophilic group [95]. A conserved glutamate is envisaged to promote the initial attack at C4 of cytosine ring by protonating the adjacent N3-position and deprotonating the nucleophilic water, then again using general acid/base chemistry to facilitate breakdown of the tetrahedral intermediate [95]. The N-terminal core domain provides pyrimidine nucleoside and zinc-binding pockets, and the structurally homologous C-terminal core domain in the other monomer covers the active-site, completely sequestering the ligand from solvent [96-98].

Different oligomeric states were observed among CDAs from diverse species; for instance, CDA from *E. coli* was shown to be a homodimeric enzyme that possesses two active sites per dimer formed in the subunit interface. On the other hand, homotetrameric CDA enzymes have been observed in some organisms, such as *B. subtilis*, which contains one zinc atom per enzyme subunit [99], *S. cerevisiae* [100], and human CDA, where each subunit possesses one active site [101].

The *cdd* gene was identified in the genome of the MTB H37Rv strain by sequence homology [13]. MTB *cdd* was cloned and the protein was expressed in *E. coli*, purified and kinetically characterized [102]. The MTB CDA characterization provided experimental evidence that the *in silico* predicted *cdd* gene codes for a functional CDA enzyme in MTB [102]. Moreover, structural studies revealed that MTB CDA (PDB access code: 3IJF) possesses a homotetrameric structure in which each monomer comprises a single domain, and, as previously observed for the CDA from *B. subtilis* [99], the MTB CDA contained one zinc atom per subunit coordinated by three cysteines [102]. Tetrameric CDA enzymes are found in both prokaryotes and eukaryotes, and according to structural studies, it appears that tetrameric CDAs are more widely distributed among species. Furthermore, the structure of the two known oligomeric states of CDA suggest that tetrameric CDAs are constructed in the same way as dimeric CDAs, with the structural core formed from four identical subunits placed in relation to each other as in the catalytic and C-terminal domains of dimeric CDAs.

CDA is also known as APOBEC protein which possesses a role in the deamination of single-stranded DNA or RNA. Thus, the activation-induced cytidine deaminase (AID) enzyme is required for antibody affinity maturation in active germinal B cells. AID presumably initiates somatic hypermutation by introducing deoxycytidine to deoxyuridine mutations in the VDJ region of the immunoglobulin gene [103, 104]. Additionally, CDA plays an important role in the metabolism of a number of analogues of cytosine nucleoside used as antitumoral and antiviral agents, leading to their pharmacological inactivation [105]. Thus, CDA is an interesting (and intriguing) target to the development of inhibitors through the rational drug design for therapeutic use and to the understanding of its role in the biology of *M. tuberculosis*.

### 2.7. Pyrimidine Nucleoside Phosphorylase

Pyrimidine nucleoside phosphorylase (PyNP), also known as pyrimidine phosphorylase and thymidine phosphorylase (encoded by *deoA* gene, 1284 bp, MTB Rv3314c, EC 2.4.2.4, 427 aa, 44,453.9 Da, and PI = 6.96) catalyzes the reversible phosphorolysis of pyrimidine nucleosides. The catalysis of glycosidic bond cleavage between atom N1 of the pyrimidine base and atom C1' of sugar deoxynucleoside in the presence of inorganic phosphate ($P_i$) leads to the production of free pyrimidine base and D-2-deoxyribose-1-phosphate (dRP; Fig. **10**) [106].

Some organisms, including mammals and several bacteria such as *E. coli*, have two distinct PyNPs: uridine phosphorylase (UP) and thymidine phosphorylase (TP). UP, a member of the nucleoside phosphorylase I (NP-I) family, is specific to uridine nucleosides, but it also accepts 2'-deoxypyrimidine nucleosides. TP, a member of the nucleoside phosphorylase II (NP-II) family, is highly specific for 2'-deoxyribonucleosides of thymidine [106-108]. TP and UP have been characterized from a wide variety of species and tissues, such as mouse liver [109], horse liver [110], *E. coli* [111], and *L. casei* [112]. The main difference between TP and UP enzymes was shown to be the high specificity of TP for the 2'-deoxyribose moiety.

On the other hand, other organisms, such as *Bacillus stearothermophilus* [113] and *Haemophilus influenzae* [114], pos-
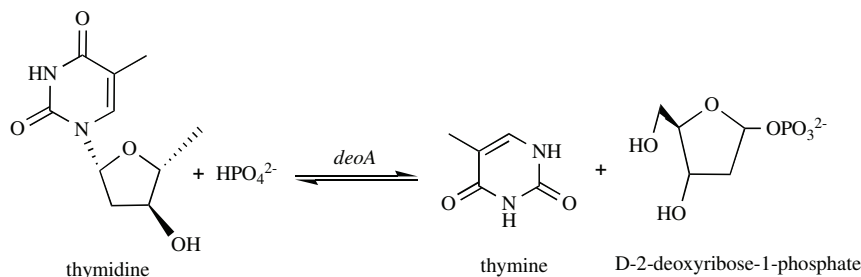


**Fig. (10).** Chemical reaction catalyzed by PyNP (*deoA*). The enzyme catalyzes the reversible phosphorolysis of pyrimidine nucleosides, thymidine or deoxyuridine, in the presence of $P_i$ to form the free pyrimidine base, thymine or uracil, respectively, and deoxyribose-1-phosphate.
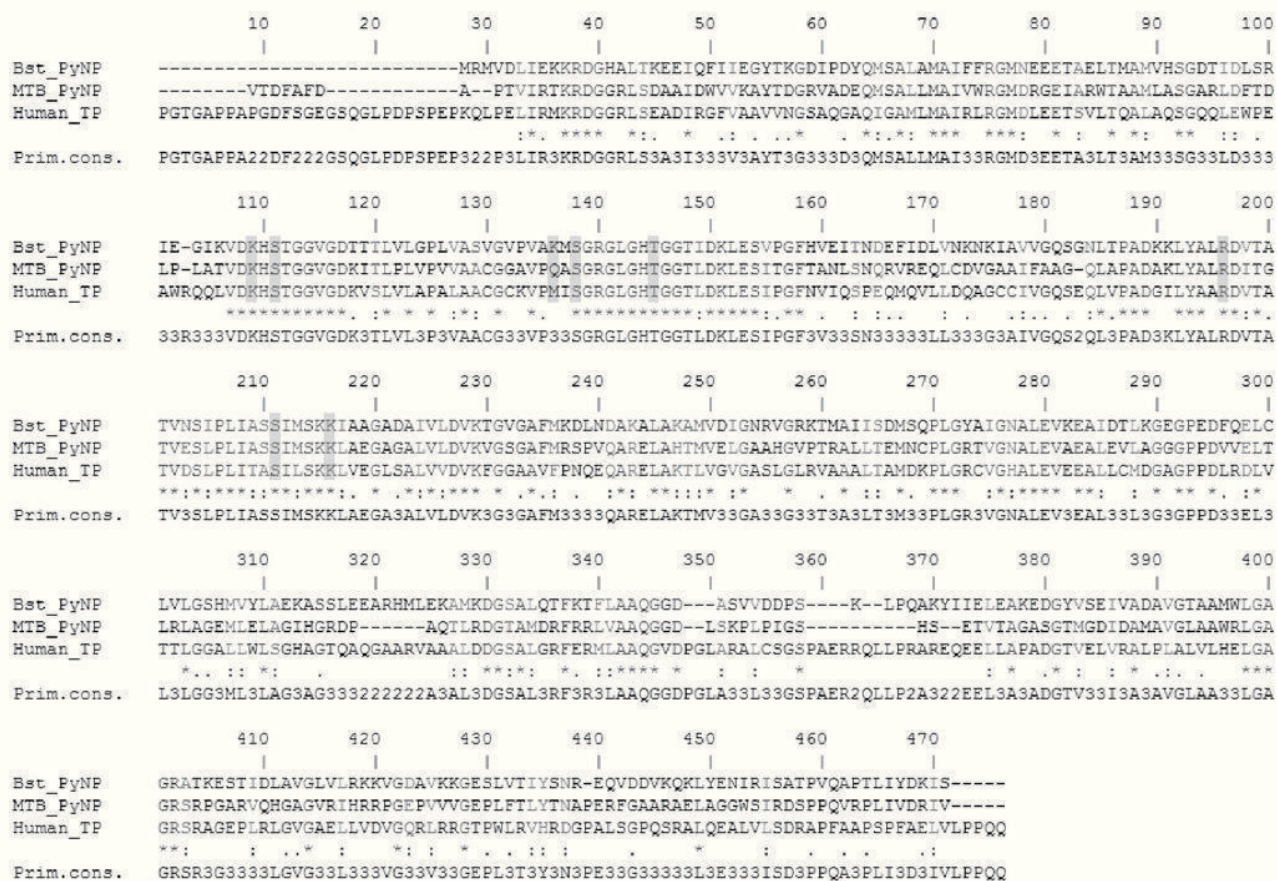
```
              10        20        30        40        50        60        70        80        90        100
               |         |         |         |         |         |         |         |         |         |
Bst_PyNP    ---------------------------MRMVDLIEKKRDGHALTKEEIQFIIEGYTKGDIPDYQMSALAMAIFFRGMNEEETAELTMAMVHSGDTIDLSR
MTB_PyNP    --------VTDFAFD------------A--PTVIRTKRDGGRLSDAAIDWVKAYTDGRVADEQMSALLMAIVWRGMDRGEIARWTAAMLASGARLDFTD
Human_TP    PGTGAPPAPGDFSGEGSQGLPDPSPEPKQLPELIRMKRDGGRLSEADIRGFVAAVVNGSAQGAQIGAMLMAIRLRGMDLEETSVLTQALAQSGQQLEWPE
Prim.cons.  PGTGAPPA22DF222GSQGLPDPSPEP322P3LIR3KRDGGRLS3A3I333V3AYT3G333D3QMSALLMAI33RGMD3EETA3LT3AM33SG33LD333

              110       120       130       140       150       160       170       180       190       200
               |         |         |         |         |         |         |         |         |         |
Bst_PyNP    IE-GIKVDKHSTGGVGDTTILVLGPLVASVGVPVAKMSGRGLGHTGGTIDKLESVPGFHVEITNDEFIDLVNKNKIAVVGQSGNLTPADKKLYALRDVTA
MTB_PyNP    LP-LATVDKHSTGGVGDKITLPLVPVVAACGGAVFQASGRGLGHTGGTLDKLESITGFTANLSNQRVREQLCDVGAAIFAAG-QLAPADAKLYALRDITG
Human_TP    AWRQQLVDKHSTGGVGDKVSLVLAPALAACGCKVPMISGRGLGHTGGTLDKLESIPGFNVIQSPEQMQVLLDQAGCCIVGQSEQLVPADGILYAARDVTA
Prim.cons.  33R333VDKHSTGGVGDK3TLVL3P3VAACG33VP33SGRGLGHTGGTLDKLESIPGF3V33SN33333LL333G3AIVGQS2QL3PAD3KLYALRDVTA

              210       220       230       240       250       260       270       280       290       300
               |         |         |         |         |         |         |         |         |         |
Bst_PyNP    TVNSIPLIASSIMSKKIAAGADAIVLDVKTGVGAFMKDLNDAKALAKAMVDIGNRVGRKTMAIISDMSQPLGYAIGNALEVKEAIDTLKGEGPEDFQELC
MTB_PyNP    TVESLPLIASSIMSKKLAEGAGALVLDVKVGSGAFMRSPVQARELAHTMVELGAAHGVPTRALLTEMNCPLGRTVGNALEVAEALEVLAGGGPPDVVELT
Human_TP    TVDSLPLITASILSKKLVEGLSALVVDVKFGGAAVFPNQEQARELAKTLVGVGASLGLRVAAALTAMDKFPLGRCVGHALEVEEALLCMDGAGPPDLRDLV
Prim.cons.  TV3SLPLIASSIMSKKLAEGA3ALVLDVK3G3GAFM3333QARELAKTMV33GA33G33T3A3LT3M33PLGR3VGNALEV3EAL33L3G3GPPD33EL3

              310       320       330       340       350       360       370       380       390       400
               |         |         |         |         |         |         |         |         |         |
Bst_PyNP    LVLGSHMVYLAEKASSLEEARHMLEKAMKDGSALQTFKTFLAAQGGD---ASVVDDPS----K--LPQAKYIIELEAKEDGYVSEIVADAVGTAAMWLGA
MTB_PyNP    LRLAGEMLELAGIHGRDP------AQTLRDGTAMDRFRRLVAAQGGD--LSKPLPIGS-----------HS--ETVTAGASGTMGDIDAMAVGLAAWRLGA
Human_TP    TTLGGALLWLSGHAGTQAQGAARVAAALDDGSALGRFERMLAAQGVDPGLARALCSGSPAERRQLLPRAREQEELLAPADGTVELVRALPLALVLHELGA
Prim.cons.  L3LGG3ML3LAG3AG333222222A3AL3DGSAL3RF3R3LAAQGGDPGLA33L33GSPAER2QLLP2A322EEL3A3ADGTV33I3A3AVGLAA33LGA

              410       420       430       440       450       460       470
               |         |         |         |         |         |         |
Bst_PyNP    GRATKESTIDLAVGLVLRKKVGDAVKKGESLVTIYSNR-EQVDDVKQKLYENIRISATPVQAPTLIYDKIS-----
MTB_PyNP    GRSRPGARVQHGAGVRIHRRPGEPVVVGEPLFTLYTNAPERFGAARAELAGGWSIRDSPPQVRPLIVDRIV-----
Human_TP    GRSRAGEPLRLGVGAELLVDVGQRLRRGTPWLRVHRDGPALSGPQSRALQEALVLSDRAPFAAPSPFAELVLPPQQ
Prim.cons.  GRSR3G3333LGVG33L3333VG33V33GEPL3T3Y3N3PE33G33333L3E333ISD3PPQA3PLI3D3IVLPPQQ
```

**Fig. (11).** Multiple sequence alignment of MTB PyNP with *B. stearothermophilus* PyNP (Bst_PyNP) and human TP (Human_TP). Identical conserved residues are identified in gray and are also indicated by asterisk below the alignment.

sess only one PyNP enzyme, which accepts both thymidine and uridine as substrates and does not have selectivity for either ribonucleosides or deoxyribonucleosides. This enzyme was classified as a member of the NP-II family [115]. According to amino acid sequence alignments, MTB PyNP shares 40% of sequence identity with human TP and 43% with *B. stearothermophilus* PyNP (Fig. **11**); the MTB enzyme also possesses high sequence homology with other bacteria, such as *H. influenzae*. The crystal structure of PyNP from *B. stearothermophilus* (PDB access code: 1BRW) demonstrates that the protein is an asymmetric dimer and the enzyme active site is between the two subunits [116]. The amino acid sequence of PyNP from *B. stearothermophilus* shared significant similarity with those of human, *E. coli* TP, and MTB PyNP [116]. Structurally, the active site is composed of a phosphate binding site and a (deoxy)ribonucleoside binding site within the cleft region, which is highly conserved between TP and PyNP enzymes of the NP-II group [116]. Amino acid residues from the active site that interact with phosphate include Lys109, Ser111, Lys 136, Ser138, and Thr148; and residues that interact with the pyrimidine nucleoside moiety include Arg196, Ser211, and Lys216 [116]. According to the alignment shown in Fig. (**11**), these residues which are involved in substrate binding are conserved in MTB PyNP and human TP. Sequence comparison between the active site amino acid residues of *B. stearothermophilus* and MTB enzymes reveals only one difference in residue 136, which has been proposed to mediate substrate specificity. MTB PyNP amino acid position 136 is occupied by a glutamine instead of a lysine in *B. stearothermophilus* enzyme, and this replacement by similar amino acid residues keeps an interaction between MTB PyNP active site and ribose [117].

PyNP is widely studied for the design of inhibitors because it is considered an important chemotherapeutic target for cancer, as some tumor cells depend heavily on this pathway for their proliferation [118, 119]. Moreover, PyNP is an attractive target to the design of novel inhibitors to be used in the treatment of TB. Accordingly, MTB PyNP was recently cloned, expressed, purified, and characterized by our research group (unpublished results).

## 2.8. Uracil Phosphoribosyltransferase

Uracil phosphoribosyltransferase (UPRTase), also known as UMP pyrophosphorylase and UMP diphosphorylase (encoded by *upp* gene, 624 bp, MTB Rv3309c, EC 2.4.2.9, 207 aa, 21,866.1 Da, and PI = 4.73) catalyzes the conversion of uracil and 5'-phosphoribosyl-α-1'-pyrophosphate (PRPP) to UMP and $PP_i$ (Fig. **12**). UPRTase is a key enzyme in the pyrimidine salvage pathway as it allows direct reutilization of uracil bases. Uridine nucleosidase and uridine phosphorylase, which catalyze the conversion of uracil to uridine, were not found in the MTB genome [13]. In addition, uridine kinase and uridine monophosphatase, which convert uridine to UMP, were also not found in the MTB genome [13]. UPRTase appears thus to play an important role in the pyrimidine salvage pathway, since it is the only operative enzyme that converts preformed pyrimidine bases to the nucleotide level.

UPRTase is a member of type I phosphoribosyl transferases, which share a characteristic fold consisting of a core region with a flexible loop and a hood [120]. The core region comprises 5 parallel β-strands and at least 3 α-helices [121]. The hood provides the residues required for binding of the uracil formed by C-terminal resi-
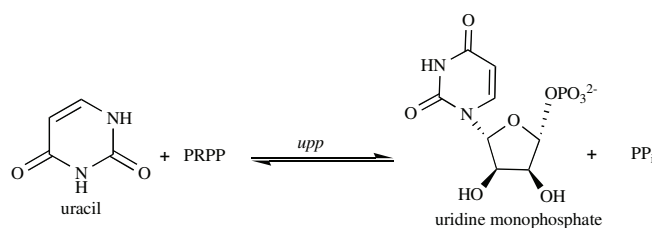
**Fig. (12).** Chemical reaction catalyzed by UPRTase (*upp*). The enzyme catalyzes the conversion of uracil and PRPP to UMP and PP$_i$.

dues [120]. The active site is formed by the hood and the PRPP binding motif, and the catalytic residues from the flexible loop cover the active site, protecting the transition state from hydrolysis [120, 122]. The three-dimensional structure of some UPRTases have been determined, including enzymes from *Thermus termophilus* (PDB access code: 1V9S, to be published), *Bacillus caldolyticus* (PDB access code: 1I5E) [120], *Thermotoga maritime* (PDB access code: 1O5O, to be published), *E. coli* (PDB access code: 2EHJ, to be published), *Aquifex aeolicus* (PDB access code: 2E55, to be published), *S. solfataricus* (PDB access code: 1XTT) [123], and *Toxoplasma gondii* (PDB access code: 1UPU) [124]. The amino acid sequence alignment of each of these UPRTase species with MTB sequence shows overall identities ranging from 30% to 46% (data not shown). Furthermore, it also demonstrates strong conservation of the active site residues comprising four short regions that display sequence identity which are important to substrate recognition and catalysis, as described previously [124]. UPRTase from some species are allosterically activated by GTP such as *T. gondii* [125], *Giardia intestinalis* [126], *E. coli* [127], and *S. solfataricus* [122, 123] enzymes. Besides that, *S. solfataricus* enzyme was shown to be allosterically inhibited by CTP [122, 123].

It has recently been suggested that there is an UPRTase enzyme activity in humans due to the finding of a cDNA encoding a protein with a putative UPRTase domain isolated from the human fetal brain library [128]. However, the cloning, expression, and purification of the putative human enzyme resulted in a protein without UPRTase catalytic activity [128]. Accordingly, no solid and convincing experimental evidence has been presented showing the presence of UPRTase enzyme activity in humans. Thus, UPRTase is an attractive target, unless shown otherwise, for the design of selective chemotherapeutic agents due to the possibility of finding specific inhibitors against the pathogen enzyme. Accordingly, MTB UPRT was recently cloned, expressed, purified, and kinetically characterized by our research group (unpublished results). Moreover, the construction of a strain of MTB having the *upp* gene knocked out is underway, as an attempt to establish the role, if any, of UPRTase in mycobacterial survival and latency by the Wayne model [4].

## 3. CONCLUDING REMARKS

Enzymes of the pyrimidine salvage pathway are shown to be attractive targets for the development of inhibitors to be used in cancer and infectious disease treatments, as some pyrimidine analogues were already found to be toxic for cell growth. For instance, a series of derivates of deoxyuridine were shown to possess antimalarial activity *in vitro*, inhibiting specifically the *Plasmodium* enzyme dUTPase versus the human enzyme [35]. Several anticancer drugs used clinically, such as 5-FU through the metabolite FdUMP, inhibit thymidylate synthase. Moreover, analogues of phenolphthalein were found to have higher activity and specificity against thymidylate synthase from bacterial organisms, such as *L. casei*, *P. carinii* or *C. neoformans*, than to the human enzyme [39-42]. A series of nucleotide analogues with modifications at the carbon-5 of the pyrimidine ring and/or at the sugar ring were found to inhibit MTB dTMP kinase [51, 57, 61]. Thus, although humans also possess some enzymes of the pyrimidine salvage pathway, it is possible to

find selective inhibitors for the MTB enzymes by exploiting differences in functional and structural features. A promising target should be essential for survival of a pathogen and absent from its host. Alternatively, a promising target may play an important role in adaptation of the pathogen to a particular physiological state of the host. An emerging drug discovery strategy is to identify and target protein factors essential for pathogen survival and replication in the host. It has been proposed that in addition to targeting virulence, new antimicrobial development strategies should be expanded to include targeting bacterial gene functions that are essential for *in vivo* viability [129]. Accordingly, an understanding of the role played by the enzymes of the pyrimidine salvage pathway in *M. tuberculosis* may unveil molecular targets that are pivotal to survival in the host context, but not necessarily essential for *in vitro* survival. In addition, the enzymes of the pyrimidine salvage pathway might have an important role in the mycobacterial latent state as the bacilli have to recycle bases and/or nucleosides to survive in the host. Consistent with this proposal, it has recently been shown that inhibiting an enzymatic virulence factor secreted by *M. tuberculosis* into the host's macrophage prevented the growth of the bacilli in host cells [130].

## REFERENCES

[1]     World Health Organization, Global Tuberculosis Control. A short update to the 2009 report, **2009**.
[2]     Lienhardt, C.; Ogden, J.A. Tuberculosis control in resource-poor countries: have we reached the limits of the universal paradigm? *Trop. Med. Int. Health.*, **2004**, *9*(7), 833-841.
[3]     Ducati, R.G.; Ruffino-Netto, A.; Basso, L.A.; Santos, D.S. The resumption of consumption - a review on tuberculosis. *Mem. Inst. Oswaldo Cruz.*, **2006**, *101*(7), 697-714.
[4]     Wayne, L.G.; Hayes, L.G. An *in vitro* model for sequential study of shift-down of *Mycobacterium tuberculosis* through two stages of nonreplicating persistence. *Infect. Immun.*, **1996**, *64*(6), 2062-2069.
[5]     Stewart, G.R.; Robertson, B.D.; Young, D.B. Tuberculosis: a problem with persistence. *Nat. Rev. Microbiol.*, **2003**, *1*(2), 97-105.
[6]     Pieters, J. *Mycobacterium tuberculosis* and the macrophage: maintaining a balance. *Cell Host Microbe.*, **2008**, *3*(6), 399-407.
[7]     Corbett, E.L.; Watt, C.J.; Walker, N.; Maher, D.; Williams, B.G.; Raviglione, M.C.; Dye, C. The growing burden of tuberculosis: global trends and interactions with the HIV epidemic. *Arch. Intern. Med.*, **2003**, *163*(9), 1009-1021.
[8]     Colditz, G.A.; Berkey, C.S.; Mosteller, F.; Brewer, T.F.; Wilson, M.E.; Burdick, E.; Fineberg, H.V. The efficacy of bacillus Calmette-Guérin vaccination of newborns and infants in the prevention of tuberculosis: meta-analyses of the published literature. *Pediatrics*, **1995**, *96*(1 Pt 1), 29-35.
[9]     Colditz, G.A.; Brewer, T.F.; Berkey, C.S.; Wilson, M.E.; Burdick, E.; Fineberg, H.V.; Mosteller, F. Efficacy of BCG vaccine in the prevention of tuberculosis. Meta-analysis of the published literature. *JAMA*, **1994**, *271*(9), 698-702.

[10] Fine, P.E. Variation in protection by BCG: implications of and for heterologous immunity. *Lancet*, **1995**, *346*(8986), 1339-1345.

[11] Shah, N.S.; Wright, A.; Bai, G.; Barrera, L.; Boulahbal, F.; Martín-Casabona, N.; Drobniewski, F.; Gilpin, C.; Havelková, M.; Lepe, R.; Lumb, R.; Metchock, B.; Portaels, F.; Rodrigues, M.F.; Rüsch-Gerdes, S.; Van Deun, A.; Vincent, V.; Laserson, K.; Wells, C.; Cegielski, J.P. Worldwide emergence of extensively drug-resistant tuberculosis. *Emerg. Infect. Dis.*, **2007**, *13*(3), 380-387.

[12] Matteelli, A.; Migliori, G.B.; Cirillo, D.; Centis, R.; Girard, E.; Raviglioni, M. Multidrug-resistant and extensively drug-resistant *Mycobacterium tuberculosis*: epidemiology and control. *Expert Rev. Anti Infect. Ther.*, **2007**, *5*(5), 857-871.

[13] Cole, S.T.; Brosch, R.; Parkhill, J.; Garnier, T.; Churcher, C.; Harris, D.; Gordon, S.V.; Eiglmeier, K.; Gas, S.; Barry, C.E.; Tekaia, F.; Badcock, K.; Basham, D.; Brown, D.; Chillingworth, T.; Connor, R.; Davies, R.; Devlin, K.; Feltwell, T.; Gentles, S.; Hamlin, N.; Holroyd, S.; Hornsby, T.; Jagels, K.; Krogh, A.; McLean, J.; Moule, S.; Murphy, L.; Oliver, K.; Osborne, J.; Quail, M.A.; Rajandream, M.A.; Rogers, J.; Rutter, S.; Seeger, K.; Skelton, J.; Squares, R.; Squares, S.; Sulston, J.E.; Taylor, K.; Whitehead, S.; Barrell, B.G. Deciphering the biology of *Mycobacterium tuberculosis* from the complete genome sequence. *Nature*, **1998**, *393*(6685), 537-544.

[14] Ducati, R.G.; Basso, L.A.; Santos, D.S. Mycobacterial shikimate pathway enzymes as targets for drug design. *Curr. Drug Targets*, **2007**, *8*(3), 423-435.

[15] Taylor Ringia, E.A.; Tyler, P.C.; Evans, G.B.; Furneaux, R.H.; Murkin, A.S.; Schramm, V.L. Transition state analogue discrimination by related purine nucleoside phosphorylases. *J. Am. Chem. Soc.*, **2006**, *128*(22), 7126-7127.

[16] Kim, S.; Park, D.; Kim, T.H.; Hwang, M.; Shim, J. Functional analysis of pyrimidine biosynthesis enzymes using the anticancer drug 5-fluorouracil in *Caenorhabditis elegans*. *FEBS J.*, **2009**, *276*(17), 4715-4726.

[17] Islam, M.R.; Kim, H.; Kang, S.; Kim, J.; Jeong, Y.; Hwang, H.; Lee, S.; Woo, J.; Kim, S. Functional characterization of a gene encoding a dual domain for uridine kinase and uracil phosphoribosyltransferase in *Arabidopsis thaliana*. *Plant Mol. Biol.*, **2007**, *63*(4), 465-477.

[18] Beck, D.A.; O'Donovan, G.A. Pathways of pyrimidine salvage in *Pseudomonas* and former *Pseudomonas*: detection of recycling enzymes using high-performance liquid chromatography. *Curr. Microbiol.*, **2008**, *56*(2), 162-167.

[19] Neuhard, J.; Kelln, R.A. In: *Escherichia coli* and *Salmonella* cellular and molecular biology; Neidhardt, F.C. Ed.; ASM Press: Washington, D.C., **1996**; Vol. *1*, pp. 580-599.

[20] O'Donovan, G.A.; Neuhard, J. Pyrimidine metabolism in microorganisms. *Bacteriol. Rev.*, **1970**, *34*(3), 278-343.

[21] Helt, S.S.; Thymark, M.; Harris, P.; Aagaard, C.; Dietrich, J.; Larsen, S.; Willemoes, M. Mechanism of dTTP inhibition of the bifunctional dCTP deaminase:dUTPase encoded by *Mycobacterium tuberculosis*. *J. Mol. Biol.*, **2008**, *376*(2), 554-569.

[22] Björnberg, O.; Neuhard, J.; Nyman, P.O. A bifunctional dCTP deaminase-dUTP nucleotidohydrolase from the hyperthermophilic archaeon *Methanocaldococcus jannaschii*. *J. Biol. Chem.*, **2003**, *278*(23), 20667-20672.

[23] Li, H.; Xu, H.; Graham, D.E.; White, R.H. The *Methanococcus jannaschii* dCTP deaminase is a bifunctional deaminase and diphosphatase. *J. Biol. Chem.*, **2003**, *278*(13), 11100-11106.

[24] Siggaard, J.H.B.; Johansson, E.; Vognsen, T.; Helt, S.S.; Harris, P.; Larsen, S.; Willemoës, M. Concerted bifunctionality of the dCTP deaminase-dUTPase from *Methanocaldococcus jannaschii*: a structural and pre-steady state kinetic analysis. *Arch. Biochem. Biophys.*, **2009**, *490*(1), 42-49.

[25] Wang, L.; Weiss, B. dcd (dCTP deaminase) gene of *Escherichia coli*: mapping, cloning, sequencing, and identification as a locus of suppressors of lethal *dut* (dUTPase) mutations. *J. Bacteriol.*, **1992**, *174*(17), 5647-5653.

[26] Vértessy, B.G.; Tóth, J. Keeping uracil out of DNA: physiological role, structure and catalytic mechanism of dUTPases. *Acc. Chem. Res.*, **2009**, *42*(1), 97-106.

[27] Johansson, E.; Thymark, M.; Bynck, J.H.; Fano, M.; Larsen, S.; Willemoës, M. Regulation of dCTP deaminase from *Escherichia coli* by nonallosteric dTTP binding to an inactive form of the enzyme. *FEBS J.*, **2007**, *274*(16), 4188-4198.

[28] Thymark, M.; Johansson, E.; Larsen, S.; Willemoës, M. Mutational analysis of the nucleotide binding site of *Escherichia coli* dCTP deaminase. *Arch. Biochem. Biophys.*, **2008**, *470*(1), 20-26.

[29] Johansson, E.; Fano, M.; Bynck, J.H.; Neuhard, J.; Larsen, S.; Sigurskjold, B.W.; Christensen, U.; Willemoës, M. Structures of dCTP deaminase from *Escherichia coli* with bound substrate and product: reaction mechanism and determinants of mono- and bifunctionality for a family of enzymes. *J. Biol. Chem.*, **2005**, *280*(4), 3051-3059.

[30] Dos Vultos, T.; Mestre, O.; Tonjum, T.; Gicquel, B. DNA repair in *Mycobacterium tuberculosis* revisited. *FEMS Microbiol. Rev.*, **2009**, *33*(3), 471-487.

[31] el-Hajj, H.H.; Wang, L.; Weiss, B. Multiple mutant of *Escherichia coli* synthesizing virtually thymineless DNA during limited growth. *J. Bacteriol.*, **1992**, *174*(13), 4450-4456.

[32] Chan, S.; Segelke, B.; Lekin, T.; Krupka, H.; Cho, U.S.; Kim, M.; So, M.; Kim, C.; Naranjo, C.M.; Rogers, Y.C.; Park, M.S.; Waldo, G.S.; Pashkov, I.; Cascio, D.; Perry, J.L.; Sawaya, M.R. Crystal structure of the *Mycobacterium tuberculosis* dUTPase: insights into the catalytic mechanism. *J. Mol. Biol.*, **2004**, *341*(2), 503-517.

[33] Varga, B.; Barabás, O.; Takács, E.; Nagy, N.; Nagy, P.; Vértessy, B.G. Active site of mycobacterial dUTPase: structural characteristics and a built-in sensor. *Biochem. Biophys. Res. Commun.*, **2008**, *373*(1), 8-13.

[34] McIntosh, E.M. Haynes, R.H. dUTP pyrophosphatase as a potential target for chemotherapeutic drug development. *Acta Biochim. Pol.*, **1997**, *44*(2), 159-171.

[35] Whittingham, J.L.; Leal, I.; Nguyen, C.; Kasinathan, G.; Bell, E.; Jones, A.F.; Berry, C.; Benito, A.; Turkenburg, J.P.; Dodson, E.J.; Ruiz Perez, L.M.; Wilkinson, A.J.; Johansson, N.G.; Brun, R.; Gilbert, I.H. Gonzalez Pacanowska, D.; Wilson, K.S. dUTPase as a platform for antimalarial drug design: structural basis for the selectivity of a class of nucleoside inhibitors. *Structure*, **2005**, *13*(2), 329-338.

[36] Curtin, N.J.; Harris, A.L.; Aherne, G.W. Mechanism of cell death following thymidylate synthase inhibition: 2'-deoxyuridine-5'-triphosphate accumulation, DNA damage, and growth inhibition following exposure to CB3717 and dipyridamole. *Cancer Res.*, **1991**, *51*(9), 2346-2352.

[37] Touroutoglou, N. Pazdur, R. Thymidylate synthase inhibitors. *Clin. Cancer Res.*, **1996**, *2*(2), 227-243.

[38] Myllykallio, H.; Lipowski, G.; Leduc, D.; Filee, J.; Forterre, P.; Liebl, U. An alternative flavin-dependent mechanism for thymidylate synthesis. *Science*, **2002**, *297*(5578), 105-107.

[39] Stout, T.J.; Tondi, D.; Rinaldi, M.; Barlocco, D.; Pecorari, P.; Santi, D.V.; Kuntz, I.D.; Stroud, R.M.; Shoichet, B.K.; Costi, M.P. Structure-based design of inhibitors specific for bacterial thymidylate synthase. *Biochemistry*, **1999**, *38*(5), 1607-1617.

[40] Costi, P.M.; Rinaldi, M.; Tondi, D.; Pecorari, P.; Barlocco, D.; Ghelli, S.; Stroud, R.M.; Santi, D.V.; Stout, T.J.; Musiu, C.; Marangiu, E.M.; Pani, A.; Congiu, D.; Loi, G.A.; La Colla, P. Phthalein derivatives as a new tool for selectivity in thymidylate synthase inhibition. *J. Med. Chem.*, **1999**, *42*(12), 2112-2124.

[41] Shoichet, B.K.; Stroud, R.M.; Santi, D.V.; Kuntz, I.D.; Perry, K.M. Structure-based discovery of inhibitors of thymidylate synthase. *Science*, **1993**, *259*(5100), 1445-1450.

[42] Costi, M.P. Thymidylate synthase inhibition: a structure-based rationale for drug design. *Med. Res. Rev.*, **1998**, *18*(1), 21-42.

[43] Hunter, J.H.; Gujjar, R.; Pang, C.K.T.; Rathod, P.K. Kinetics and ligand-binding preferences of *Mycobacterium tuberculosis* thymidylate synthases, ThyA and ThyX. *PLoS ONE*, **2008**, *3*(5), e2237.

[44] Jiang, L.; Lee, P.C.; White, J.; Rathod, P.K. Potent and selective activity of a combination of thymidine and 1843U89, a folate-based thymidylate synthase inhibitor, against *Plasmodium falciparum*. *Antimicrob. Agents Chemother.*, **2000**, *44*(4), 1047-1050.

[45] Ricart, A.D.; Berlin, J.D.; Papadopoulos, K.P.; Syed, S.; Drolet, D.W.; Quaratino-Baker, C.; Horan, J.; Chick, J.; Vermeulen, W.; Tolcher, A.W.; Rowinsky, E.K.; Rothenberg, M.L. Phase I, pharmacokinetic and biological correlative study of OSI-7904L, a novel liposomal thymidylate synthase inhibitor, and cisplatin in patients with solid tumors. *Clin. Cancer Res.*, **2008**, *14*(23), 7947-7955.

[46] Yan, H. Tsai, M.D. Nucleoside monophosphate kinases: structure, mechanism, and substrate specificity. *Adv. Enzymol. Relat. Areas Mol. Biol.*, **1999**, 73103-134, x.

[47] Vonrhein, C.; Schlauderer, G.J.; Schulz, G.E. Movie of the structural changes during a catalytic cycle of nucleoside monophosphate kinases. *Structure*, **1995**, *3*(5), 483-490.

[48] Segura-Peña, D.; Sekulic, N.; Ort, S.; Konrad, M.; Lavie, A. Substrate-induced conformational changes in human UMP/CMP kinase. *J. Biol. Chem.*, **2004**, *279*(32), 33882-33889.

[49] Ofiteru, A.; Bucurenci, N.; Alexov, E.; Bertrand, T.; Briozzo, P.; Munier-Lehmann, H.; Gilles, A. Structural and functional consequences of single amino acid substitutions in the pyrimidine base binding pocket of *Escherichia coli* CMP kinase. *FEBS J.*, **2007**, *274*(13), 3363-3373.

[50] Bertrand, T.; Briozzo, P.; Assairi, L.; Ofiteru, A.; Bucurenci, N.; Munier-Lehmann, H.; Golinelli-Pimpaneau, B.; Bârzu, O.; Gilles, A. Sugar specificity of bacterial CMP kinases as revealed by crystal structures and mutagenesis of *Escherichia coli* enzyme. *J. Mol. Biol.*, **2002**, *315*(5), 1099-1110.

[51] Vanheusden, V.; Van Rompaey, P.; Munier-Lehmann, H.; Pochet, S.; Herdewijn, P.; Van Calenbergh, S. Thymidine and thymidine-5'-O-monophosphate analogues as inhibitors of *Mycobacterium tuberculosis* thymidylate kinase. *Bioorg. Med. Chem. Lett.*, **2003**, *13*(18), 3045-3048.

[52] Jong, A.Y.; Kuo, C.L.; Campbell, J.L. The CDC8 gene of yeast encodes thymidylate kinase. *J. Biol. Chem.*, **1984**, *259*(17), 11052-11059.

[53] Sclafani, R.A.; Fangman, W.L. Yeast gene CDC8 encodes thymidylate kinase and is complemented by herpes thymidine kinase gene TK. *Proc. Natl. Acad. Sci. U.S.A.*, **1984**, *81*(18), 5821-5825.

[54] Li de la Sierra, I.; Munier-Lehmann, H.; Gilles, A.M.; Bârzu, O.; Delarue, M. X-ray structure of TMP kinase from *Mycobacterium tuberculosis* complexed with TMP at 1.95 Å resolution. *J. Mol. Biol.*, **2001**, *311*(1), 87-100.

[55] Familiar, O.; Munier-Lehmann, H.; Negri, A.; Gago, F.; Douguet, D.; Rigouts, L.; Hernández, A.; Camarasa, M.; Pérez-Pérez, M. Exploring acyclic nucleoside analogues as inhibitors of *Mycobacterium tuberculosis* thymidylate kinase. *Chem. Med. Chem.*, **2008**, *3*(7), 1083-1093.

[56] Munier-Lehmann, H.; Chaffotte, A.; Pochet, S.; Labesse, G. Thymidylate kinase of *Mycobacterium tuberculosis*: a chimera sharing properties common to eukaryotic and bacterial enzymes. *Protein Sci.*, **2001**, *10*(6), 1195-1205.

[57] Vanheusden, V.; Munier-Lehmann, H.; Pochet, S.; Herdewijn, P.; Van Calenbergh, S. Synthesis and evaluation of thymidine-5'-O-monophosphate analogues as inhibitors of *Mycobacterium tuberculosis* thymidylate kinase. *Bioorg. Med. Chem. Lett.*, **2002**, *12*(19), 2695-2698.

[58] Lavie, A.; Konrad, M.; Brundiers, R.; Goody, R.S.; Schlichting, I.; Reinstein, J. Crystal structure of yeast thymidylate kinase complexed with the bisub-strate inhibitor P1-(5'-adenosyl) P5-(5'-thymidyl) pentaphosphate (TP5A) at 2.0 Å resolution: implications for catalysis and AZT activation. *Biochemistry*, **1998**, *37*(11), 3677-3686.

[59] Lavie, A.; Ostermann, N.; Brundiers, R.; Goody, R.S.; Reinstein, J.; Konrad, M.; Schlichting, I. Structural basis for efficient phosphorylation of 3'-azidothymidine monophosphate by *Escherichia coli* thymidylate kinase. *Proc. Natl. Acad. Sci. U.S.A.*, **1998**, *95*(24), 14045-14050.

[60] Fioravanti, E.; Adam, V.; Munier-Lehmann, H.; Bourgeois, D. The crystal structure of *Mycobacterium tuberculosis* thymidylate kinase in complex with 3'-azidodeoxythymidine monophosphate suggests a mechanism for competitive inhibition. *Biochemistry*, **2005**, *44*(1), 130-137.

[61] Haouz, A.; Vanheusden, V.; Munier-Lehmann, H.; Froeyen, M.; Herdewijn, P.; Van Calenbergh, S.; Delarue, M. Enzymatic and structural analysis of inhibitors designed against *Mycobacterium tuberculosis* thymidylate kinase. New insights into the phosphoryl transfer mechanism. *J. Biol. Chem.*, **2003**, *278*(7), 4963-4971.

[62] Van Daele, I.; Munier-Lehmann, H.; Hendrickx, P.M.S.; Marchal, G.; Chavarot, P.; Froeyen, M.; Qing, L.; Martins, J.C.; Van Calenbergh, S. Synthesis and biological evaluation of bicyclic nucleosides as inhibitors of *M. tuberculosis* thymidylate kinase. *Chem. Med. Chem.*, **2006**, *1*(10), 1081-1090.

[63] Van Daele, I.; Munier-Lehmann, H.; Froeyen, M.; Balzarini, J.; Van Calenbergh, S. Rational design of 5'-thiourea-substituted alpha-thymidine analogues as thymidine monophosphate kinase inhibitors capable of inhibiting mycobacterial growth. *J. Med. Chem.*, **2007**, *50*(22), 5281-5292.

[64] Serina, L.; Blondin, C.; Krin, E.; Sismeiro, O.; Danchin, A.; Sakamoto, H.; Gilles, A.M.; Bârzu, O. *Escherichia coli* UMP-kinase, a member of the aspartokinase family, is a hexamer regulated by guanine nucleotides and UTP. *Biochemistry*, **1995**, *34*(15), 5066-5074.

[65] Marco-Marín, C.; Escamilla-Honrubia, J.M.; Rubio, V. First-time crystallization and preliminary X-ray crystallographic analysis of a bacterial-archaeal type UMP kinase, a key enzyme in microbial pyrimidine biosynthesis. *Biochim. Biophys. Acta*, **2005**, *1747*(2), 271-275.

[66] Briozzo, P.; Evrin, C.; Meyer, P.; Assairi, L.; Joly, N.; Barzu, O.; Gilles, A. Structure of *Escherichia coli* UMP kinase differs from that of other nucleoside monophosphate kinases and sheds new light on enzyme regulation. *J. Biol. Chem.*, **2005**, *280*(27), 25533-25540.

[67] Gagyi, C.; Bucurenci, N.; Sîrbu, O.; Labesse, G.; Ionescu, M.; Ofiteru, A.; Assairi, L.; Landais, S.; Danchin, A.; Bârzu, O.; Gilles, A. UMP kinase from the Gram-positive bacterium *Bacillus subtilis* is strongly dependent on GTP for optimal activity. *Eur. J. Biochem.*, **2003**, *270*(15), 3196-3204.

[68] Jensen, K.S.; Johansson, E.; Jensen, K.F. Structural and enzymatic investigation of the *Sulfolobus solfataricus* uridylate kinase shows competitive UTP inhibition and the lack of GTP stimulation. *Biochemistry*, **2007**, *46*(10), 2745-2757.

[69] Meyer, P.; Evrin, C.; Briozzo, P.; Joly, N.; Bârzu, O.; Gilles, A. Structural and functional characterization of *Escherichia coli* UMP kinase in complex with its allosteric regulator GTP. *J. Biol. Chem.*, **2008**, *283*(51), 36011-36018.

[70] Evrin, C.; Straut, M.; Slavova-Azmanova, N.; Bucurenci, N.; Onu, A.; Assairi, L.; Ionescu, M.; Palibroda, N.; Bârzu, O.; Gilles, A. Regulatory mechanisms differ in UMP kinases from gram-negative and gram-positive bacteria. *J. Biol. Chem.*, **2007**, *282*(10), 7242-7253.

[71] Fassy, F.; Krebs, O.; Lowinski, M.; Ferrari, P.; Winter, J.; Collard-Dutilleul, V.; Salahbey Hocini, K. UMP kinase from *Streptococcus pneumoniae*: evidence for co-operative ATP binding and allosteric regulation. *Biochem. J.*, **2004**, *384*(Pt 3), 619-627.

[72] Tu, J.; Chin, K.; Wang, A.H.; Chou, S. Unique GTP-binding pocket and allostery of uridylate kinase from a gram-negative phytopathogenic bacterium. *J. Mol. Biol.*, **2009**, *385*(4), 1113-1126.

[73] Yamanaka, K.; Ogura, T.; Niki, H.; Hiraga, S. Identification and characterization of the smbA gene, a suppressor of the mukB null mutant of *Escherichia coli*. *J. Bacteriol.*, **1992**, *174*(23), 7517-7526.

[74] Robertson, D.; Carroll, P.; Parish, T. Rapid recombination screening to test gene essentiality demonstrates that *pyrH* is essential in *Mycobacterium tuberculosis* (*Edinb*). *Tuberculosis (Edinb)*, **2007**, *87*(5), 450-458.

[75] Bucurenci, N.; Sakamoto, H.; Briozzo, P.; Palibroda, N.; Serina, L.; Sarfati, R.S.; Labesse, G.; Briand, G.; Danchin, A.; Bârzu, O.; Gilles, A.M. CMP kinase from *Escherichia coli* is structurally related to other nucleoside monophosphate kinases. *J. Biol. Chem.*, **1996**, *271*(5), 2856-2862.

[76] Briozzo, P.; Golinelli-Pimpaneau, B.; Gilles, A.M.; Gaucher, J.F.; Burlacu-Miron, S.; Sakamoto, H.; Janin, J.; Bârzu, O. Structures of *Escherichia coli* CMP kinase alone and in complex with CDP: a new fold of the nucleoside monophosphate binding domain and insights into cytosine nucleotide specificity. *Structure*, **1998**, *6*(12), 1517-1527.

[77] Sorokin, A.; Serror, P.; Pujic, P.; Azevedo, V.; Ehrlich, S.D. The *Bacillus subtilis* chromosome region encoding homologues of the *Escherichia coli* mssA and rpsA gene products. *Microbiology (Reading, Engl.)*, **1995**, *141*(Pt 2)311-319.

[78] Yu, L.; Mack, J.; Hajduk, P.J.; Kakavas, S.J.; Saiki, A.Y.C.; Lerner, C.G.; Olejniczak, E.T. Solution structure and function of an essential CMP kinase of *Streptococcus pneumoniae*. *Protein Sci.*, **2003**, *12*(11), 2613-2621.

[79] Sassetti, C.M.; Boyd, D.H.; Rubin, E.J. Genes required for mycobacterial growth defined by high density mutagenesis. *Mol. Microbiol.*, **2003**, *48*(1), 77-84.

[80] Thum, C.; Schneider, C.Z.; Palma, M.S.; Santos, D.S.; Basso, L.A. The Rv1712 Locus from *Mycobacterium tuberculosis* H37Rv codes for a functional CMP kinase that preferentially phosphorylates dCMP. *J. Bacteriol.*, **2009**, *191*(8), 2884-2887.

[81] Caceres, R.A.; Macedo Timmers, L.F.S.; Vivan, A.L.; Schneider, C.Z.; Basso, L.A.; De Azevedo, W.F.; Santos, D.S. Molecular modeling and dynamics studies of cytidylate kinase from *Mycobacterium tuberculosis* H37Rv. *J. Mol. Model.*, **2008**, *14*(5), 427-434.

[82] Chopra, P.; Singh, A.; Koul, A.; Ramachandran, S.; Drlica, K.; Tyagi, A.K.; Singh, Y. Cytotoxic activity of nucleoside diphosphate kinase secreted from *Mycobacterium tuberculosis*. *Eur. J. Biochem.*, **2003**, *270*(4), 625-634.

[83] Tiwari, S.; Kishan, K.V.R.; Chakrabarti, T.; Chakraborti, P.K. Amino acid residues involved in autophosphorylation and phosphotransfer activities are distinct in nucleoside diphosphate kinase from *Mycobacterium tuberculosis*. *J. Biol. Chem.*, **2004**, *279*(42), 43595-43603.

[84] Lascu, I.; Chaffotte, A.; Limbourg-Bouchon, B.; Véron, M. A Pro/Ser substitution in nucleoside diphosphate kinase of *Drosophila melanogaster* (mutation killer of prune) affects stability but not catalytic efficiency of the enzyme. *J. Biol. Chem.*, **1992**, *267*(18), 12775-12781.

[85] Chakrabarty, A.M. Nucleoside diphosphate kinase: role in bacterial growth, virulence, cell signalling and polysaccharide synthesis. *Mol. Microbiol.*, **1998**, *28*(5), 875-882.

[86] Sun, J.; Wang, X.; Lau, A.; Liao, T.A.; Bucci, C.; Hmama, Z. Mycobacterial nucleoside diphosphate kinase blocks phagosome maturation in murine raw 264.7 macrophages. *PLoS ONE*, **2010**, *5*(1), e8769.

[87] Chen, Y.; Morera, S.; Mocan, J.; Lascu, I.; Janin, J. X-ray structure of *Mycobacterium tuberculosis* nucleoside diphosphate kinase. *Proteins*, **2002**, *47*(4), 556-557.

[88] Moréra, S.; Lacombe, M.L.; Xu, Y.; LeBras, G.; Janin, J. X-ray structure of human nucleoside diphosphate kinase B complexed with GDP at 2 Å resolution. *Structure*, **1995**, *3*(12), 1307-1314.

[89] Janin, J.; Dumas, C.; Moréra, S.; Xu, Y.; Meyer, P.; Chiadmi, M.; Cherfils, J. Three-dimensional structure of nucleoside diphosphate kinase. *J. Bioenerg. Biomembr.*, **2000**, *32*(3), 215-225.

[90] Dumas, C.; Lascu, I.; Moréra, S.; Glaser, P.; Fourme, R.; Wallet, V.; Lacombe, M.L.; Véron, M.; Janin, J. X-ray structure of nucleoside diphosphate kinase. *EMBO J.*, **1992**, *11*(9), 3203-3208.

[91] Kumar, P.; Verma, A.; Saini, A.K.; Chopra, P.; Chakraborti, P.K.; Singh, Y.; Chowdhury, S. Nucleoside diphosphate kinase from *Mycobacterium tuberculosis* cleaves single strand DNA within the human c-myc promoter in an enzyme-catalyzed reaction. *Nucleic Acids Res.*, **2005**, *33*(8), 2707-2714.

[92] Lascu, L.; Giartosio, A.; Ransac, S.; Erent, M. Quaternary structure of nucleoside diphosphate kinases. *J. Bioenerg. Biomembr.*, **2000**, *32*(3), 227-236.

[93] Williams, R.L.; Oren, D.A.; Muñoz-Dorado, J.; Inouye, S.; Inouye, M.; Arnold, E. Crystal structure of *Myxococcus xanthus* nucleoside diphosphate kinase and its interaction with a nucleotide substrate at 2.0 A resolution. *J. Mol. Biol.*, **1993**, *234*(4), 1230-1247.

[94] Carter, C.W. The nucleoside deaminases for cytidine and adenosine: structure, transition state stabilization, mechanism, and evolution. *Biochimie*, **1995**, *77*(1-2), 92-98.

[95] Carlow, D.C.; Smith, A.A.; Yang, C.C.; Short, S.A.; Wolfenden, R. Major contribution of a carboxymethyl group to transition-state stabilization by cytidine deaminase: mutation and rescue. *Biochemistry*, **1995**, *34*(13), 4220-4224.

[96] Johansson, E.; Neuhard, J.; Willemoës, M.; Larsen, S. Structural, kinetic, and mutational studies of the zinc ion environment in tetrameric cytidine deaminase. *Biochemistry*, **2004**, *43*(20), 6020-6029.

[97] Betts, L.; Xiang, S.; Short, S.A.; Wolfenden, R.; Carter, C.W. Cytidine deaminase. The 2.3 A crystal structure of an enzyme: transition-state analog complex. *J. Mol. Biol.*, **1994**, *235*(2), 635-656.

[98] Ashley, G.W.; Bartlett, P.A. Purification and properties of cytidine deaminase from *Escherichia coli*. *J. Biol. Chem.*, **1984**, *259*(21), 13615-13620.

[99] Johansson, E.; Mejlhede, N.; Neuhard, J.; Larsen, S. Crystal structure of the tetrameric cytidine deaminase from *Bacillus subtilis* at 2.0 A resolution. *Biochemistry*, **2002**, *41*(8), 2563-2570.

[100] Ipata, P.L.; Cercignani, G.; Balestreri, E. Partial purification and properties of cytidine deaminase from baker's yeast. *Biochemistry*, **1970**, *9*(17), 3390-3395.

[101] Wentworth, D.F. Wolfenden, R. Cytidine deaminases (from *Escherichia coli* and human liver). *Meth. Enzymol.*, **1978**, 51401-51407.

[102] Sánchez-Quitian, Z.A.; Schneider, C.Z.; Ducati, R.G.; de Azevedo, W.F.; Bloch, C.; Basso, L.A.; Santos, D.S. Structural and functional analyses of *Mycobacterium tuberculosis* Rv3315c-encoded metal-dependent homotetrameric cytidine deaminase. *J. Struct. Biol.*, **2010**, *169*(3), 413-423.

[103] Neuberger, M.S.; Harris, R.S.; Di Noia, J.; Petersen-Mahrt, S.K. Immunity through DNA deamination. *Trends Biochem. Sci.*, **2003**, *28*(6), 305-312.

[104] Muramatsu, M.; Kinoshita, K.; Fagarasan, S.; Yamada, S.; Shinkai, Y.; Honjo, T. Class switch recombination and hypermutation require activation-

induced cytidine deaminase (AID), a potential RNA editing enzyme. *Cell*, **2000**, *102*(5), 553-563.

[105] Bouffard, D.Y.; Laliberté, J.; Momparler, R.L. Kinetic studies on 2',2'-difluorodeoxycytidine (Gemcitabine) with purified human deoxycytidine kinase and cytidine deaminase. *Biochem. Pharmacol.*, **1993**, *45*(9), 1857-1861.

[106] Krenitsky, T.A.; Mellors, J.W.; Barclay, R.K. Pyrimidine nucleosidases. Their classification and relationship to uric acid ribonucleoside phosphorylase. *J. Biol. Chem.*, **1965**, *240*, 1281-1286.

[107] Gallo, R.C.; Perry, S.; Breitman, T.R. The enzymatic mechanisms for deoxythymidine synthesis in human leukocytes. I. Substrate inhibition by thymine and activation by phosphate or arsenate. *J. Biol. Chem.*, **1967**, *242*(21), 5059-5068.

[108] Paege, L.M.; Schlenk, F. Bacterial uracil riboside phosphorylase. *Arch. Biochem. Biophys.*, **1952**, *40*(1), 42-49.

[109] Krenitsky, T.A.; Barclay, M.; Jacquez, J.A. Specificity of mouse uridine phosphorylase. Chromatography, purification, and properties. *J. Biol. Chem.*, **1964**, *239*, 805-812.

[110] Friedkin, M.; Roberts, D. The enzymatic synthesis of nucleosides. I. Thymidine phosphorylase in mammalian tissue. *J. Biol. Chem.*, **1954**, *207*(1), 245-256.

[111] Razzell, W.E.; Khorana, H.G. Purification and properties of a pyrimidine deoxyriboside phosphorylase from *Escherichia coli. Biochim. Biophys. Acta*, **1958**, *28*(3), 562-566.

[112] Avraham, Y.; Grossowicz, N.; Yashphe, J. Purification and characterization of uridine and thymidine phosphorylase from *Lactobacillus casei. Biochim. Biophys. Acta*, **1990**, *1040*(2), 287-293.

[113] Saunders, P.P.; Wilson, B.A.; Saunders, G.F. Purification and comparative properties of a pyrimidine nucleoside phosphorylase from *Bacillus stearothermophilus. J. Biol. Chem.*, **1969**, *244*(13), 3691-3697.

[114] Scocca, J.J. Purification and substrate specificity of pyrimidine nucleoside phosphorylase from *Haemophilus influenzae. J. Biol. Chem.*, **1971**, *246*(21), 6606-6610.

[115] Pugmire, M.J.; Ealick, S.E. Structural analyses reveal two distinct families of nucleoside phosphorylases. *Biochem. J.*, **2002**, *361*(Pt 1), 1-25.

[116] Pugmire, M.J.; Ealick, S.E. The crystal structure of pyrimidine nucleoside phosphorylase in a closed conformation. *Structure*, **1998**, *6*(11), 1467-1479.

[117] Hamamoto, T.; Noguchi, T.; Midorikawa, Y. Purification and characterization of purine nucleoside phosphorylase and pyrimidine nucleoside phosphorylase from *Bacillus stearothermophilus* TH 6-2. *Biosci. Biotechnol. Biochem.*, **1996**, *60*(7), 1179-1180.

[118] Schwartz, P.M.; Milstone, L.M. Thymidine phosphorylase in human epidermal keratinocytes. *Biochem. Pharmacol.*, **1988**, *37*(2), 353-355.

[119] Schwartz, E.L.; Baptiste, N.; Megati, S.; Wadler, S.; Otter, B.A. 5-Ethoxy-2'-deoxyuridine, a novel substrate for thymidine phosphorylase, potentiates the antitumor activity of 5-fluorouracil when used in combination with interferon, an inducer of thymidine phosphorylase expression. *Cancer Res.*, **1995**, *55*(16), 3543-3550.

[120] Kadziola, A.; Neuhard, J.; Larsen, S. Structure of product-bound *Bacillus caldolyticus* uracil phosphoribosyltransferase confirms ordered sequential substrate binding. *Acta Crystallogr. D Biol. Crystallogr.*, **2002**, *58*(Pt 6 Pt 2), 936-945.

[121] Kukimoto-Niino, M.; Shibata, R.; Murayama, K.; Hamana, H.; Nishimoto, M.; Bessho, Y.; Terada, T.; Shirouzu, M.; Kuramitsu, S.; Yokoyama, S. Crystal structure of a predicted phosphoribosyltransferase (TT1426) from *Thermus thermophilus* HB8 at 2.01 A resolution. *Protein Sci.*, **2005**, *14*(3), 823-827.

[122] Christoffersen, S.; Kadziola, A.; Johansson, E.; Rasmussen, M.; Willemoës, M.; Jensen, K.F. Structural and kinetic studies of the allosteric transition in *Sulfolobus solfataricus* uracil phosphoribosyltransferase: Permanent activation by engineering of the C-terminus. *J. Mol. Biol.*, **2009**, *393*(2), 464-477.

[123] Arent, S.; Harris, P.; Jensen, K.F.; Larsen, S. Allosteric regulation and communication between subunits in uracil phosphoribosyltransferase from *Sulfolobus solfataricus. Biochemistry*, **2005**, *44*(3), 883-892.

[124] Schumacher, M.A.; Carter, D.; Scott, D.M.; Roos, D.S.; Ullman, B.; Brennan, R.G. Crystal structures of *Toxoplasma gondii* uracil phosphoribosyltransferase reveal the atomic basis of pyrimidine discrimination and prodrug binding. *EMBO J.*, **1998**, *17*(12), 3219-3232.

[125] Schumacher, M.A.; Bashor, C.J.; Song, M.H.; Otsu, K.; Zhu, S.; Parry, R.J.; Ullman, B.; Brennan, R.G. The structural mechanism of GTP stabilized oligomerization and catalytic activation of the *Toxoplasma gondii* uracil phosphoribosyltransferase. *Proc. Natl. Acad. Sci. U.S.A.*, **2002**, *99*(1), 78-83.

[126] Dai, Y.P.; Lee, C.S.; O'Sullivan, W.J. Properties of uracil phosphoribosyltransferase from *Giardia intestinalis. Int. J. Parasitol.*, **1995**, *25*(2), 207-214.

[127] Jensen, K.F.; Mygind, B. Different oligomeric states are involved in the allosteric behavior of uracil phosphoribosyltransferase from *Escherichia coli. Eur. J. Biochem.*, **1996**, *240*(3), 637-645.

[128] Li, J.; Huang, S.; Chen, J.; Yang, Z.; Fei, X.; Zheng, M.; Ji, C.; Xie, Y.; Mao, Y. Identification and characterization of human uracil phosphoribosyltransferase (UPRTase). *J. Hum. Genet.*, **2007**, *52*(5), 415-422.

[129] Clatworthy, A.E.; Pierson E.; Hung D.T. Targeting virulence: a new paradigm for antimicrobial therapy. *Nat. Chem. Biol.*, **2007**, *3*(9), 541-548.

[130] Zhou, B.; He, Y.; Zhang, X.; Xu, J.; Luo, Y.; Wang, Y.; Franzblau, S.G.; Yang, Z.; Chan, R.J.; Liu, Y.; Zheng, J.; Zhang, Z.Y. Targeting mycobacterium protein tyrosine phosphatase B for antituberculosis agents. *Proc. Natl. Acad. Sci. U.S.A.,* **2010**, *107*(10), 4573-4578.

# Capítulo 3

Biochemical characterization of uracil phosphoribosyltransferase from *Mycobacterium tuberculosis*

Anne Drumond Villela, Rodrigo Gay Ducati, Leonardo Astolfi Rosado, Carlos Bloch Junior, Maura Vianna Prates, Carlos Henrique Inacio Ramos, Luiz Augusto Basso, Diógenes Santiago Santos

**Biochemical characterization of uracil phosphoribosyltransferase from *Mycobacterium tuberculosis***

Anne Drumond Villela[a,b], Rodrigo Gay Ducati[a], Leonardo Astolfi Rosado[a,b,c], Carlos Bloch Junior[d], Maura Vianna Prates[d], Carlos Henrique Inacio Ramos[e], Luiz Augusto Basso[a,b*], Diógenes Santiago Santos[a,b*]


[a]Centro de Pesquisas em Biologia Molecular e Funcional (CPBMF), Instituto Nacional de Ciência e Tecnologia em Tuberculose (INCT-TB), Pontifícia Universidade Católica do Rio Grande do Sul (PUCRS), Av. Ipiranga 6681/92-A, 90619-900, Porto Alegre, RS, Brazil.
[b]Programa de Pós-Graduação em Biologia Celular e Molecular, Pontifícia Universidade Católica do Rio Grande do Sul (PUCRS), Porto Alegre, RS, Brazil.
[c]Programa de Pós-Graduação em Medicina e Ciências da Saúde, Pontifícia Universidade Católica do Rio Grande do Sul (PUCRS), Porto Alegre, RS, Brazil.
[d]Laboratório de Espectrometria de Massa, Empresa Brasileira de Pesquisa Agropecuária - Recursos Genéticos e Biotecnologia, Estação Parque Biológico, Brasília, DF, Brazil.
[e]Instituto de Química, Departamento de Bioquímica, Universidade Estadual de Campinas (UNICAMP), Campinas, SP, Brazil.


*Corresponding authors. Telephone/Fax: +55-51-33203629.
E-mail addresses: luiz.basso@pucrs.br (Luiz A. Basso) or diogenes@pucrs.br (Diógenes S. Santos).

# Abstract

Uracil phosphoribosyltransferase (UPRT) catalyzes the conversion of uracil and 5-phosphoribosyl-$\alpha$-1-pyrophosphate (PRPP) to uridine 5'-monophosphate (UMP) and pyrophosphate ($PP_i$). UPRT plays an important role in the pyrimidine salvage pathway since UMP is a common precursor of all pyrimidine nucleotides. Here we describe cloning, expression and purification to homogeneity of *upp*-encoded UPRT from *Mycobacterium tuberculosis* (*Mt*UPRT). Mass spectrometry and N-terminal amino acid sequencing unambiguously identified the homogeneous protein as *Mt*UPRT. Analytical ultracentrifugation showed that native *Mt*UPRT follows a monomer-tetramer association model. *Mt*UPRT is specific for uracil. GTP is not a modulator of *Mt*UPRT ativity. *Mt*UPRT was not significantly activated or inhibited by ATP, UTP, and CTP. Initial velocity and isothermal titration calorimetry studies suggest that catalysis follows a sequential ordered mechanism, in which PRPP binding is followed by uracil, and $PP_i$ product is released first followed by UMP. The pH-rate profiles indicated that groups with p*K* values of 5.7 and 8.1 are important for catalysis, and a group with a p*K* value of 9.5 is involved in PRPP binding. Pre-steady-state kinetic data suggested that product release is likely to have no contribution to rate-limiting step of *Mt*UPRT-catalyzed chemical reaction. Stopped-flow measurements of changes in intrinsic protein fluorescence upon PRPP binding to *Mt*UPRT suggested that there appears to be a slow pre-existing equilibrium process between two forms of free enzyme in solution followed by a fast bimolecular association process. The results here described provide a solid foundation on which to base *upp* gene knockout aiming at the development of strategies to prevent tuberculosis.

## Introduction

The major etiological agent of human tuberculosis (TB), *Mycobacterium tuberculosis*, currently infects one-third of the world's population. This pathogen was responsible for 8.5 – 9.2 million new TB cases in 2010, resulting in 1.5 million deaths worldwide.[1] Despite the availability of the Bacille Calmette-Guérin (BCG) vaccine and effective short-course chemotherapy, the increasing global burden of TB has been associated with co-infection with HIV,[1] emergence of multi, extensively[2] and totally drug-resistant strains.[3] Furthermore, the ability of *M. tuberculosis* to remain viable within infected hosts in a long-term asymptomatic infection is an additional problem for the control of TB, since roughly 10% of people infected with latent TB develop the active form of the disease.[4,5] There is thus a need for the development of new therapeutic strategies to control TB.[6]

The complete genome sequencing of *M. tuberculosis* H37Rv has been an important progress towards a better understanding of the biology of bacilli and validation of molecular targets as candidates for rational drug design.[7] The knowledge of functional and structural features of enzymes involved in fundamental metabolic pathways is an important step for the target-based development of selective chemotherapeutic agents to treat TB.[8-13] Enzymes involved in pyrimidine biosynthesis have important roles in cellular metabolism, as they provide pyrimidine nucleosides that are essential components of a number of biomolecules.[14] Uridine 5'-monophosphate (UMP) is a common precursor of all pyrimidine nucleotides and can be synthesized either *de novo* from simple molecules or by the salvage pathway of preformed pyrimidine bases or nucleosides.[15,16] Cells use the salvage pathway to reutilize pyrimidine bases and nucleosides because it represents a significant energy saving as the *de novo* synthesis is energy demanding.[15,16] Uracil phosphoribosyltransferase (UPRT) is a key enzyme in the pyrimidine salvage pathway as it allows direct reutilization of uracil bases.

Enzymes that catalyze the interconversion of uracil and uridine (uridine nucleosidase or uridine phosphorylase) and of uridine and UMP (uridine kinase or uridine monophosphatase) have not been identified by sequence homology in the *M. tuberculosis* genome.[7] Thus, UPRT appears to be the only operative enzyme that converts preformed pyrimidine bases to the nucleotide level.[8]

UPRTs catalyze the conversion of uracil and 5-phosphoribosyl-$\alpha$-1-pyrophosphate (PRPP) to UMP and pyrophosphate (PP$_i$) (Fig. 1). In *M. tuberculosis* H37Rv, two genes have been identified by sequence homology to likely encode proteins with UPRT activity (EC 2.4.2.9):[7] *upp* (Rv3309c) and *pyrR* (Rv1379). Even though *pyrR* proteins are evolutionarily related to UPRTs as demonstrated by sequence and structural similarities, *M. tuberculosis pyrR* was shown to encode a protein with weak UPRT catalytic activity.[17] Thus, most of the UPRT activity and uracil salvage in *M. tuberculosis* probably arises from the *upp* gene product. Unlike enzymes from the *de novo* synthesis of UMP, UPRTs have mostly been characterized in lower organisms. Human UPRT has been isolated from the human fetal brain cDNA library.[18] However cloning, expression, and purification yielded a recombinant protein with no detectable UPRT catalytic activity.[18] Therefore, there is no solid experimental evidence for the presence of UPRT in humans. Although the *upp* gene has been predicted to be non-essential by Himar 1-based transposon mutagenesis in the H37Rv strain[19], *M. tuberculosis* UPRT (*Mt*UPRT) might be an attractive target for the development of specific inhibitors due to its absence from the host. In addition, the apparently pivotal role of *Mt*UPRT in pyrimidine salvage pathway suggests that it may have a key role in the latent state and/or virulence of the tubercle bacilli. Thus, biochemical studies on *Mt*UPRT seem to be worth pursuing.

In this work, we present PCR amplification of *M. tuberculosis upp* gene, cloning, and purification to homogeneity of recombinant *Mt*UPRT. Mass spectrometry analysis and N-

terminal amino acid sequencing confirmed the identity of recombinant *Mt*UPRT protein.

Results on initial velocity measurements and isothermal titration calorimetry (ITC) data on

substrate(s)/product(s) binding suggest that *Mt*UPRT follows a sequential ordered

mechanism, in which PRPP binding is followed by uracil, and $PP_i$ dissociation is followed by

UMP release into solution. Pre-steady state kinetics suggests that product release appears not

to contribute to the rate-limiting step for catalysis. In addition, stopped-flow measurements of

enhancements in protein fluorescence upon PRPP binding to free *Mt*UPRT suggest a

bimolecular process in which there are two forms of free enzyme in solution and only one can

bind the ligand. The latter is consistent with analytical centrifugation results suggesting a

monomer-tetramer equilibrium process of *Mt*UPRT. pH-rate profiles provided the apparent

p*K* values of amino acid residues involved in catalysis and substrate binding. The results

described here may contribute to functional efforts towards a better understanding of *M.*

*tuberculosis* biology, and provide a solid support on which to base gene replacement efforts.


## Results and Discussion


**PCR amplification and cloning of *M. tuberculosis upp* gene, and expression and**

**purification of recombinant *Mt*UPRT**

The 624 bp *upp* gene was amplified from *M. tuberculosis* H37Rv genomic DNA, cloned into

the pCR-Blunt cloning vector, and subcloned into the pET-23a(+) expression vector between

the *Nde*I and *Bam*HI restriction sites. Automatic DNA sequencing of the recombinant plasmid

confirmed both identity and integrity of the *upp* gene, showing that no mutations were

introduced during the PCR amplification steps.

Sodium dodecyl sulfate-polyacrylamide gel electrophoresis (SDS-PAGE) analysis of

BL21(DE3) *Escherichia coli* electrocompetent host cells transformed with recombinant pET-

23a(+)::*upp* plasmid revealed that cell extracts contained a protein in the soluble fraction with an apparent molecular mass of 22 kDa (Fig. 2, lane 2). This is in agreement with the expected mass (21.898 kDa) of *Mt*UPRT (Expasy - compute pI/Mw programme kDa). Among the protocols tested, in our hands, the best experimental protocol for recombinant *Mt*UPRT protein expression was the following: BL21(DE3) *E. coli* electrocompetent host cells grown in Luria-Bertani (LB) medium at 37ºC for 18 hours after cell culture reaching an $OD_{600\,nm}$ of 0.4 without isopropyl-β-D-thiogalactopyranoside (IPTG) induction. The pET expression vector system has a strong IPTG-inducible bacteriophage T7 *lacUV5* late promoter that controls the T7 RNA polymerase to transcribe cloned target genes.[20] However, *lac*-controlled systems could have high level protein expression in the absence of inducer due to derepression of the system when cells approach stationary phase in complex medium, as previously reported for other enzymes.[21-27]

*Mt*UPRT was purified to homogeneity by three steps of liquid chromatography. The purification protocol included an anion-exchange column (DEAE Sepharose CL6B), a gel filtration column (Sephacryl S-300), followed by desorption of homogeneous *Mt*UPRT protein from a strong anion-exchange column (Mono Q) as assessed by SDS-PAGE (Fig. 2). This 2.1-fold purification protocol yielded 20 mg of homogeneous *Mt*UPRT from 2 g of wet cells, indicating a 31% protein yield (Table 1). Enzyme activity assays confirmed that recombinant *Mt*UPRT catalyses the conversion of uracil and PRPP to UMP and $PP_i$. Homogeneous *Mt*UPRT was stored at –80ºC with no loss of activity for up to 1 year.

**Mass spectrometry analysis and N-terminal amino acid sequencing.**
The *Mt*UPRT subunit molecular mass was determined by mass spectrometry analysis to be 21,898.1 Da, consistent with the expected molecular mass of 21,898.2 Da (Expasy - compute pI/Mw programme). The predicted subunit molecular mass of *E. coli* UPRT is 23,500 Da. The

first 51 N-terminal *Mt*UPRT amino acid residues identified by the Edman degradation method correspond to those predicted for the *upp* gene protein product. These results unambiguously identify the homogeneous recombinant protein as *Mt*UPRT.

**Determination of oligomeric state of *Mt*UPRT in solution**

The molecular mass of native *Mt*UPRT was determined by the sedimentation equilibrium (SE) method of analytical ultracentrifugation (AUC). The molecular mass of a sedimenting particle was derived independently of sedimentation and diffusion coefficients and obtained from fitting the concentration distribution of macromolecules at equilibrium. The experiment was carried out with protein concentrations ranging from 0.5 to 1.5 mg mL$^{-1}$ and rotor speed from 3,000 to 11,000 rpm at 4ºC with scan data acquisition at 275 nm. Data analysis involved fitting a model of absorbance versus cell radius data by applying nonlinear regression using Origin software. The best results were obtained with 1.5 mg mL$^{-1}$ of protein at 9,000 and 11,000 rpm which were determined by the distribution randomness of residuals and by the minimization of variance ($3.8 \times 10^{-5}$). Variances for single species were: monomer, $1.8 \times 10^{-4}$; dimer, $9.2 \times 10^{-5}$; trimer, $4.7 \times 10^{-5}$; and tetramer, $4.1 \times 10^{-5}$. The random distribution of residuals (Fig. 3) indicates appropriate fitting and is in agreement with the monomer-tetramer association model, with an estimated equilibrium dissociation constant of approximately $2.8 \times 10^{2}$ M.

Different oligomeric states were found for UPRTs from several organisms. The *Toxoplasma gondii* UPRT behaved as a dimer in solution, whereas in the presence of guanosine 5'-triphosphate (GTP), the enzyme is a tetramer.[28] *Sulfolobus solfataricus* and *Sulfolobus shibatae* UPRTs present tetrameric oligomeric states,[29,30] whereas both *Giardia intestinalis*[31] and *Bacillus caldolyticus*[32] enzymes are dimeric proteins. *E. coli* UPRT was shown to be a dimer or trimer in the absence of ligands, while in the presence of PRPP and

GTP it was shown to be a pentamer or hexamer with both forms existing in a dynamic equilibrium.[33,34] Even though *Mt*UPRT was shown to be present in a monomer-tetramer equilibrium model by AUC, the tetramer seems to be more abundant as no monomer could be detected by size exclusion chromatography (data not shown).

**Substrate specificity, apparent steady-state kinetic parameters, and evaluation of nucleotides as allosteric effectors**

Prior to embarking on determination of the true steady-state kinetic parameters and *Mt*UPRT enzyme mechanism, studies on substrate specificity, assessment of apparent steady-state kinetic parameters, and evaluation of nucleotides as possible allosteric effectors were carried out.

### Evaluation of pyrimidine bases as substrates

Uracil, thymine and cytosine pyrimidine bases were evaluated as possible *Mt*UPRT substrates. The bases were added to *Mt*UPRT reaction mixtures and protein separated by ultrafiltration, and product formation analyzed by HPLC monitoring absorbance at 254, 260, and 280 nm. The results show that *Mt*UPRT is specific for uracil, as no product formation could be detected for both cytosine and thymine bases (data not shown). This result was confirmed using liquid chromatography coupled to electrospray ionization tandem mass spectrometry (LC-ESI-MS/MS).[35] UPRT from several organisms were also shown to be specific for uracil and some uracil analogues.[30, 33] The *Mt*UPRT enzyme activity measurements henceforth described were carried out using uracil as substrate and a continuous spectrophotometric assay.

**Apparent steady-state kinetic parameters**

The dependence of initial velocity on PRPP as a variable substrate at fixed-saturating uracil concentration (10 µM) followed hyperbolic Michaelis-Menten[36] kinetics (Fig. 4A). Accordingly, the data were fitted to the Michaelis-Menten equation $v = V_{max}[S]/(K_M + [S])$, in which $v$ is the steady-state velocity, $V_{max}$ is the maximal rate, [S] is the substrate concentration, and $K_M$ is the Michaelis-Menten constant. This analysis yielded the following values for the apparent constants: $K_M = 34 \pm 2$ µM and $V_{max} = 2.6 \pm 0.1$ U mg$^{-1}$ ($k_{cat} = 0.96 \pm 0.04$ s$^{-1}$). The saturation curve for uracil at a fixed-saturating PRPP concentration (100 µM) was sigmoidal (Fig. 4B). These data were thus fitted to the Hill equation $v = V_{max}[S]^n/(K_{0.5}^n + [S]^n)$, in which $v$ is the measured reaction velocity, $V_{max}$ is the maximal velocity, $S$ is the substrate concentration, $n$ is the Hill coefficient (indicating the cooperative index), and $K_{0.5}$ is the substrate concentration in which $v = 0.5V_{max}$. Data fitting to the Hill equation yielded the following values for uracil: $K_{0.5} = 3.5 \pm 0.2$ µM, $V_{max} = 2.0 \pm 0.1$ U mg$^{-1}$ ($k_{cat} = 0.74 \pm 0.04$ s$^{-1}$), and $n = 2.4 \pm 0.2$. The positive value for $n$ indicates positive homotropic cooperativity for uracil. The $K_M$ value for PRPP is similar to one reported for *B. caldolyticus* UPRT (50 µM).[32] Although *B. caldolyticus* UPRT displayed hyperbolic saturation curve,[32] the $K_M$ value for uracil (2 µM) is similar to the $K_{0.5}$ here reported.

Apparent steady-state kinetic parameters were also determined in the presence of 100 µM GTP (Fig. 4C and D). The values were $K_M = 26 \pm 3$ µM and $V_{max} = 2.2 \pm 0.1$ U mg$^{-1}$ ($k_{cat} = 0.81 \pm 0.04$ s$^{-1}$) for hyperbolic saturation curve for PRPP as the variable substrate at fixed-saturating uracil concentration (10 µM); and $K_{0.5} = 1.9 \pm 0.1$ µM, $V_{max} = 1.7 \pm 0.1$ U mg$^{-1}$ ($k_{cat} = 0.63 \pm 0.04$ s$^{-1}$), and $n = 2.8 \pm 0.2$ for sigmoidal saturation curve for uracil as the variable substrate at fixed-saturating PRPP concentration (100 µM).

In contrast to reports on UPRTs from *E. coli*,[33,34] *S. solfataricus*,[29] and *S. shibatae*,[30] the kinetic parameters for *Mt*UPRT were not affected by GTP (Fig. 4C and D). GTP lowered the $K_M$ value for PRPP, changing saturation curves from slightly sigmoidal to strictly hyperbolic without affecting $V_{max}$ for *E. coli* UPRT.[34] GTP was also shown to cause a dramatic increase in the activity of *G. intestinalis* UPRT.[31] The enzyme from *T. gondii* was shown to be activated by GTP, which also stabilizes the more active tetrameric form of the enzyme.[28] GTP was shown to increase $k_{cat}$ and $K_M$ values for PRPP and uracil of *S. solfataricus* UPRT, whereas cytidine 5'-triphosphate (CTP) inhibited the enzyme in the presence of UMP.[29] UPRTs whose enzyme activity are regulated by GTP and CTP are truncated with a conserved C-terminal glycine residue.[37] It has been shown that extending the polypeptide chain from the C-terminal glycine by adding a threonine and methionine of *S. solfataricus* UPRT resulted in an endogenously activated mutant protein since high activity was detected in the absence of GTP.[37] This result is in agreement with UPRT enzymes from other organisms whose activity are not regulated by GTP, and that have the conserved C-terminal glycine residue followed by one or a few more amino acid residues.[37] *B. caldolyticus* UPRT and *Mt*UPRT, which possess an amino acid sequence identity of approximately 45%, have 2 amino acid residues after the conserved glycine, which might be the reason for GTP not having any effect on the activity of these enzymes.

### Evaluation of nucleotides as allosteric effectors

UPRTs from several organisms are allosterically regulated by nucleotides. Accordingly, a number of nucleotides were evaluated as possible allosteric effectors of *Mt*UPRT by monitoring the enzyme-catalyzed chemical reaction for 500 s (Fig. 5). The absorbance was converted to UMP concentration using the following equation: $C = A/\Delta\varepsilon\, b$, where $C$ is the UMP concentration, $A$ is the absorbance at 280 nm, $\Delta\varepsilon$ is the molar absorptivity based on

differential absorption between uracil and UMP ($\Delta\varepsilon$= 2.5 x $10^3$ $M^{-1}$ $cm^{-1}$), and $b$ is the optical

path (0.5 cm). $Mt$UPRT was not significantly activated or inhibited by 500 μM of any of the

following nucleotides: adenosine 5'-triphosphate (ATP), uridine 5'-triphosphate (UTP), GTP,

and CTP. As expected, enzyme inhibition was observed in the presence of 100 μM of the

product UMP. However, no increase in UMP inhibition occurred in the presence of CTP, as

has been reported for *S. solfataricus* UPRT.[29]

**Determination of $Mt$UPRT kinetic mechanism**

Initial velocity patterns and isothermal titration calorimetry (ITC) of ligand binding to

$Mt$UPRT were employed to assess the enzyme mechanism.

**Initial velocity pattern**

The initial velocity pattern for the $Mt$UPRT catalyzed reaction at varying concentrations of

PRPP at fixed-varying uracil concentrations is shown in Fig. 6, as a double-reciprocal plot

(Lineweaver-Burk plot). A pattern of intersecting lines to the left of *y*-axis (Fig. 6) was

observed for PRPP, which is consistent with ternary complex formation and a sequential

mechanism.[38] The plots of $Mt$UPRT activity versus uracil concentration in the presence of

different PRPP concentrations were all sigmoidal (data not shown), thereby giving non-linear

double-reciprocal plots that precluded the analysis based on patterns of lines. Accordingly, the

only enzyme mechanism that could be ruled out is the ping-pong (double-displacement) that

gives a parallel pattern of lines. At any rate, the pattern of intersecting line given in Fig. 6

indicates that productive catalysis only occurs when both substrates are bound to the enzyme

active site.[39] The data (Fig. 6) were fitted to $v=VAB/(K_{ia}K_B+K_aB+K_bA+AB)$, yielding the

following true steady-state kinetic parameters: $k_{cat}$ = 0.58 ± 0.02 $s^{-1}$, $K_{PRPP}$ = 14 ± 1 μM, $K_{uracil}$

= 2.6 ± 0.4 μM, $k_{cat}/K_{PRPP}$ = 4.1 (± 0.2) x $10^4$ $M^{-1}$ $s^{-1}$, and $k_{cat}/K_{uracil}$ = 2.2 (± 0.3) x $10^5$ $M^{-1}$ $s^{-1}$.

### Equilibrium binding of ligands to *Mt*UPRT assessed by ITC

To try to ascertain whether or not there is an order of substrate addition to *Mt*UPRT, ITC

experiments were carried out. ITC was also employed to evaluate the relative affinity of

ligand binding to free *Mt*UPRT enzyme. ITC measures the heat that is transferred upon

formation of a ligand-macromolecule complex at a constant temperature and pressure. The

measure of the heat released upon binding of the ligand allows determination of the

association constant ($K_a$) and the binding enthalpy ($\Delta H$) of the process. The dissociation

constant at equilibrium ($K_d$) is calculated as the inverse of $K_a$ ($K_d = 1/K_a$). Moreover, the

entropy of the binding reaction ($\Delta S$) and the Gibbs free energy ($\Delta G$) are obtained from the

equation: $\Delta G = -RT\ln K_a = \Delta H - T\Delta S$, where $R$ is the gas constant (8.314 J $K^{-1}$ $mol^{-1}$) and $T$ is

the temperature in Kelvin ($T = $ ºC+273.15).[40] The heat change upon binding for each

individual injection was plotted as a function of the molar ligand-to-protein ratio. To derive

the thermodynamic parameters, the binding isotherms were fitted to a four sequential binding

sites model, which was the best fit obtained for ITC data, which is also consistent with the

native molecular mass of *Mt*UPRT determined by AUC. PRPP (Fig. 7A) and UMP (Fig. 7C)

binding isotherms to free *Mt*UPRT showed significant heat changes, providing a

thermodynamic signature of non-covalent interactions for each ligand and allowing the

determination of the thermodynamic parameters for each binding site (Table 2). Direct and

reverse titrations with PRPP and UMP were conducted to check the stoichiometry and the

suitability of the model.[41] Since the direct titrations generated large standard errors for the

thermodynamic parameters, only the reverse titrations for PRPP (Fig. 7A) and UMP (Fig. 7C)

are presented here. The binding of PRPP to free *Mt*UPRT enzyme generated both exothermic

and endothermic profiles, exhibiting a biphasic behavior (Fig. 7A), while the binding of UMP

exhibited an exothermic binding process (Fig. 7C). Notwithstanding, the affinity of binding

for both PRPP and UMP among *Mt*UPRT subunits were similar, except subunit 2 bound to

PRPP (Table 2). The thermodynamic analysis revealed different types of interactions between

the ligand and enzyme subunits. Negative enthalpy suggests favorable hydrogen bond

contacts or van der Waals interactions. Negative entropy implies conformational changes,

whereas positive entropy indicates that the reaction is dominated by solvent rearrangement

and hydrophobic forces.[40] The signature of non-covalent interactions leading to

*Mt*UPRT:PRPP binary formation suggests that the first and second binding processes are

guided by the release of "bound" water molecules. The third and fourth binding processes

suggest that there may be favorable hydrogen bond formation or van der Waals interactions

(negative $\Delta H$), followed by an unfavorable redistribution of the hydrogen bond network

between the reacting species (positive $\Delta H$). In addition, the third process of PRPP binding

appears to be associated with conformational changes in either the ligand or protein (negative

$\Delta S$), and the fourth process appears to be dominated by the release of water molecules to the

bulk solvent (positive $\Delta S$).[40] The non-covalent signatures of *Mt*UPRT:UMP complex

formation processes are somewhat similar to PRPP. At any rate, the $\Delta G$ values are similar and

all binding processes are favorable (negative $\Delta G$) for PRPP and UMP.

      The ligand binding isotherms showed no significant heat changes upon either uracil

(Fig. 7B) or $PP_i$ (Fig. 7D) interaction with free *Mt*UPRT enzyme. These data suggest that both

uracil and $PP_i$ cannot bind to free enzyme. Furthermore, no binding of GTP either to the free

enzyme or to the enzyme bound to PRPP was detected by ITC (data not shown). The

incubation of PRPP with *Mt*UPRT prior to the titration of GTP was tested to determine

whether the binding of PRPP to *Mt*UPRT generates conformational changes on the enzyme

that could enable GTP binding. However, no binding of GTP to *Mt*UPRT:PRPP binary

complex could be detected (data now shown). These results are in agreement with the steady-state kinetic results showing that GTP does not have any effect on $Mt$UPRT enzyme activity, and therefore $Mt$UPRT is not allosterically regulated by this nucleotide.

**Proposed kinetic mechanism**

The initial velocity pattern of intersecting lines (Fig. 6) suggested a sequential mechanism (either random or ordered). On the other hand, the ITC data allowed determination of order of substrate addition and product release (Fig. 7). Accordingly, the $Mt$UPRT enzyme mechanism consistent with these results is ordered addition of substrate, in which binding of PRPP precedes the binding of uracil, and ordered product release, $PP_i$ release from $Mt$UPRT:UMP:$PP_i$ ternary complex is followed by UMP release to yield free enzyme for the next round of catalysis (Fig. 8). Ordered sequential mechanisms of substrate binding have been reported for $E.\ coli$[42], $S.\ solfataricus$[29], $G.\ intestinalis$,[31] and $B.\ caldolyticus$[16] UPRTs.

**pH-rate profiles**

The pH dependence of the kinetic parameters was evaluated to probe acid-base catalysis in the $Mt$UPRT mode of action. The pH-rate profile for $k_{cat}$ was best fitted to an equation for bell-shaped curve: $\log y = \log[C/(1+H/K_a+K_b/H)]$, where $y$ is the kinetic parameter ($k_{cat}$), $C$ is the pH independent value of $y$, $H$ is the proton concentration, and $K_a$ and $K_b$ are, respectively, the apparent acid and base dissociation constants for the ionizing groups. The bell-shaped pH profile for $k_{cat}$ indicates participation of a single ionizing group in the acidic limb (slope value of +1) that must be unprotonated for catalysis, and participation of a single ionizing group for the basic limb (slope value of −1) that must be protonated for catalysis. Data fitting yielded p$K$ values of 5.7 (± 0.5) and 8.1 (± 0.8). This result indicates that probably Asp198 and Arg102 of $Mt$UPRT are involved in catalysis (Fig. 9A). A catalytic mechanism has been

proposed for UPRT from *B. caldolyticus* in which the O2 of the tautomeric enol form of uracil donates a hydrogen forming a hydrogen bond with the carboxylate group of aspartate (Asp200 for *B. caldolyticus* UPRT) and the $\alpha$-phosphate group of PRPP, thereby simultaneously activating uracil as a nucleophile and $PP_i$ as a leaving group.[16] It is just tempting to suggest that Asp198 in *M. tuberculosis* UPRT plays the role of Asp200 in *B. caldolyticus* UPRT. The role played by Arg102 of *Mt*UPRT in catalysis will have to await site-directed mutagenesis to provide solid experimental data.

The $k_{cat}/K_M$ data for PRPP (Fig. 9B) were fitted to the following equation: $\log y = \log[C/(1+K_b/H)]$. This equation describes pH-rate profiles that show a decrease in $\log y$ with a slope of -1 as the pH values increase, in which $y$ is the apparent kinetic parameter, $C$ is the pH-independent plateau value of $y$, $H$ is the hydrogen ion concentration, and $K_b$ is the apparent base dissociation constant for ionizing groups. Data fitting of pH dependence of $\log k_{cat}/K_M$ for PRPP to this equation yielded a single ionizing group with a p$K$ value of 9.5 ($\pm$ 1.1) that must be protonated for substrate binding (Fig. 9B). This result indicates that either Arg77 or Arg102 of *Mt*UPRT may play a role in PRPP binding. These residues were previously shown to be conserved among UPRTs from different organisms, such as *T. gondii*, *B caldolyticus* and *E. coli*.[43] Although there is a high conservation of residues involved in ligand binding and catalysis, amino acid sequences of different UPRT species are fairly dissimilar with identities ranging from 20 to 45%.[28,44]

The dependence of $k_{cat}/K_M$ for uracil on different pHs could not be analyzed because the saturation curves for uracil at pH values ranging from 7.0 to 8.5 fitted to a sigmoidal curve. Since the enzyme-catalyzed chemical reaction at these pH values does not obey Michaelis-Menten kinetics, it was not possible to determined $K_M$ values.

**Pre-steady-state kinetics**

Stopped-flow measurements in absorbance mode were carried out to ascertain whether or not

product release contributes to the rate-limiting step. In addition, stopped-flow measurements

in fluorescence mode were carried out to determine the kinetics of *Mt*UPRT:PRPP binary

complex formation.


**Absorbance mode**

Pre-steady-state kinetic measurements of product formation by *Mt*UPRT were carried out to

determine whether the enzyme displays burst kinetics, in which the products are released

more slowly than they are formed. Substrate concentrations above their $K_M$ values (250 µM of

both PRPP and uracil, mixing chamber concentrations) were used to discard any possible

binding effect on enzyme activity. In addition, these concentrations are in excess over enzyme

concentration (25 µM, mixing chamber concentration), so as to reliably detect any burst in

product formation.[45] The pre-steady-state trace was fitted to a single exponential equation: $S =$

$A\mathrm{e}^{-kt} + E$, in which $S$ is the absorbance signal at time $t$, $A$ is the amplitude, $k$ is the first-order

rate constant for product formation, and $E$ is the floating endpoint. This analysis yielded

values for the first-order rate constants for product formation of, respectively, 0.94 ($\pm$ 0.02) s$^{-}$

$^{1}$ (Fig. 10A) and 0.58 $\pm$ 0.01 s$^{-1}$ (Fig. 10B) in the absence and presence of 1 mM of GTP (0.1

cm pathlength). These results are in agreement with the catalytic rate constant values obtained

from steady-state kinetics ($k_{cat}$), and showed negligible GTP effect on *Mt*UPRT enzyme

activity in accordance with steady-state kinetic data (Fig. 4C, Fig. 4D, and Fig. 5).

Considering the portion of the signal that could not be detected due to the dead time of the

equipment (1.37 ms), the change in absorbance lost corresponds to roughly 154 µM and 264

µM of product formation in, respectively, the absence and in the presence of GTP. These

values indicate that there were multiple turnovers that occurred in the dead time of the

equipment, since the enzyme concentration in the mixing chamber is 25 μM. Although these results do not unequivocally rule out burst formation in the dead time of the equipment, there appears to be no burst in product formation.

**Fluorescence mode**

The kinetics of PRPP binding to *Mt*UPRT was investigated by stopped-flow spectroscopy in the fluorescence mode. The binary complex formation measured was characterized by a monophasic enhancement in fluorescence. Accordingly, all data sets were fitted to a single exponential function, yielding values for observed apparent rate constants ($k_{obs}$) and observable amplitude ($A_{obs}$). A plot of $k_{obs}$ values against increasing PRPP concentrations ($c$) showed a hyperbolic decrease in the apparent rate constant (Fig. 11). These results are consistent with a model of a slow pre-existing equilibrium process between two forms of free *Mt*UPRT enzyme in solution followed by a fast bimolecular association process (Fig. 12).[46] This model predicts that the rate constant of association of PRPP to *Mt*UPRT is limited by the first-order isomerization rate constant ($k_2$) from *Mt*UPRT* to *Mt*UPRT when PRPP concentration is brought to infinite, since only *Mt*UPRT binds PRPP considerably (Fig. 12). The isomerization process is assumed to be slower than the bimolecular interaction ($k_1$[PRPP]+$k_{-1}$ >> $k_2$+$k_{-2}$). The data were thus fitted to the following equation: $k_{obs}$ = [($k_{-2}K_d$)/([PRPP]+$K_d$)]+$k_2$, where $K_d$ is the dissociation constant ($K_d = k_{-1}/k_1$), and $k_2$ and $k_{-2}$ are, respectively, the limiting forward and reverse first-order rate constants for the isomerization process of free enzyme that occur before substrate binding. This analysis yielded the following values: $k_2 = 1.4 \pm 0.7$ s$^{-1}$, $k_{-2} = 43 \pm 23$ s$^{-1}$, and $K_d = 0.42 \pm 0.35$ μM. These values allow determination of the overall dissociation constant of the whole process ($K_{D(overall)}$). To calculate $K_{D(overall)}$, it is assumed that [*Mt*UPRT:PRPP] is much larger than [*Mt*UPRT*:PRPP] as binding of PRPP to the latter form is negligible. Accordingly, the

overall dissociation constant ($K_{D(\text{overall})}$) is given by the following equation: $K_{D(\text{overall})} = K_d[(1/K_2)+1]$, where is the equilibrium constant for the isomerization process ($K_2 = [MtUPRT]/[MtUPRT^*] = k_2/k_{-2}$). This analysis yielded a value of $13 \pm 7$ µM for $K_{D(\text{overall})}$, which is in agreement with the ITC data (Table 2) and amplitude analysis of stopped-flow signal (Fig. 11 – inset) described in the next paragraph. It is tempting to suggest that the isomerization process may be related to the monomer-tetramer association model proposed by the AUC experiment for MtUPRT. In addition, GTP has been shown to stabilize the more active tetrameric form of T. gondii UPRT enzyme.[28] However, whether or not the pre-existing equilibrium process of two forms of MtUPRT in solution can be ascribed the monomer (less active) and tetramer (more active) equilibrium in solution needs more experimental evidence. At any rate, the model of a pre-existing equilibrium proposed to explain the stopped-flow data on the kinetics of PRPP binding to MtUPRT is consistent with the positive homotropic cooperativity for uracil (Fig. 4B) as PRPP is the first substrate to bind to free enzyme.

The observed amplitude changes of the stopped-flow signal lost in the dead time of the equipment were corrected to obtain the total amplitude of the signal using the following equation: $\ln A = k_{\text{obs}}t_d + \ln A_{\text{obs}}$, where $A$ is the corrected amplitude change, $k_{\text{obs}}$ is the observed apparent association rate constant, $t_d$ is the stopped-flow dead time, and $A_{\text{obs}}$ is the observable signal amplitude. The corrected total amplitudes were plotted against increasing PRPP concentrations. This plot displayed a hyperbolic curve (Fig. 11, inset), and the data were accordingly fitted to the following equation: $F = F_{\text{max}}A/(K+A)$, where $F$ is the observed fluorescence signal, $F_{\text{max}}$ is the maximal fluorescence, $A$ is the substrate concentration, and $K$ is the dissociation constant that gives half the maximal response. This analysis for the amplitude of fluorescence signal yielded a value of $8.2 \pm 3.9$ µM for the dissociation constant ($K$). This value is in agreement with the dissociation constant values derived from ITC

measurements (Table 2) and the overall dissociation constant described in the previous paragraph.

## Experimental procedures

### Materials

All chemicals were of analytical or reagent grade and were used without further purification, unless stated otherwise. *Pfu* DNA polymerase was from Stratagene. Restriction enzymes were from New England Biolabs. T4 DNA ligase and pCR-Blunt cloning vector were from Invitrogen, and pET-23a(+) expression vector and *E. coli* BL21(DE3) electrocompetent cells were from Novagen. FPLC and HPLC were carried out using an Äkta Purifier system from GE Healthcare; all chromatographic columns and the low molecular weight and high molecular weight gel filtration calibration kits were also from GE Healthcare. Amicon ultrafiltration membranes and Centricon (centrifugal filter devices) were purchased from Millipore. Bovine serum albumin and Bradford reagent were from Bio-Rad Laboratories. Mass spectrometry analysis (MALDI-TOF/TOF) was performed using an ABI 4700 Proteomics Analyzer from Applied Biosystems, an Ultraflex II from Bruker Daltonics, and a Q-TOF Ultima API from Micromass. N-terminal sequencing was carried out using a PPSQ 23 protein peptide sequencer from Shimadzu. AUC experiments were performed with a Beckman Optima XL-A analytical ultracentrifuge using an AN-60Ti rotor. LC-ESI-MS/MS and Eclipse plus C18 4.6/150 column were purchased from Agilent, and LC detector was an ESI coupled to the 3200 Q-Trap from Applied Biosystems MDS SCIEX. Uracil, PRPP, UMP, $PP_i$, GTP, CTP, ATP, and UTP, along with lysozyme and streptomycin sulfate, were all purchased from Sigma-Aldrich. Dithiothreitol (DTT) was from Acros Organics. All steady-state activity assays were performed in a Shimadzu UV-2550 UV/Visible spectrophotometer.

ITC was performed with an iTC$_{200}$ Microcalorimeter from MicroCal Inc and the respective experimental data were evaluated using the Origin 7 SR4 software from MicroCal. Pre-steady-state measurements were carried out using an Applied Photophysics SX.18MV-R stopped-flow spectrofluorimeter in either absorbance or fluorescence mode.

**Amplification and cloning of the *M. tuberculosis upp* gene**

Two oligonucleotides (5'-AC<u>CATATG</u>CAGGTCCATGTCGTTGACCA-3' and 5'-GT<u>GGATCC</u>TCAGCGCGGGCCGAACTG-3') complementary to the amino-terminal coding and carboxy-terminal noncoding strands of *M. tuberculosis upp* gene were designed to, respectively, contain *Nde*I and *Bam*HI restriction sites (underlined). These primers were used to PCR amplify the *upp* gene from *M. tuberculosis* H37Rv genomic DNA. The PCR product, in agreement with the expected size (624 bp), was cloned into the pCR-Blunt cloning vector and subcloned into the pET-23a(+) expression vector. The recombinant plasmid (pET-23a(+)::*upp*) was analyzed by automatic DNA sequencing.

**Expression and purification of recombinant *Mt*UPRT**

The pET-23a(+)::*upp* recombinant plasmid was transformed into BL21(DE3) *E. coli* electrocompetent host cells and selected on LB agar plates containing 50 µg mL$^{-1}$ ampicillin. A single colony was used to inoculate 50 mL LB medium containing 50 µg mL$^{-1}$ ampicillin and grown overnight at 37ºC. This liquid culture was used to inoculate 500 mL of LB medium (in a 2 L flask) containing 50 µg mL$^{-1}$ ampicillin and grown at 37ºC and 180 rpm up to an OD$_{600\,nm}$ of 0.4. Cells were grown for an additional period of eighteen hours (with no IPTG induction), harvested by centrifugation at 15,900$g$ for 30 min at 4ºC, and stored at –20ºC. The same protocol was employed for BL21(DE3) *E. coli* electrocompetent host cells transformed

with empty pET-23a(+) expression vector, as control. The expression of *Mt*UPRT was analyzed by 12% SDS-PAGE stained with Coomassie Brilliant Blue.[47]

The cell pellet (2 g of wet cells) was suspended in 20 mL of 50 mM Tris pH 7.6 (buffer A) containing lysozyme (0.2 mg mL$^{-1}$) and incubated for 30 min at 4ºC. Cells were disrupted by sonication and cell debris was removed by centrifugation (48,000$g$ 30 min 4ºC). The supernatant was treated with 1% (wt/vol) streptomycin sulfate, stirred for 30 min, and centrifuged (48,000$g$ 30 min 4ºC). The resulting supernatant, containing soluble *Mt*UPRT, was dialyzed against buffer A. An FPLC Äkta Purifier system was utilized in all purification steps at 4ºC. The dialyzed crude extract was loaded on a DEAE Sepharose CL6B anion exchange column previously equilibrated with buffer A and the adsorbed material eluted with a linear gradient from 0 to 350 mM NaCl in buffer A at a 1 mL min$^{-1}$ flow rate. Fractions containing the target protein were pooled (157.5 mL), concentrated (8.0 mL) using an Amicon ultrafiltration membrane (10,000 Da molecular weight cut off), and loaded on a HiPrep 26/60 Sephacryl S-300 gel filtration column. The target protein was isocratically eluted with buffer A at 0.25 mL min$^{-1}$ flow rate. Pooled fractions (26 mL) were loaded on a Mono Q 16/10 anion exchange column and protein elution was achieved with a linear gradient from 0 to 350 mM NaCl in buffer A. The pooled sample was dialyzed against buffer A and concentrated using an Amicon ultrafiltration membrane (10,000 Da molecular weight cut off). Homogeneous recombinant *Mt*UPRT protein was immediately frozen in liquid nitrogen and stored at –80ºC. All protein purification steps were analyzed by 12% SDS-PAGE stained with Coomassie Brilliant Blue[47] and protein concentration was determined by the method of Bradford using the Bio-Rad protein assay kit and bovine serum albumin as standard.[48]

**Mass spectrometry analysis and N-terminal amino acid sequencing**

The subunit molecular mass of homogeneous recombinant *Mt*UPRT protein was assessed by mass spectrometry, using a MALDI-TOF/TOF on an ABI 4700 Proteomics Analyzer, an Ultraflex II, and a Q-TOF Ultima API as described elsewhere.[49] The N-terminal amino acid residues of homogeneous *Mt*UPRT were identified by automated Edman degradation sequencing using a PPSQ 23 protein peptide sequencer.

**Determination of *Mt*UPRT molecular mass**

Analytical ultracentrifugation (AUC) experiments were performed at 20ºC and analyzed as described elsewhere.[50-52]. Experiments were carried out from 3,000 to 11,000 rpm at 4ºC with scan data acquisition at 275 nm and protein concentration from 500 to 1,500 µg mL$^{-1}$ in 100 mM Hepes pH 7.5 containing 10 mM $MgCl_2$ and 150 mM NaCl. Sedimentation equilibrium (SE) analysis involved fitting a model of absorbance versus cell radius data by nonlinear regression using the Origin software package. The self-association method was used to analyze the experiments with several models of association for UPRT. The distribution of the protein along the cell was fitted to the following equation: $C=C_o\exp[M(1-V_{bar}\rho)\omega^2(r^2-r_o)/2RT]$, in which $C$ is the protein concentration at radial position $r$, $C_o$ is the protein concentration at radial position $r_o$, $M$ is the molecular mass, $V_{bar}$ is the protein partial specific volume, $\rho$ is the buffer density, $\omega$ is the centrifugal angular velocity, $R$ is the gas constant, and $T$ is the absolute temperature. The Sednterp software was used to estimate protein partial specific volume and buffer density at 4ºC.

**Evaluation of pyrimidine bases as substrates using a discontinuous assay**

Reaction mixtures containing 50 mM Tris pH 7.8, 10 mM $MgCl_2$, 1 mM PRPP, and 0.1 mM of the pyrimidine base to be tested (uracil, cytosine, or thymine) were initiated by the addition

of 54 nM of homogeneous *Mt*UPRT. The reactions were incubated at 37ºC for 30 min and then boiled for 3 min to stop the reaction. The mixtures were passed through a Centricon (10,000 Da molecular weight cut off) to remove the protein content prior to analysis. The nucleotide contents of the samples were analyzed using an HPLC Äkta Purifier system and a Sephasil peptide C18 5 µm ST 4.6/250 column. A 500 µL aliquot of each sample was loaded on the column and adsorbed material isocratically eluted with 5 mM potassium phosphate pH 4.0 containing 5% acetonitrile for 10 min at 1 mL min$^{-1}$flow rate. Nucleotides and bases were monitored at 254, 260, and 280 nm.

Another method used to analyze the nucleotide content was the LC-ESI-MS/MS. This experiment was employed to confirm results obtained in the analysis described above. The chromatography was carried out with an Eclipse plus C18 4.6/150 column. The injected sample volume was 20 µL, which was eluted isocratically with 10 mM ammonium acetate containing 40% acetonitrile at 0.8 ml min$^{-1}$ flow rate. The LC detector was an ESI coupled to the 3200 Q-Trap, employing the ESI-MS/MS parameters as described by others.[35] During the chromatography run, precursor ion scan (Prec) and enhance product ion scan (EPI) were monitored. Prec monitored precursors of mass over charge ratio (*m/z*) of compounds containing a phosphate group ($H_2PO_4^-$, *m/z* 97) and EPI gave the fragmentation spectra of the nucleotides *m/z*.[35]

**Initial velocity measurements of recombinant *Mt*UPRT by a continuous assay**

*Mt*UPRT enzyme activity was determined spectrophotometrically by measuring the conversion of uracil into UMP essentially as described by others[53] with a few changes. Enzyme activity measurements were performed using a UV-2550 UV/Vis Spectrophotometer at 25ºC, and reactions initiated by the addition of enzyme to assay mixtures containing 10 µM uracil, 100 µM PRPP, 5 mM MgCl$_2$, 100 mM Hepes pH 7.5, and 10 mM DTT in a final

volume of 0.5 mL, and time courses followed for 60 s. This assay was based on the differential molar absorption between uracil and UMP at 280 nm ($\Delta\varepsilon$= 2.5 x $10^3$ $M^{-1}$ $cm^{-1}$), in which an increase in absorbance is observed due to the formation of UMP. One unit of *Mt*UPRT is defined as the amount of enzyme that catalyses the conversion of 1 µmol of uracil in UMP per min.

**Evaluation of nucleotides as allosteric effectors**

*Mt*UPRT activation or inhibition by allosteric effectors was evaluated and the following nucleotides were tested: 500 µM GTP, 500 µM CTP, 500 µM ATP, 500 µM UTP, and 100 µM UMP. The experimental conditions were 10 µM uracil, 100 µM PRPP, 5 mM MgCl$_2$, 10 mM DTT, 100 mM Hepes pH 7.5, and 108 nM *Mt*UPRT, using 0.5 cm pathlength quartz cuvettes. Enzyme activity was measured for 500 s as described for the standard reaction.

**Kinetic parameters and initial velocity pattern**

Determination of the steady-state kinetic parameters, $k_{cat}$ and $K_M$, was carried out at varying concentrations of one substrate while the concentration of the other substrate was fixed at constant saturating level. The concentrations of uracil were 2, 3, 6, 8, 10, 12 ,and 20 µM at a fixed PRPP concentration of 100 µM, while the concentrations of PRPP were 6, 20, 40, 60, 80, and 100 µM at a fixed uracil concentration of 10 µM. The reaction was initiated by adding 108 nM *Mt*UPRT and monitoring the change in absorbance at 280 nm for 60 s. Steady-state kinetic parameters were also determined in the presence of 100 µM GTP. Initial velocity patterns were also determined from measurements of *Mt*UPRT activity in the presence of varying concentrations of PRPP (6 - 100 µM) at several fixed-varied concentrations of uracil (2 - 10 µM).

**Isothermal titration calorimetry (ITC)**

ITC experiments were carried out using an $iTC_{200}$ Microcalorimeter. Ligands and enzyme were prepared in 100 mM Hepes pH 7.5 containing 10 mM $MgCl_2$. For direct titrations the sample cell was filled with 139 µM of *Mt*UPRT (200 µL) and titrated (39.7 µL) with different concentrations of either substrates or products: 200 µM of uracil, 500 µM of PRPP, 500 µM of UMP, and 350 µM of $PP_i$. In addition, titration was performed with 10 mM of GTP and the sample cell was filled with either free *Mt*UPRT (139 µM) or *Mt*UPRT (139 µM) incubated with 100 µM PRPP for 1 hour before starting the measurements. Reverse titrations were also carried out where the sample cell was filled with either 90 µM of PRPP or 150 µM of UMP and titrated with 633 µM of UPRT.

A stirring speed of 500 rpm and a temperature of 25ºC were employed for all ITC experiments. For direct titrations, the first injection (0.5 µL) was not used in data analysis and it was followed by either 17 injections (2.2 µL) for uracil, PRPP, $PP_i$, and GTP or 21 injections (1.85 µL) for UMP. For the reverse titrations, the first injection (0.5 µL) was not used in data analysis and it was followed by either 30 injections (1.3 µL) for PRPP or 24 injections (1.6 µL) for UMP. The corresponding heat of dilution of each ligand (direct titrations) or UPRT (reverse titrations) titrated into buffer was used to correct data. The experimental data were evaluated using the Origin 7 SR4 software.


**pH-rate profiles**

The pH dependence of the kinetic parameters was determined by measuring initial velocities in the presence of varying concentrations of one substrate and a saturating level of the other, in a buffer mixture of Mes/Hepes/Ches over the following pH values: 6.0, 6.5, 7.0, 7.5, 8.0, 8.5, and 9.0.[54] Prior to performing the pH-rate profile determinations, the enzyme was

incubated over this pH range and assayed under standard conditions to identify denaturing pH values and to ensure enzyme stability at the tested pH range. The pH-rate data were plotted as the dependence of either $\log k_{cat}$ or $\log k_{cat}/K_M$ on pH values.

**Pre-steady-state kinetics in absorbance mode**

The increase in absorbance upon uracil conversion to UMP was monitored at 280 nm (1 mm slit width = 4.65 nm spectral band), at 25°C, using a split time base (50-500 s; 200 data points for each time base), and 0.1 cm pathlength. The experimental conditions were 25 µM *Mt*UPRT, 250 µM PRPP, and 250 µM uracil in 100 mM Hepes pH 7.5 containing 10 mM MgCl$_2$ (mixing chamber concentrations). Experiments were initiated by mixing enzyme with substrates, and, when present, 1 mM GTP was included in both solutions. The dead time of the stopped-flow equipment is 1.37 ms.

**Pre-steady-state kinetics in fluorescence mode**

The kinetics of PRPP binding to *Mt*UPRT was assessed by stopped-flow measurements. The rate of formation of MtUPRT:PRPP binary complex was determined by monitoring the rate of enhancement in intrinsic protein fluorescence upon PRPP binding to *Mt*UPRT at 25°C using an SX-18MV-R stopped-flow spectrofluorimeter (Applied Photophysics) in fluorescence mode (dead time 6 1.37 ms). Excitation wavelength was 280 nm (1 mm slit width = 4.65 nm spectral band), and fluorescence signal captured using a cut off filter of 295 nm positioned between the photomultiplier and the sample cell and a split time base of 0.1-1.0 s. The experimental conditions were 6 µM *Mt*UPRT and PRPP concentrations ranging from 0.5 to 12 µM in 100 mM Hepes pH 7.5 containing 10 mM MgCl$_2$ (mixing chamber concentrations). An apparent rate constant and an amplitude change were obtained for each PRPP concentration upon curve fitting to a single exponential increase equation.

## Conclusion

Efficient prophylactic strategies are urgently needed to decrease the global incidence of TB. Live attenuated strains to be used as a vaccine offer a great promise against intracellular pathogens.[55] An ideal vaccine candidate would lead to limited replication *in vivo*, have the potential to induce immune response and improved safety comparing to BCG vaccine.[56] *Mt*UPRT is a key enzyme of the pyrimidine salvage pathway that might be an attractive target for the development of attenuated strains. Accordingly, the biochemical studies on *Mt*UPRT mode of action here described provide a solid support on which to base future efforts on gene replacement towards the development of efficient prophylactic strategies to combat TB. Moreover, attempts to ascertain the role of *Mt*UPRT in *M. tuberculosis* survival *in vivo* during latent TB is also worth pursuing. Understanding the mode of action of *Mt*UPRT may also be useful to chemical biologists interested in designing function-based chemical compounds to elucidate the biological role of this enzyme in the context of whole *M. tuberculosis* cells.

## Acknowledgements

# References

1.      World Health Organization, Global Tuberculosis Control: WHO report 2011.

2.      A. Jain and R. Mondal, *FEMS Immunol. Med. Microbiol.*, 2008, **53**, 145-150.

3.      A. A. Velayati, P. Farnia, M. R. Masjedi, T. A. Ibrahim, P. Tabarsi, R. Z. Haroun, H. O. Kuan, J. Ghanavi, P. Farnia and M. Varahram, *Eur. Respir. J.*, 2009, **34**, 1202-1203.

4.      R. G. Ducati, A. Ruffino-Netto, L. A. Basso and D. S. Santos, *Mem. Inst. Oswaldo Cruz,* 2006, **101**, 697-714.

5.      J. Pieters, *Cell Host Microbe*, 2008, **12**, 399-407.

6.      G. R. Stewart, B. D. Robertson and D. B. Young, *Nat. Rev. Microbiol.*, 2003, **1**, 97-105.

7.      S. T. Cole, R. Brosch, J. Parkhill, T. Garnier, C. Churcher, D. Harris, S. V. Gordon, K. Eiglmeier, S. Gas, C. E. 3rd Barry, F. Tekaia, K. Badcock, D. Basham, D. Brown, T. Chillingworth, R. Connor, R. Davies, K. Devlin, T. Feltwell, S. Gentles, N. Hamlin, S. Holroyd, T. Hornsby, K. Jagels, A. Krogh, J. McLean, S. Moule, L. Murphy, K. Oliver, J. Osborne, M. A. Quail, M. A. Rajandream, J. Rogers, S. Rutter, K. Seeger, J. Skelton, R. Squares, S. Squares, J. E. Sulston, K. Taylor, S. Whitehead and B. G. Barrell, *Nature*, 1998, **11**, 537-544.

8.      A. D. Villela, Z. A. Sánchez-Quitian, R. G. Ducati, D. S. Santos and L. A. Basso, *Curr. Med. Chem.*, 2011, **18**, 1286-1298.

9.      R. G Ducati, A. Breda, L. A Basso and D. S. Santos, *Curr. Med. Chem.*, 2011, **18**, 1258-1275.

10.     R. G. Ducati, A. A. Souto, R. A. Caceres, W. F. de Azevedo Jr, L. A. Basso and D. S. Santos, *Int. Rev. Biophys. Chem.*, 2010, **1**, 34-40.

11.     R. G. Ducati, L. A. Basso, D. S. Santos and W. F. de Azevedo Jr, *Bioorg. Med. Chem.*, 2010, **18**, 4769-4774.

12.     R. G. Ducati, D. S. Santos and L. A. Basso, *Arch. Biochem. Biophys.*, 2009, **486**, 155-164.

13.     R. G. Ducati, L. A. Basso and D. S. Santos, *Curr. Drug Targets*, 2007, **8**, 423-435.

14.     S. Kim, D. H. Park, T. H. Kim, M. Hwang and J. Shim. *FEBS J.*, 2009, **276**, 4715-4726.

15.     B. A. Moffatt and H. Ashihara, *The Arabidopsis Book*, 2002, 1-20.

16.     A. Kadziola, J. Neuhard and S. Larsen, *Acta Crystallogr. D. Biol. Crystallogr.*, 2002, **58**, 936-945.

17.     K. A. Kantardjieff, C. Vasquez, P. Castro, N. M. Warfel, B. S. Rho, T. Lekin, C. Y. Kim, B. W. Segelke, T. C. Terwilliger and B. Rupp, *Acta Crystallogr. D. Biol. Crystallogr.*, 2005, **61**, 355-364.

18.     J. Li, S. Huang, J. Chen, Z. Yang, X. Fei, M. Zheng, C. Ji, Y. Xie and Y. Mao, *J. Hum. Genet.*, 2007, **52**, 415-422.

19.     C. M. Sassetti and E. J. Rubin, *Proc. Natl. Acad. Sci. USA*, 2003, **100**, 12989-12994.

20.     K. C. Kelley, K. J. Huestis, D. A. Austen, C. T. Sanderson, M. A. Donoghue, S. K. Stickel, E. S. Kawasaki and M. S. Osburne, *Gene*, 1995, **156**, 33-36.

21.     T. H. Grossman, E. S. Kawasaki, S. R. Punreddy and M. S. Osburne, *Gene*, 1998, **209**, 95-103.

22.     Z. A. Sánchez-Quitian, C. Z. Schneider, R. G. Ducati, W. F. de Azevedo Jr, C. Bloch Jr, L. A. Basso and D. S. Santos, *J. Struct. Biol.*, 2010, **169**, 413-423.

23.     D. Renck, R. G. Ducati, M. S. Palma, D. S. Santos and L. A. Basso, *Arch. Biochem. Biophys.*, 2010, **497**, 35-42.

24.	D. C. Rostirolla, A. Breda, L. A. Rosado, M. S. Palma, L. A. Basso and D. S. Santos, *Arch. Biochem. Biophys.*, 2011, **505**, 202-212.

25.	J. E. Nunes, R. G. Ducati, A. Breda, L. A. Rosado, B. M. de Souza, M. S. Palma, D. S. Santos and L. A. Basso, *Arch. Biochem. Biophys.*, 2011, **512**, 143-153.

26.	L. K. B. Martinelli, R. G. Ducati, L. A. Rosado, A. Breda, B. P. Selbach, D. S. Santos and L. A. Basso, *Mol. Biosyst.*, 2011, **7**, 1289-1305.

27.	J. D. de Mendonça, O. Adachi, L. A. Rosado, R. G. Ducati, D. S. Santos and L. A. Basso, *Mol. Biosyst.*, 2011, **7**, 119-128.

28.	M. A. Schumacher, C. J. Bashor, M. H. Song, K. Otsu, S. Zhu, R. J. Parry, B. Ullman and R. G. Brennan, *Proc. Natl. Acad. Sci. USA*, 2002, **99**, 78-83.

29.	K. F. Jensen, S. Arent, S. Larsen and L. Schack, *FEBS J.*, 2005, **272**, 1440-1453.

30.	L. Linde and K. F. Jensen, *Biochim. Biophys. Acta*, 1996, **1296**, 16-22.

31.	Y. P. Dai, C. S. Lee and W. J. O'Sullivan, *Int. J. Parasitol.*, 1995, **25**, 207-214.

32.	H. K. Jensen, N. Mikkelsen and J. Neuhard, *Protein Expr. Purif.*, 1997, **10**, 356-364.

33.	U. B. Rasmussen, B. Mygind and P. Nygaard, *Biochim. Biophys. Acta*, 1986, **881**, 268-275.

34.	K. F. Jensen and B. Mygind, *Eur. J. Biochem.*, 1996, **240**, 637-645.

35.	H. De Brabandere, N. Forsgard, L. Israelsson, J. Petterson, E. Rydin, M. Waldebäck and P. J. Sjöberg, *Anal. Chem.*, 2008, **80**, 6689-6697.

36.	V. Henri, L. Michaelis and M. L. Menten, *Biochem. Z.*, 1913, **49**, 333-369.

37.	S. Christoffersen, A. Kadziola, E. Johansson, M. Rasmussen, M. Willemoës and K. F. Jensen, *J. Mol. Biol.*, 2009, **393**, 464-477.

38.	I. H. Segel, *Enzyme kinetics, behavior and analysis of rapid equilibrium and steady-state enzyme systems*, John Wiley and Sons, Inc., New York, 1975.

39.     R. A. Copeland, *Evaluation of enzyme inhibitors in drug discovery, a guide for medicinal chemists and pharmacologists*, John Wiley and Sons, Inc., New Jersey, 2005.

40.     J. E. Ladbury and M. L. Doyle, *Biocalorimetry II*, Wiley, London, 2004.

41.     A. Brown, *Int. J. Mol. Sci.*, 2009, **10**, 3457-3477.

42.     C. Lundegaard and K. F. Jensen, *Biochemistry*, 1999, **38**, 3327-3334.

43.     M. A. Schumacher, D. Carter, D. M. Scott, D. S. Roos, B. Ullman and R. G. Brennan, *EMBO J.*, 1998, **17**, 3219-3232.

44.     S. Arent, P. Harris, K. F. Jensen and S. Larsen, *Biochemistry*, 2005, **44**, 883-892.

45.     K. Hiromi, in *Kinetics of fast enzyme reactions*, Halsted press, New York, 1979, pp. 226-236.

46.     H. Nakatani and K. Hiromi, *J. Biochem.*, 1980, **87**, 1805-10.

47.     U. K. Laemmli, *Nature*, 1970, **227**, 680-685.

48.     M. M. Bradford, *Anal. Biochem.*, 1976, **72**, 248-254.

49.     G. D. Brand, F. C. Krause, L. P. Silva, J. R. Leite, J. A. Melo, M. V. Prates, J. B. Pesquero, E. L. Santos, C. R. Nakaie, C. M. Costa-Neto and C. Bloch Jr, *Peptides*, 2006, **27**, 2137-2146.

50.     S.E. Harding and D.J. Winzor, in *Protein-Ligand Interactions: Hydrodynamics and Calorimetry: Practical approach,* ed. S.E. Harding and B.Z. Chowdhry, Oxford University Press, Oxford, 2001, pp. 105-135.

51.     D.J. Winzor and S.E. Harding, in *Protein-Ligand Interactions: Hydrodynamics and Calorimetry: Practical approach,* ed. S.E. Harding and B.Z. Chowdhry, Oxford University Press, Oxford, 2001, pp. 75-104.

52.     J. C. Borges and C. H. I. Ramos, *Curr. Med. Chem.*, 2011, **18**, 1276-1285.

53.     P. Natalini, S. Ruggieri, I. Santarelli, A. Vita and G. Magni, *J. Biol. Chem.*, 1979, **254**, 1558-1563.

54.     P. F. Cook and W. W. Cleland, *Enzyme kinetics and mechanism*, Garland Science

Publishing, New York, 2007.

55.     V. K. Sambandamurthy and W. R. Jacobs Jr., *Microbes Infect.*, 2005, **7**, 955-961.

56.     A. T.  Kamath, U. Fruth, M. J. Brennan, R.  Dobbelaer, P. Hubrechts, M. M. Ho, R. E.

Mayner, J. Thole, K. B. Walker, M. Liu, P. H. Lambert, AERAS Global TB Vaccine

Foundation and World Health Organization, *Vaccine*, 2005, **23**, 3753-61.

# Figure legends

**Fig. 1** Chemical reaction catalyzed by *Mt*UPRT.

**Fig. 2** SDS-PAGE analysis of *Mt*UPRT purification steps. Lane 1, molecular weight protein marker; lane 2, crude extract; lane 3, sample loaded onto DEAE Sepharose CL6B column; lane 4, sample loaded onto Sephacryl S-300 column; lane 5, sample loaded onto Mono Q column; lane 6, homogeneous recombinant *Mt*UPRT eluted from the Mono Q column.

**Fig. 3** Sedimentation equilibrium experiment. Data analysis involved fitting a model of absorbance versus cell radius data by applying nonlinear regression. The experimental data for 1.5 mg/mL of protein at 9,000 and 11,000 rpm are shown. The random distribution of the residues (top panel) indicated a good quality fit in agreement with monomer-tetramer equilibrium.

**Fig. 4** Apparent steady-state kinetic parameters. (A) Specific activity of *Mt*UPRT (U mg$^{-1}$) as a function of increasing PRPP concentration in the presence of constant uracil concentration (10 µM). (B) Specific activity of *Mt*UPRT as a function of increasing uracil concentration in the presence of constant PRPP concentration (100 µM). (C) Specific activity of *Mt*UPRT as a function of increasing PRPP concentration in the presence of constant concentrations of uracil (10 µM) and GTP (100 µM). (D) Specific activity of *Mt*UPRT as a function of increasing uracil concentration in the presence of constant concentrations of PRPP (100 µM) and GTP (100 µM).

**Fig. 5** Evaluation of nucleotides as allosteric effectors. All reactions contained 100 μM PRPP and 10 μM uracil. (●) standard reaction, (○) standard reaction containing 500 μM GTP, (□) standard reaction containing 500 μM CTP, (Δ) standard reaction containing 500 μM ATP, (×) standard reaction containing 500 μM UTP, (■) standard reaction containing 100 μM UMP, (▲)standard reaction containing both 100 μM UMP and 500 μM CTP.

**Fig. 6** Initial velocity patterns for *Mt*UPRT. Double-reciprocal plot of enzyme specific activity$^{-1}$ (mg U$^{-1}$) versus [PRPP]$^{-1}$ (μM$^{-1}$). Concentrations of uracil were: 6 μM (open circles), 8 μM (filled triangle), and 10 μM (open squares).

**Fig. 7** Isothermal titration (ITC) curves of binding of ligands to *Mt*UPRT. (A) Reverse titration of PRPP substrate. (B) Titration of uracil substrate. (C) Reverse titration of UMP product. (D) Titration of PP$_i$ product.

**Fig. 8** Proposed kinetic mechanism for *Mt*UPRT.

**Fig. 9** Dependence of kinetic parameters on pH. (A) pH dependence of log $k_{cat}$. (B) pH dependence of log $k_{cat}/K_{PRPP}$.

**Fig. 10** Representative stopped-flow trace for product formation. The first-order rate constant for product formation yielded values of $0.94 \pm 0.02$ s$^{-1}$ and $0.58 \pm 0.01$ s$^{-1}$ in the absence (A) and presence (B) of 1 mM GTP, respectively. The bottom stopped-flow traces represent the control experiment in the absence of *Mt*UPRT.

**Fig. 11** Pre-steady-state kinetics of *Mt*UPRT-PRPP binary complex formation. The dependence of observed association rate constant on PRPP concentration is shown. Inset presents the PRPP-dependent variation in signal amplitude.


**Fig 12** Kinetics of PRPP binding to *M. tuberculosis* UPRT. The fast bimolecular process of binary complex formation is preceded by a slow isomerization process of free enzyme.

**Table 1**

Purification of *Mt*UPRT from *E. coli* BL21(DE3) electrocompetent host cells.[a]

| Purification step | Total protein (mg) | Total enzyme activity (U) | Specific activity (U mg$^{-1}$) | Purification fold | Yield (%) |
|---|---|---|---|---|---|
| Crude extract | 132.74 | 100.47 | 0.76 | 1.0 | 100 |
| DEAE Sepharose CL6B | 86.70 | 95.92 | 1.11 | 1.5 | 95 |
| Sephacryl S-300 | 41.32 | 35.63 | 0.86 | 1.1 | 35 |
| Mono Q | 20.23 | 31.61 | 1.56 | 2.1 | 31 |

[a] Typical purification protocol starting from 2 g of wet cells.

**Table 2**

Thermodynamic parameters of PRPP and UMP ligands binding to *Mt*UPRT.[a]

| Ligands | $K_a$ (M$^{-1}$) | $\Delta H$ (kcal mol$^{-1}$) | $\Delta S$ (cal mol$^{-1}$ deg$^{-1}$) | $\Delta G$ (kcal mol$^{-1}$) | $K_d$ (μM) |
|---|---|---|---|---|---|
| **PRPP** | | | | | |
| Subunit 1 | $2.0 \,(\pm 3.6) \times 10^5$ | $2.8 \pm 0.3$ | $34 \pm 6$ | $-7 \pm 1$ | $5.0 \pm 0.9$ |
| Subunit 2 | $2.1 \,(\pm 0.6) \times 10^4$ | $-3 \pm 16$ | $10 \pm 3$ | $-6 \pm 2$ | $48 \pm 15$ |
| Subunit 3 | $1.6 \,(\pm 0.5) \times 10^5$ | $-41 \pm 32$ | $-114 \pm 33$ | $-7 \pm 2$ | $6 \pm 2$ |
| Subunit 4 | $1.1 \,(\pm 0.4) \times 10^5$ | $58 \pm 22$ | $217 \pm 85$ | $-7 \pm 3$ | $9 \pm 4$ |
| **UMP** | | | | | |
| Subunit 1 | $7 \,(\pm 2) \times 10^4$ | $-5.1 \pm 0.4$ | $5 \pm 1$ | $-7 \pm 2$ | $14 \pm 3$ |
| Subunit 2 | $1.5 \,(\pm 5) \times 10^5$ | $6 \pm 3$ | $45 \pm 16$ | $-7 \pm 2$ | $7 \pm 2$ |
| Subunit 3 | $1.2 \,(\pm 0.4) \times 10^5$ | $-24 \pm 11$ | $-56 \pm 21$ | $-7 \pm 3$ | $8 \pm 3$ |
| Subunit 4 | $8 \,(\pm 3) \times 10^4$ | $28 \pm 18$ | $117 \pm 43$ | $-7 \pm 2$ | $13 \pm 5$ |

[a] $K_a$ = association constant; $\Delta H$ = binding enthalpy; $\Delta S$ = binding entropy; $\Delta G$ = Gibbs free energy; $K_d$ = dissociation constant.

**Figure 1.**

**Figure 2.**

**Figure 3.**



UPRT 1.5 mg/mL

● 11,000 rpm
○ 9,000 rpm
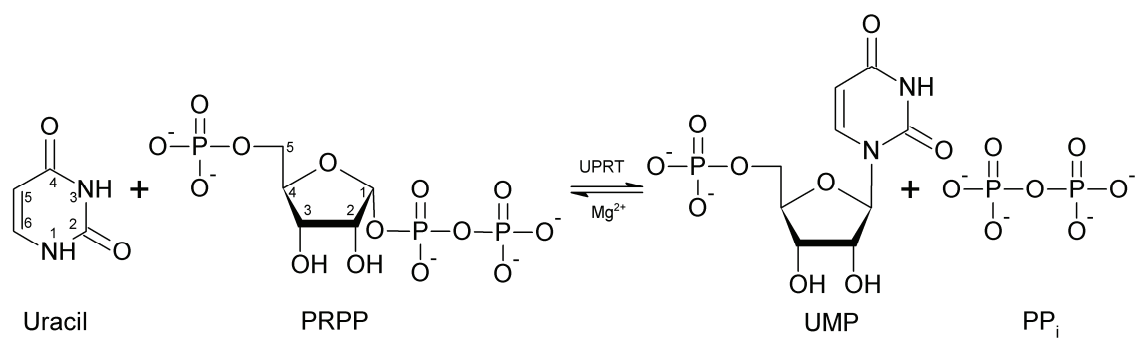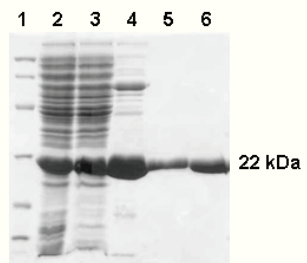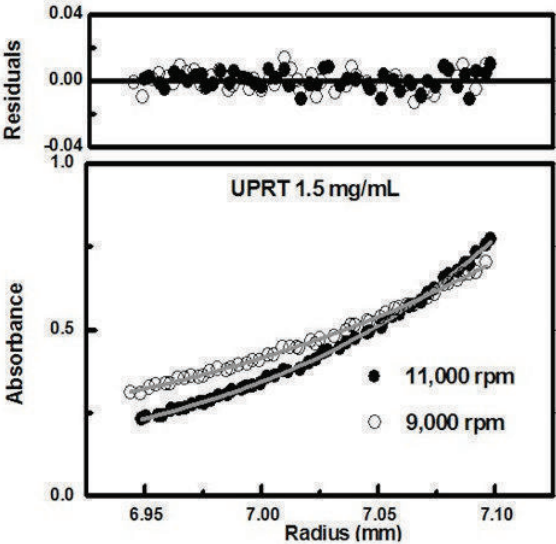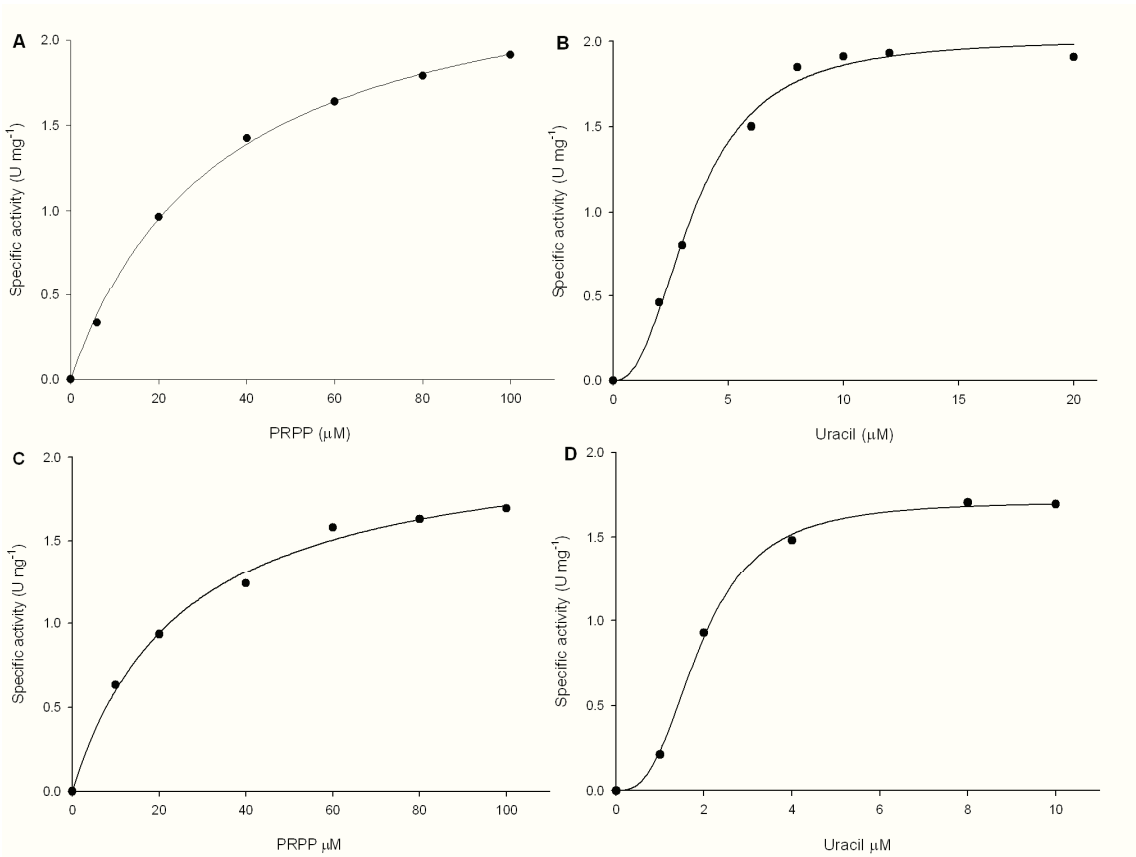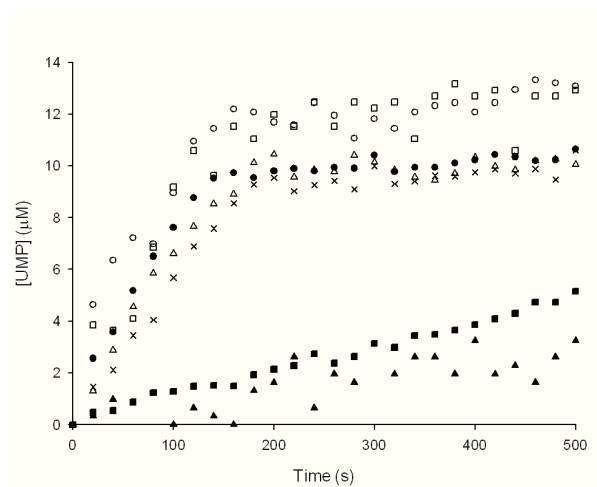
**Figure 4.**

**Figure 5.**

**Figure 6.**

**Figure 7.**

**Figure 8.**

$$\text{PRPP.Mg}^{2+} \qquad\qquad \text{uracil} \qquad\qquad\qquad\qquad\qquad\qquad\qquad\qquad\qquad \text{PP}_i.\text{Mg}^{2+} \qquad\qquad \text{UMP}$$

E　　　E-PRPP.Mg²⁺　　　E-PRPP.Mg²⁺-uracil ⇌ E-PP_i.Mg²⁺-UMP　　　E-UMP　　　E
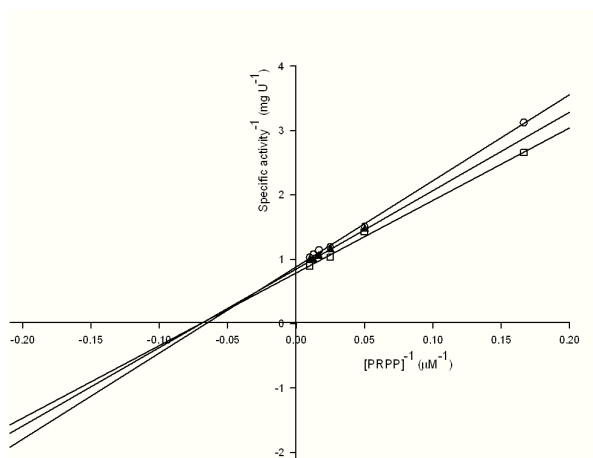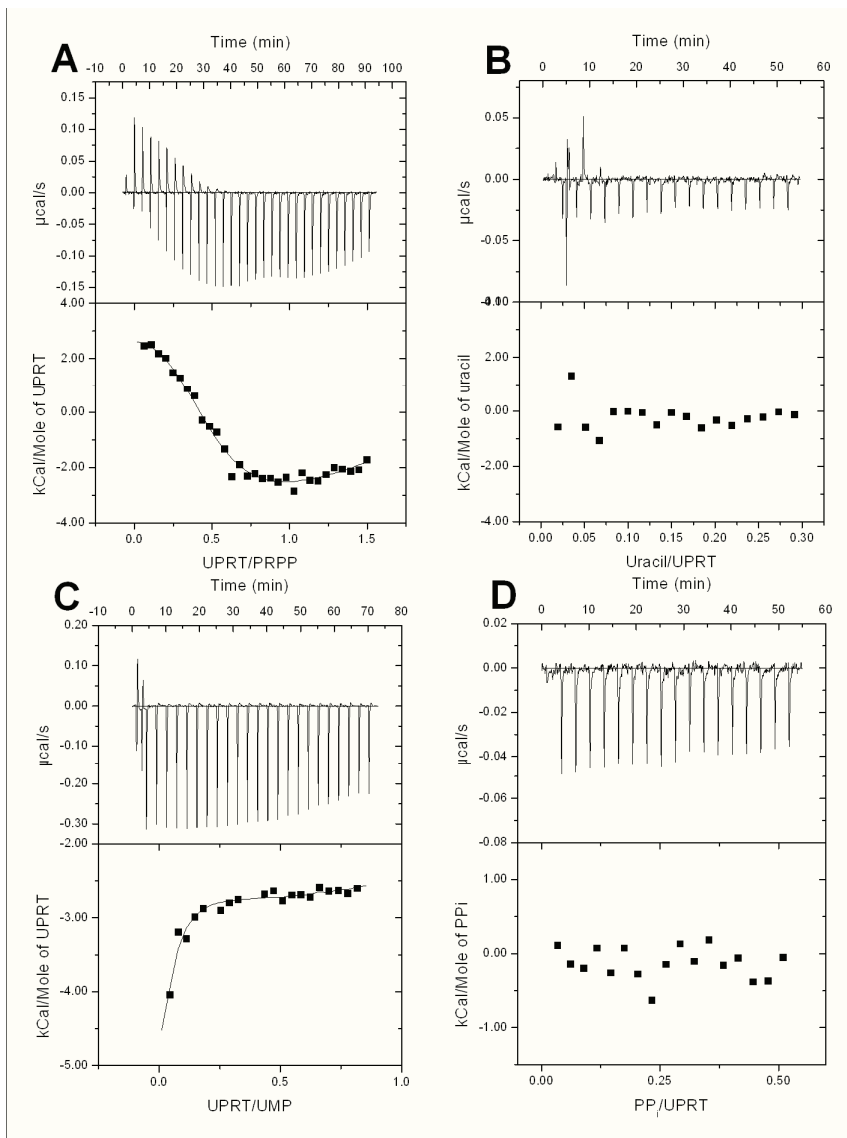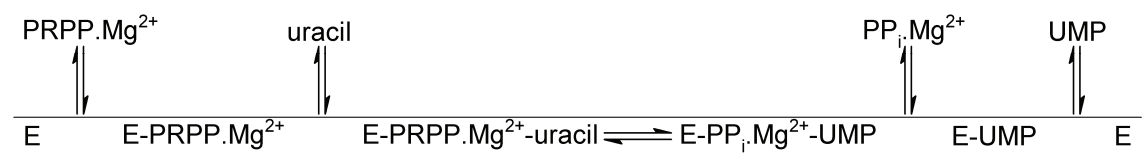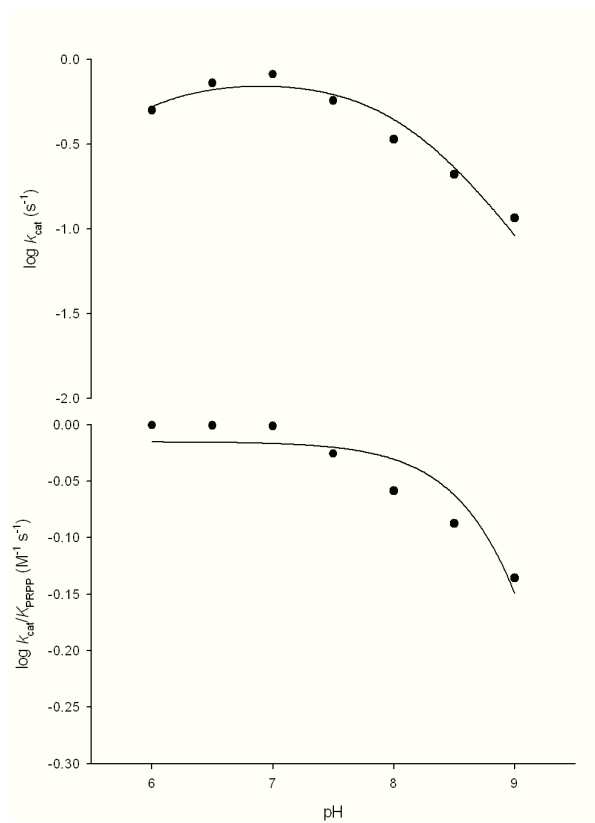
**Figure 9.**

**Figure 10.**

**Figure 11.**

**Figure 12.**

$$Mt\text{UPRT*} \underset{k_{-2}}{\overset{k_2}{\rightleftarrows}} Mt\text{UPRT} + \text{PRPP} \underset{k_{-1}}{\overset{k_1}{\rightleftarrows}} Mt\text{UPRT:PRPP}$$

$$\underbrace{\qquad\qquad\qquad\qquad}_{\textbf{SLOW}} \qquad \underbrace{\qquad\qquad\qquad\qquad}_{\textbf{FAST}}$$
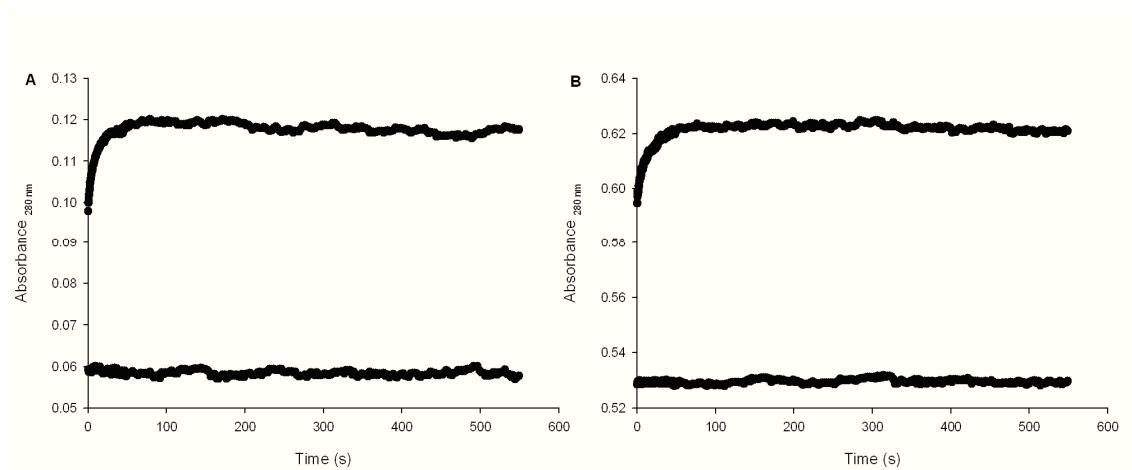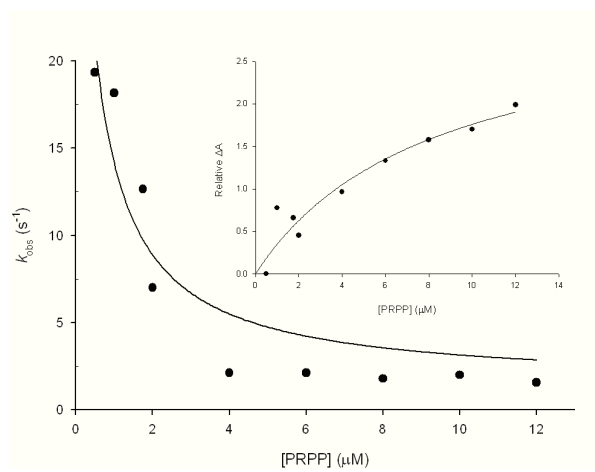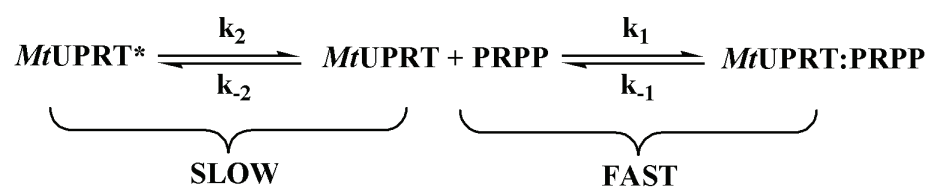
# Capítulo 4

**4. Nocaute do gene *upp***

   4.1 Construção da cepa de *M. tuberculosis* H37Rv mutante para o gene *upp*

   4.2 Construção da cepa de *M. tuberculosis* H37Rv mutante para o gene *upp* complementada com uma cópia extra do gene *upp*

   4.3 Curvas de crescimento das cepas de *M. tuberculosis* H37Rv mutante para o gene *upp*, complementada e tipo selvagem

**5. Análise da expressão da UPRT em diferentes condições de crescimento de *M. tuberculosis* H37Ra**

**6. Metabólito ativo do *isoxyl* como inibidor da *Mt*UPRT**

   6.1 Análises da incorporação de bases e nucleosídeos marcados com trítio em culturas de *M. tuberculosis* H37Ra

   6.2 Ensaio de atividade da *Mt*UPRT e reação de ativação do *isoxyl*

   6.3 Concentração inibitória mínima do *isoxyl* para as cepas de *M. tuberculosis* mutante para o gene *upp*, complementada e tipo selvagem

## 4. Nocaute do gene *upp*

A mutagênese sítio-dirigida por substituição gênica é uma técnica genética importante que permite a obtenção de mutações definidas em um gene específico, onde a substituição do alelo tipo selvagem do gene pelo alelo mutado é obtida por recombinação homóloga. A substituição gênica visa caracterizar funções de proteínas do *M. tuberculosis* e identificar fatores de virulência, representando uma abordagem única para: (1) confirmar que um gene identificado por homologia de sequência por ter determinada atividade biológica realmente tem a função predita; (2) medir a importância qualitativa e quantitativa de determinada atividade biológica tanto na fisiologia da bactéria como *in vivo* durante a infecção no hospedeiro (47).

Em micobactérias, e especialmente no *M. tuberculosis*, a recombinação homóloga ocorre em frequência baixa, abaixo de $10^{-3}$ eventos por célula, o que dificulta a obtenção de mutantes definidos em *M. tuberculosis* (48). Assim, o sucesso no isolamento de mutantes em *M. tuberculosis* é dependente da habilidade de técnicas genéticas e protocolos utilizados para compensar pela baixa eficiência de transformação e possibilitar a detecção eficiente ou seleção de mutantes de troca alélica entre a população total de transformantes (47). Portanto, o uso de um vetor replicativo e integrativo evita os problemas decorrentes da baixa eficiência de transformação, admite que o vetor seja eficientemente perdido em determinadas condições e permite a eliminação de clones que ainda contenham o vetor, possibilitando assim a detecção de eventos genéticos muito raros (19). Um sistema assim foi desenvolvido, que utiliza as propriedades seletivas do gene *sacB*, do gene

*xylE* e da origem de replicação micobacteriana termossensível, permitindo a seleção de mutantes de inserção positivos (19). O protocolo utilizado está descrito detalhadamente abaixo.

**4.1 Construção da cepa de *M. tuberculosis* H37Rv mutante para o gene *upp*:**

O fragmento de DNA incluindo o gene *upp* (624 pb) e regiões flanqueadoras *upstream* (911 pb) e *downstream* (471 pb) ao gene (tamanho total de 2.006 pb) (**Figura 7A**) foi amplificado a partir do DNA genômico de *M. tuberculosis* H37Rv utilizando dois oligonucleotídeos iniciadores (5'-AG<u>TCTAGA</u>GTAGTGGCTGATGGTCT-3' e 5'-CT<u>TCTAGA</u>AAGCGATCGGGCACTG-3') complementares as porções 5' e 3' das regiões flanqueadoras do gene *upp*, contendo sítios para a enzima de restrição *Xba*I (New England Biolabs) (sublinhado). Este fragmento de DNA foi clonado no vetor pUC19 (Invitrogen) utilizando o sítio de restrição *Xba*I. O sequenciamento automático de DNA confirmou a identidade e integridade do gene *upp* e das regiões flanqueadoras, mostrando que nenhuma mutação ocorreu na etapa de amplificação. O cassete contendo o gene que confere resistência à canamicina (Can$^R$) (1252 pb, extraído do vetor pUC4K com a enzima de restrição *Hinc*II) foi inserido no gene *upp* utilizando o sítio de restrição *Afe*I (New England Biolabs), o qual está presente naturalmente na sequência do gene (**Figura 7B**). O fragmento foi então clonado no vetor pPR27*xylE* utilizando o sítio de restrição *Xba*I.
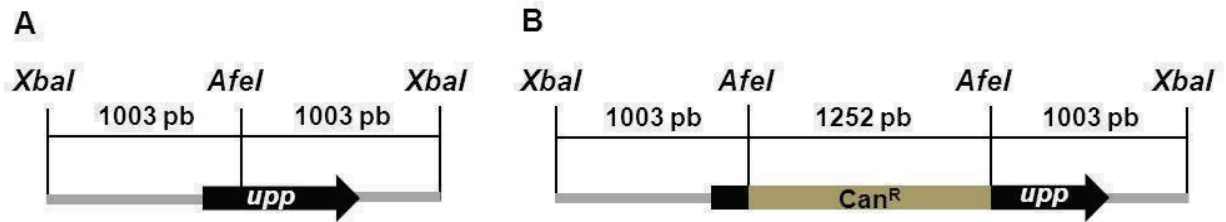
**Figura 7.** Etapas de construção do nocaute do gene *upp*. A. Fragmento amplificado a partir do DNA genômico de *M. tuberculosis* H37Rv, mostrando o sítio para a enzima de restrição *Afe*I que existe naturalmente na sequência do gene *upp* (tipo selvagem). 2. O cassete contendo o gene que confere resistência à canamicina (Can[R]) foi inserido no gene *upp* utilizando o sítio para a enzima de restrição *Afe*I (Δ*upp*::Can). Em cinza estão representadas as regiões que flanqueiam o gene *upp* que foram incluídas na construção.

O vetor pPR27*xylE* tem algumas características que facilitam a seleção positiva de mutantes por inserção em *M. tuberculosis*, como:

- Origem de replicação micobacteriana termossensível: a 32ºC o vetor replica e 39ºC ele não replica facilitando o evento de recombinação homóloga;

- Presença do gene *sacB*: a expressão do gene é letal na presença de sacarose;

- Presença do gene *xylE*: expressão do gene pode ser verificada com catecol, colônias amarelas são obtidas (19).

A construção pPR27*xylE* Δupp::can foi transformada por eletroporação em *M. tuberculosis* H37Rv. As células foram recuperadas em 5 mL do meio de cultura Middlebrook 7H9 tween 80 0,05%, ADC 10% (complexo contendo albumina, dextrose e catalase), canamicina 25 μg/mL por 48 horas a 32ºC, foram plaqueadas em meio de cultura Middlebrook 7H11 OADC 10% (complexo contendo ácido oleico, albumina, dextrose e catalase), canamicina 25 μg/mL e incubadas a 32ºC. Após aproximadamente 1 mês, as colônias foram verificadas com 1 % de catecol, e as colônias amarelas (Can[R] e *XylE*[+]) foram inoculadas em 5 mL do meio de cultura Middlebrook 7H9 tween 80 0,05%, ADC 10%, canamicina 25 μg/mL a 32ºC e incubadas por aproximadamente 1

mês. Então, as culturas foram diluídas (0, $10^{-1}$, $10^{-2}$, $10^{-3}$ e $10^{-4}$) utilizando meio de cultura e 200 μL de cada diluição foi plaqueado em Middlebrook 7H11 OADC 10%, canamicina 25 μg/mL contendo sacarose 2%. As placas foram incubadas a 39 ºC por aproximadamente 1 mês e então as colônias foram verificadas com 1% de catecol. Aproximadamente 90 % das colônias apresentaram coloração branca ($Sac^R$, $Can^R$ e $XylE^-$), sugerindo que a troca alélica ocorreu. As colônias brancas foram inoculadas em 5 mL do meio de cultura Middlebrook 7H9 Tween 80 0,05%, ADC 10%, canamicina 25 μg/mL a 37ºC e incubadas por aproximadamente 1 mês. O DNA genômico das cepas foi extraído.

Para verificar a obtenção de mutantes, ou seja, eventos de *double cross-over* (DCO), dois oligonucleotídeos iniciadores (5'-ACGGCGGCTAGTCGCCCCAA-3' e 5'-GCGCATCACGCTGCCGTGCA-3') que anelam fora da região clonada no vetor pPR27*xylE* foram utilizados na reação em cadeia da polimerase (PCR). Três diferentes eventos podem ter ocorrido (47):

1)      DCO: um fragmento de 3500 pb seria obtido devido a presença do cassete contendo o gene que confere resistência à canamicina interrompendo o gene *upp*.

2)      *Single cross-over* (SCO): nenhum fragmento seria observado, uma vez que o fragmento a ser amplificado seria muito grande (aproximadamente 15 kb) devido a inserção do corpo do vetor pPR27*xylE* no DNA genômico juntamente com a cópia do gene *upp* interrompida e a cópia selvagem.

3)      Recombinação ilegítima: um fragmento do tamanho de 2206 pb seria observado, que é o tamanho referente a cópia selvagem do gene *upp* e das regiões

flanqueadoras, uma vez que a recombinação do pPR27*xylE* Δupp::Can ocorreria de forma não homóloga entre qualquer parte do plasmídeo e do cromossomo, sendo inserido em qualquer região.

Dezesseis clones foram analisados e conforme mostrado na **Figura 8**, todos os clones possuíam o gene *upp* interrompido pelo cassete de canamicina (DCO) e a ausência da cópia selvagem do gene. Portanto, o gene *upp* não é essencial para o crescimento de *M. tuberculosis* H37Rv nas condições empregadas no experimento.
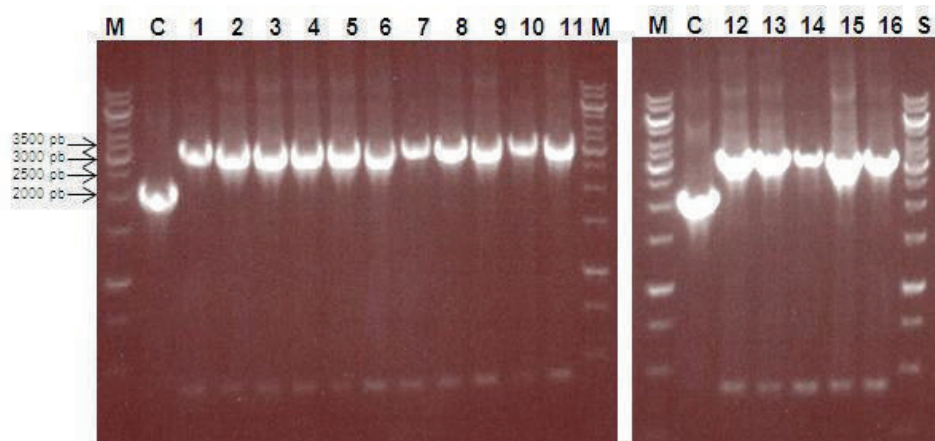


**Figura 8**. Eletroforese em gel de agarose do produto do PCR para verificação da obtenção de cepas de *M. tuberculosis* H37Rv mutantes para o gene *upp*. M: marcador de peso molecular; C: controle, PCR realizado com o DNA genômico *M. tuberculosis* H37Rv tipo selvagem; 1-16: PCR realizado com DNA genômico extraído dos mutantes.

**4.2 Construção da cepa de *M. tuberculosis* H37Rv mutante para o gene *upp* complementada com uma cópia extra do gene *upp*:**

A cepa de *M. tuberculosis* H37Rv mutante para o gene *upp* foi complementada com uma cópia extra do gene *upp,* para ser utilizada como controle nos experimentos subsequentes, mostrando que a estratégia de nocaute utilizada afetou apenas o gene em questão. Assim, dois pares de oligonucleotídeos iniciadores (5`-CCCAAACATATGGTGCAGGTCCATGTCGTTGACC-3' e 5`-CCCAAAAAGCTTTCAGCGCGGGCCGAACTGGC-3`) contendo sítios para as enzimas de restrição *Nde*I e *Hind*III (sublinhados), respectivamente, foram utilizados para amplificar o gene *upp* de *M. tuberculosis* H37Rv. Este fragmento de DNA foi clonado no vetor pMVHG1 utilizando os sítios de restrição *Nde*I e *Hind*III (pMVHG1::Mt_upp). O sequenciamento automático de DNA confirmou a identidade e integridade do gene *upp*, mostrando que nenhuma mutação ocorreu na etapa de amplificação.

Além disso, a cepa de *M. tuberculosis* H37Rv mutante para o gene *upp* foi complementada com o vetor pNIP40 contendo o gene *upp* de *Mycobacterium smegmatis* (Msmeg_1694, gene ortólogo ao gene *upp* de *M. tuberculosis*). Assim, dois pares de oligonucleotídeos iniciadores (5'-TGTCTAGATGCGCGTCGGCCTTG-3' e 5'-ACTCTAGACGACGATCTGGCCGC-3') contendo sítios para a enzima de restrição *Xba*I (sublinhados), foram utilizados para amplificar o gene *upp* de *M. smegmatis*. Este fragmento de DNA foi clonado no vetor pNIP40 utilizando o sítio de restrição *Xba*I (pNIP40::Ms_upp). O sequenciamento automático de DNA confirmou a identidade e

integridade do gene *upp*, mostrando que nenhuma mutação ocorreu na etapa de amplificação.

### 4.3 Curvas de crescimento das cepas *M. tuberculosis* H37Rv mutante para o gene *upp*, complementada e tipo selvagem:

As cepas de *M. tuberculosis* H37Rv mutante para o gene *upp* transformada com o vetor pMVHG1 e pNIP40 ambos sem inserto, complementada (pMVHG1::Mt_upp e pNIP40::Ms_upp) e tipo selvagem foram inoculadas em meio de cultura Middlebrook 7H9 tween 80 0,05%, ADC 10% a 37ºC. Os antibióticos canamicina 25 µg/mL e higromicina 50 µg/mL foram adicionados nas culturas com as cepas mutante e complementada. A densidade ótica a 600 nm ($OD_{600}$) foi monitorada após 8, 11, 13 e 19 dias de crescimento (**Figura 9**) e pode-se observar que a ausência do gene *upp* não afetou o crescimento do *M. tuberculosis* H37Rv (**Figura 9**).
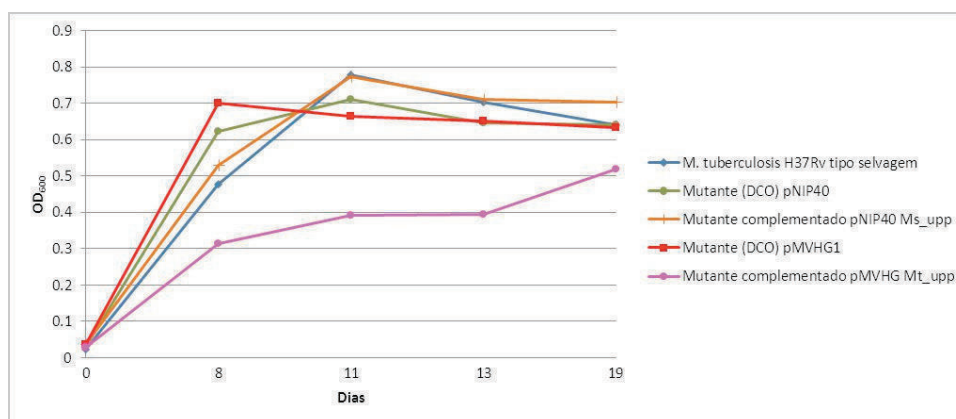


**Figura 9.** Curva de crescimento com as cepas *M. tuberculosis* H37Rv tipo selvagem, *M. tuberculosis* H37Rv mutante para o gene *upp* (DCO) transformado com pNIP40 e pMVHG1 ambos sem inserto e *M. tuberculosis* H37Rv mutante complementado com pNIP40 Ms_upp e

pMVHG1 Mt_upp. O experimento foi realizado em duplicatas e os dados apresentados são as médias dos valores obtidos.

## 5. Análise da expressão da UPRT em diferentes condições de crescimento de *M. tuberculosis* H37Ra

A expressão da UPRT foi analisada em diferentes condições de crescimento de *M. tuberculosis* H37Ra tipo selvagem. As condições de altos níveis de oxigênio foram incubadas a 37ºC e 140 rpm e estão listadas abaixo:

1) Meio de cultura Sauton com tyloxapol e adição de bases:

    a. Controle (sem a adição de bases)

    b. Adição de 20 µg/mL de uracil

    c. Adição de 20 µg/mL de cada base uracil, timina e citosina

    d. Adição de 20 µg/mL de cada base adenina e guanina

    e. Adição de 20 µg/mL de cada base uracil, timina, citosina, adenina e guanina.

2) Meio de cultura Sauton com tyloxapol foi feita uma curva de crescimento e amostras foram coletadas na $OD_{600}$ de 0,7, 1,4, 2,1 e 2,4.

3) Meio de cultura Middlebrook 7H9 tween 80 0,05%, ADC 10% foi feita uma curva de crescimento e amostras foram coletadas na $OD_{600}$ de 0,7, 1,4, 1,8 (10 dias de crescimento) e 1,8 (15 dias de crescimento).

As condições de baixos níveis de oxigênio que foram analisadas estão listadas abaixo:

1) Meio de cultura Middlebrook 7H9 tween 80 0,05%, ADC 10% em tubos de vidro com barra magnética para agitação a 37ºC, mantendo 2/3 do volume do tubo preenchido e a tampa do tubo bem fechada, para que ocorra a depleção gradual de oxigênio como descrito anteriormente por Wayne e Hayes (modelo de Wayne) (49). Para observar a depleção de oxigênio, 1,5 μg/mL de azul de metileno foi adicionado ao meio de cultura do tubo controle, na ausência de oxigênio a coloração altera de azul para branco. Além disso, como controle, alguns tubos foram mantidos com a tampa parcialmente aberta para que estes contenham oxigênio durante todo o experimento, como controle do modelo de Wayne, assim 1,5 μg/mL de azul de metileno foi adicionado ao meio de cultura do tubo controle, o qual manteve a coloração azul durante todo o experimento. Quatro diferentes tempos foram coletados, sendo que o primeiro ponto foi 1 semana e os outros 2, 3 e 4 semanas após a depleção de oxigênio.

2) Meio de cultura Sauton com tyloxapol, o modelo de Wayne e o controle foram realizados como descrito acima.

3) Meio de cultura Sauton sem tyloxapol incubado a 37ºC e com crescimento em película de superfície. As células foram coletadas no estágio inicial e final de crescimento.

Para a detecção da expressão da proteína nas diferentes condições de crescimento listadas acima, anticorpos produzidos em camundongo contra a *Mt*UPRT homogênea (anticorpo primário) e western blot foram utilizados. O anticorpo primário

(diluição 1:500) e o anticorpo secundário (diluição 1:5000), anti-IgG de camundongo acoplado à peroxidase (Sigma-Aldrich), foram diluídos em TBS 1X (tris HCl 10 mM pH 7,4 contendo NaCl 0,9%) contendo tween 20 0,05% e leite em pó 3%. A revelação do western blot foi realizada utilizando o substrato Pierce ECL western blotting (Thermo Scientific) e o filme Kodak BioMax light film (Kodak) utilizado para detecção por quimiluminescência.

Conforme mostrado na **Figura 10A e B**, a proteína UPRT não apresentou diferenças na expressão quando comparada com os controles, tanto nas condições de altos quanto baixos níveis de oxigênio. Isso significa que a expressão da UPRT é basal e que a presença de bases púricas ou pirimídicas ou também ausência de oxigênio não induzem a expressão da proteína.

### 6. Metabólito ativo do *isoxyl* como inibidor da *Mt*UPRT

O *isoxyl* (tiocarlida, 4,4'-diisoamyloxydiphenylthiourea) (**Figura 11**) é um derivado tiouréia que foi utilizado no tratamento clínico da TB nos anos 60 e descrito como sendo um inibidor da síntese de ácidos oléico e micólico em *M. tuberculosis* (50). Isolados clínicos de *M. tuberculosis* de diferentes áreas geográficas e apresentando padrões distintos de resistência a drogas mostraram-se sensíveis ao *isoxyl* na faixa de 1 à 10 μg/mL (51).

O *isoxyl* é uma pró-droga ativada por reações de oxidação no grupamento tiocarbonil (**Figura 11**), catalisadas pela proteína EthA, para expressar sua atividade antimicobacteriana. Além de ser ativadora do *isoxyl*, a proteína EthA foi descrita como

sendo ativadora de drogas de segunda linha utilizadas no tratamento da TB, como a etionamida e a tiacetazona. A proteína EthA é uma monooxigenase (codificada pelo gene ethA, Rv3854c) que está sobre o controle do regulador transcricional EthR (Rv3855), um membro da família de repressores TetR, que interage diretamente com a região promotora da proteína EthA reprimindo a sua expressão (52). Inibidores de EthR mostraram aumentar a potência da etionamida em dez vezes em culturas de *M. tuberculosis* (53).
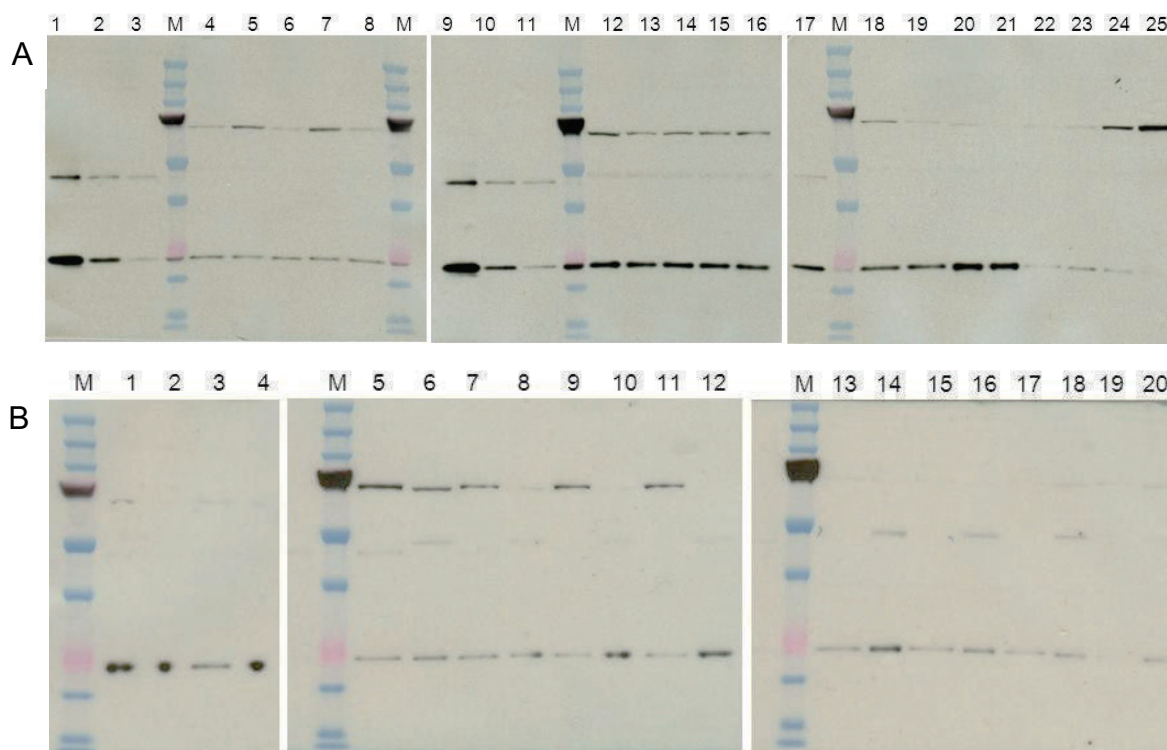


**Figura 10.** Análise da expressão da UPRT por western blot. M: marcador de peso molecular (precision plus protein dual color standards – Bio-Rad). **A.** *Mt*UPRT homogênea utilizada como controle do experimento nas quantidades de 20 (canaletas 1 e 9), 10 (canaletas 2, 10 e 17 ) e 5 ng (canaletas 3 e 11); 20 µg de proteína total foi adicionado em cada canaleta; Canaletas 4 até 8: adição das bases no meio de cultura 48 horas antes de coletar as células; Canaletas 12 até 16: adição das bases desde o ínicio da cultura; Canaletas 4 e 12: controle (sem adição de bases); Canaletas 5 e 13: adição de uracil; Canaletas 6 e 14: adição de uracil, citosina e timina; Canaletas 7 e 15: adição de adenina e guanina; Canaletas 8 e 16: adição de todas as bases; Canaleta 18: modelo de Wayne; Canaleta 19: controle do modelo de Wayne (presença de

oxigênio); Canaleta 20: crescimento em película de superfície estágio inicial; Canaleta 21: crescimento em película de superfície estágio tardio; Canaleta 22: curva de crescimento, $OD_{600}$= 0,7; Canaleta 23: curva de crescimento, $OD_{600}$= 1,4; Canaleta 24: curva de crescimento, $OD_{600}$= 2,1; Canaleta 25: curva de crescimento, $OD_{600}$= 2,4; curva de crescimento foi feita com meio de cultura sauton com tyloxapol. **B.** Canaletas 1 até 4: curva de crescimento feita com meio de cultura Middlebrook 7H9 tween 80 0,05%, ADC 10%, canaleta 1: $OD_{600}$= 0,7, canaleta 2: $OD_{600}$= 1,4, canaleta 3: $OD_{600}$= 1,8, canaleta 4: $OD_{600}$= 1,8; Canaletas 5 até 12: modelo de Wayne utilizando o meio de cultura Middlebrook 7H9 tween 80 0,05%, ADC 10%; Canaletas 13 até 20: modelo de Wayne utilizando o meio de cultura Sauton com tyloxapol; Canaleta 5 e 13: coleta após 1 semana de depleção de oxigênio; Canaleta 6 e 14: coleta do controle após 1 semana de depleção de oxigênio do modelo de Wayne; Canaleta 7 e 15: coleta após 2 semana de depleção de oxigênio; Canaleta 8 e 16: coleta do controle após 2 semana de depleção de oxigênio do modelo de Wayne; Canaleta 9 e 17: coleta após 3 semana de depleção de oxigênio; Canaleta 10 e 18: coleta do controle após 3 semana de depleção de oxigênio do modelo de Wayne; Canaleta 11 e 19: coleta após 4 semana de depleção de oxigênio; Canaleta 12 e 20: coleta do controle após 4 semana de depleção de oxigênio do modelo de Wayne.
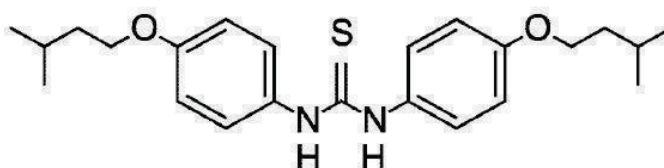


**Figura 11.** Estrutura do *isoxyl* (tiocarlida, 4,4'-diisoamyloxydiphenylthiourea) (54).

O processo de ativação do *isoxyl* pela proteína EthA *in vitro* foi proposto por Korduláková e colaboradores em 2007, onde dois metabolitos, a formimidamida (composto 3, M = 368) e o derivado de uréia (composto 5, M = 384), foram encontrados em maior quantidade por análises de cromatográfica líquida acoplada a espectrometria de massas (LC/MS) (**Figura 12**) (50).
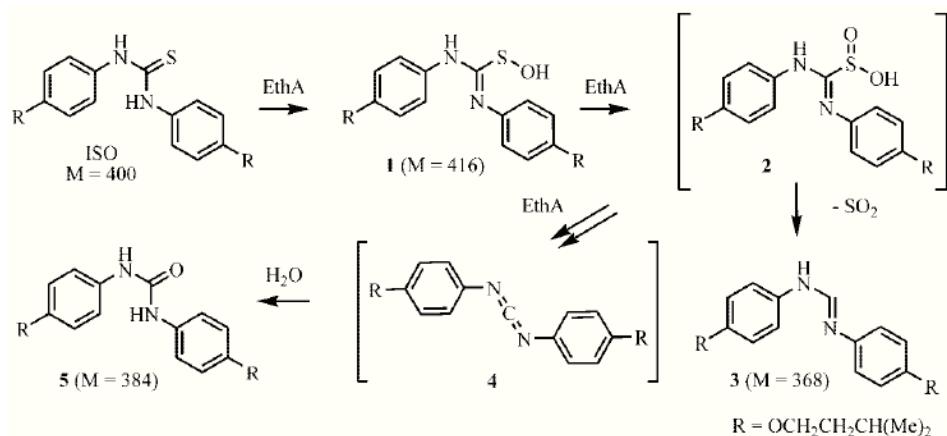
**Figura 12.** Processo de ativação proposto para o *isoxyl*. Os metabolitos formimidamida (composto 3, M = 368) e o derivado de uréia (composto 5, M = 384) foram encontrados em maior quantidade por análises de LC/MS (50).

Ainda não foi determinado como as espécies reativas derivadas do *isoxyl* desempenham a sua atividade antimicobacteriana, se é via formação de ligações covalentes dentro dos sítios ativos dos alvos enzimáticos ou através da formação de adutos dentro das células do *M. tuberculosis* (50). Assim, visando identificar novos possíveis alvos das espécies reativas derivadas do *isoxyl* no *M. tuberculosis,* como a RNA polimerase, experimentos de análise da incorporação de bases e nucleosídeos marcados com trítio em culturas de *M. tuberculosis* H37Ra foram realizados.

**6.1   Análises da incorporação de bases e nucleosídeos marcados com trítio em culturas de *M. tuberculosis* H37Ra:**

As células de *M. tuberculosis* H37Ra foram crescidas em meio de cultura Middlebrook 7H9 tween 80 0,05%, ADC 10% a 37ºC até atingir $OD_{600}$ entre 0,2 e 0,3. As células foram diluídas para uma $OD_{600}$ de 0,05, utilizando o meio de cultura mencionado acima, e incubadas a 37ºC, 140 rpm por aproximadamente 16 horas.

Então, alíquotas de 4 mL de cultura foram tratadas com uracil [³H] 2 µCi (63 pmol) e uracil 200 pmol (total de 263 pmol) ou com 4 µCi de uridina [³H] (133 pmol) , guanina [³H] (200 pmol) ou adenina [³H] (143 pmol). Além disso, 5 µg/mL de rifampicina ou 7,5 µg/mL de *isoxyl* foram adicionados às culturas, enquanto nenhuma droga foi adicionada no controle. As culturas foram incubadas a 37ºC, 140 rpm por 4 horas e todos os tratamentos foram realizados em duplicatas. As culturas foram aplicadas em filtros, o meio de cultura foi removido utilizando o vácuo e as células foram lavadas três vezes com 4 mL de PBS 1X (Fosfato 10 mM pH 7,4 contendo NaCl 137 mM e KCl 2,7 mM). Os filtros foram lavados três vezes com 2 mL de ácido trifluoroacético 10% e uma vez com 2 mL de etanol 95%. Os filtros foram removidos e transferidos para o frasco de cintilação e o líquido de cintilação foi adicionado para detecção da radioatividade incorporada pelas células.

Uma diminuição na incorporação de uracil [³H] de aproximadamente 60 % foi observada em culturas tratadas com *isoxyl* quando comparado com o controle. Esta diminuição poderia ser devido a inibição da RNA polimerase ou da incorporação de uracil. Para verificar essa hipótese um experimento utilizando uridina e uracil marcados com trítio e tratando as culturas com 5 µg/mL de rifampicina (inibidor da RNA polimerase) ou 7,5 µg/mL de *isoxyl* enquanto no controle nenhuma droga foi adicionada (**Figura 13**). Os dados foram analisados estatisticamente utilizando análise de variância com um fator (*one-way* ANOVA) e o pós-teste de comparações múltiplas de Bonferroni.

Na cultura tratada com *isoxyl* e uridina [³H] não foi observada redução significativa na incorporação de uridina comparando com o controle, enquanto que na cultura tratada com rifampicina, uma diminuição significativa de aproximadamente 40%

na incorporação de uridina foi observada em relação ao controle, o que sugere que o *isoxyl* não estaria inibindo a RNA polimerase, uma vez que se tivesse, uma inibição semelhante a obtida com a rifampicina seria observada (**Figura 13**). Por outro lado, nas culturas tratadas com *isoxyl* ou rifampicina e uracil [$^3$H] foi observada uma diminuição significativa de aproximadamente 60% e 70% na incorporação de uracil, respectivamente, quando comparado com o controle (**Figura 13**). O resultado deste experimento sugere que o *isoxyl* inibe a incorporação de uracil e não a RNA polimerase.
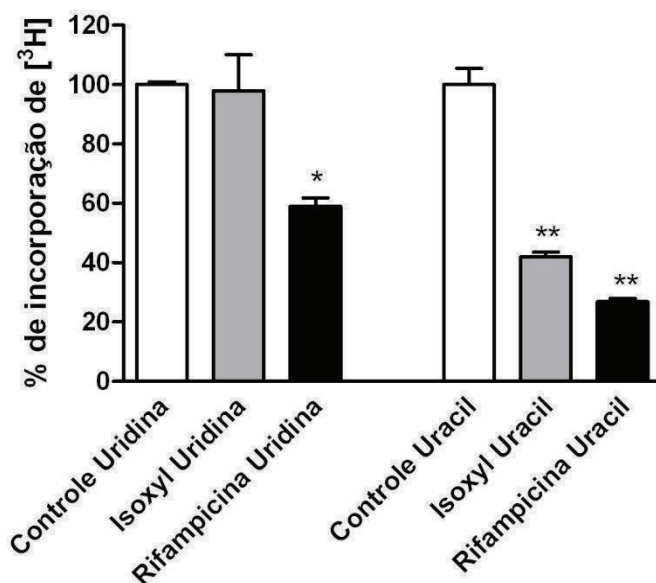


**Figura 13.** Incorporação de uridina e uracil marcados com trítio em culturas de *M. tuberculosis* H37Ra. As culturas foram tratadas com 5 μg/mL de rifampicina ou 7,5 μg/mL de *isoxyl* e no controle nenhuma droga foi adicionada. Este resultado representa a média de dois experimentos independentes. * $p < 0,05$, ** $p < 0,01$, comparados com os controles uridina e uracil, respectivamente.

Para verificar se os metabólitos ativos do *isoxyl* também inibem a incorporação das bases guanina e adenina, culturas de células de *M. tuberculosis* H37Ra foram tratadas com uracil, adenina e guanina marcados com trítio e *isoxyl*, como descrito acima. A incorporação das bases adenina e guanina não foi inibida pelos metabólitos

ativos do *isoxyl*, uma vez que não houve redução significativa na incorporação das respectivas bases quando as células foram tratadas com *isoxyl*, comparando com os controles (**Figura 14**). Nas culturas tratadas com *isoxyl* e uracil marcado com trítio, uma diminuição significativa de aproximadamente 60% na incorporação de uracil pode ser observada comparando com o controle (**Figura 14**), o que confirma o resultado obtido no experimento anterior.
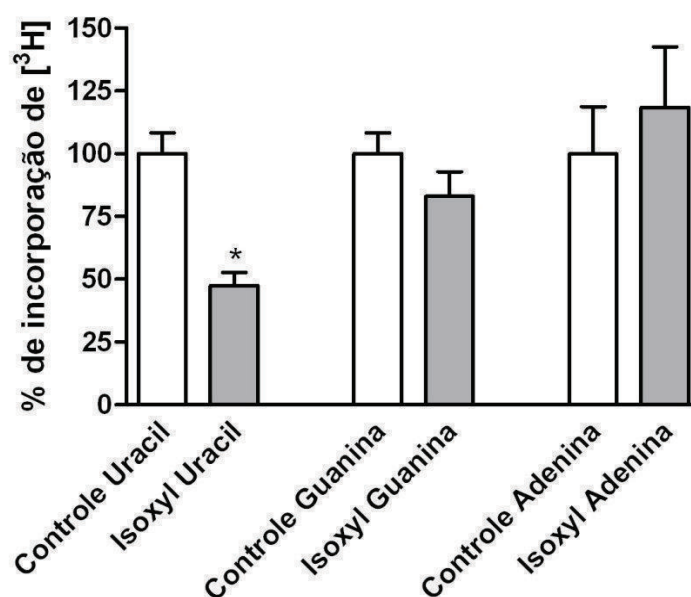


**Figura 14.** Incorporação de uracil, guanina e adenina marcados com trítio em cultura de *M. tuberculosis* H37Ra. As culturas foram tratadas com 7,5 µg/mL de *isoxyl* e no controle nenhuma droga foi adicionada. Este resultado representa a média de dois experimentos independentes. * $p < 0,05$ comparado com o controle uracil.

### 6.2 Ensaio de atividade da *Mt*UPRT e reação de ativação do *isoxyl*:

O resultado do experimento descrito acima sugeriu que o *isoxyl* inibe a incorporação de uracil, e para verificar se este fato estaria relacionado com a inibição da UPRT, a atividade da enzima foi monitorada *in vitro* por 10 min, com a adição da

reação de ativação do *isoxyl* utilizando espectrofotômetro. A reação de ativação do *isoxyl* consistiu em 6, 3 ou 0,6 μg/mL de *isoxyl*, 15 μg de proteína EthA homogênea (50), 50 mM de tris HCl pH 7,5, 200 μg/mL de BSA, 100 mM de KCl, 4 mM de NADPH e 2% dimetilsulfóxido (DMSO) (em um volume final de 250 μL) incubados por 1 h a 37ºC para que o *isoxyl* pudesse ser convertido em seus metabólitos ativos (55). Então 10 μL da reação de ativação do *isoxyl* e das reações controle, que consistem em reações de ativação do *isoxyl* na ausência de *isoxyl* ou da proteína EthA ou de ambos, foram adicionados a reação da *Mt*UPRT, em um volume final de 100 μL, e esta foi monitorada por 10 min. As reações controle foram feitas para verificar se algum componente da reação de ativação do *isoxyl* estaria interferindo na atividade da *Mt*UPRT. A reação da *Mt*UPRT consiste em hepes NaOH 100 mM pH 7,5, $MgCl_2$ 5 mM, uracil 10 μM, ditiotreitol 10 mM, PRPP 100 μM, DMSO 2 % e 0,5 μg de UPRT, onde a formação do produto UMP é monitorada a 280 nm (56).
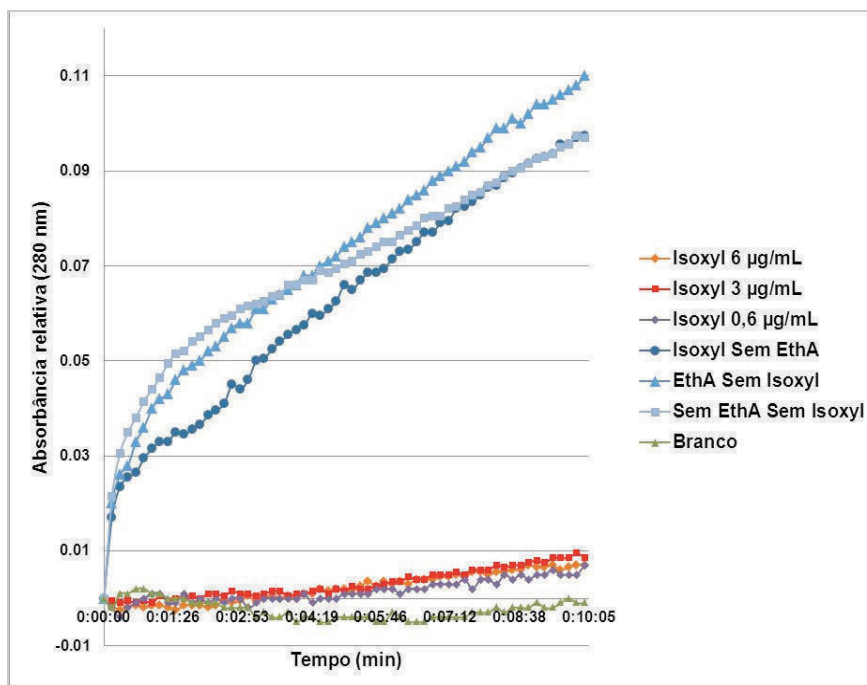
**Figura 15.** Absorbância relativa (280 nm) em função do tempo (min) da reação da *Mt*UPRT medida espectrofotometricamente. *Isoxyl* 6 µg/mL: reação de ativação do *isoxyl* com 6 µg/mL. *Isoxyl* 3 µg/mL: reação de ativação do *isoxyl* com 3 µg/mL. *Isoxyl* 0,6 µg/mL: reação de ativação do *isoxyl* com 0,6 µg/mL. *Isoxyl* Sem EthA: reação de ativação do *isoxyl* com 6 µg/mL na ausência de EthA. EthA Sem *Isoxyl*: reação de ativação do *isoxyl* na ausência de *isoxyl*. Sem EthA Sem *Isoxyl*: reação de ativação do *isoxyl* na ausência de *isoxyl* e de EthA. Branco: reação de ativação do *isoxyl* 6 µg/mL adicionada a reação da UPRT na ausência da enzima.

Como pode ser observado na **Figura 15**, algum metabolito ativo do *isoxyl* obtido com as concentrações de 6, 3 e 0,6 µg/mL da pró-droga inibiu a *Mt*UPRT, uma vez que na ausência de *isoxyl* ou EthA ou de ambos a atividade da *Mt*UPRT não foi alterada. Os componentes da reação de ativação do *isoxyl* mostraram não interferir na reação da *Mt*UPRT (**Figura 15**). O *isoxyl* não inibiu a *Mt*UPRT na ausência de EthA, mostrando que este precisa sofrer ativação pela proteína EthA para desempenhar sua ação inibitória, como descrito anteriormente (55). Além disso, a redução na incorporação de uracil marcado com trítio nas culturas tratadas com *isoxyl* (**Figura 13 e 14**) é

provavelmente devido à inibição da enzima UPRT. Entretanto, o *isoxyl* não parece inibir as outras fosforribosil transferases, como a adenina fosforribosil transferase (APRT) e a hipoxantina guanina fosforribosil transferase (HGPRT), uma vez que a incorporação das bases adenina e guanina não foram reduzidas significativamente nas culturas tratadas com *isoxyl* quando comparadas com os respectivos controles (**Figura 14**).

### 6.3 Concentração inibitória mínima de *isoxyl* para as cepas de *M. tuberculosis* mutante para o gene *upp,* complementada e tipo selvagem:

A concentração inibitória mínima (MIC) de *isoxyl* foi determinada para as cepas de *M. tuberculosis* H37Rv mutante para o gene *upp* transformada com o vetor pMVHG1 e pNIP40 (ambos sem inserto), complementada (pMVHG1::Mt_upp e pNIP40::Ms_upp) e tipo selvagem. A MIC foi determinada utilizando o método de diluições sucessivas com meio de cultura Middlebrook 7H9 tween 80 0,05 %, OADC 10 % suplementado com casitona 0,1 % e glicerol 0,5% (Middlebrook 7H9-S). Diluições seriadas de base dois foram realizadas, obtendo concentrações de *isoxyl* nos poços da placa de cultura variando de 12,8 a 0,1 µg/mL. As cepas foram inoculadas em meio de cultura Middlebrook 7H9 tween 80 0,05 %, OADC 10 %, e incubadas a 37ºC, 140 rpm até atingir uma $OD_{600}$ de aproximadamente 0,5. As culturas foram diluídas para $OD_{600}$ de 0,003 com meio de cultura Middlebrook 7H9-S e 200 µL das culturas foram adicionados em cada poço da placa. As placas de cultura foram incubadas a 37ºC por 11 dias e dois critérios foram analisados para a determinação da MIC: o tamanho do pellet celular no fundo do poço e a coloração obtida com a adição de resazurina 0,01 %. Após a adição

de resazurina, as placas foram re-incubadas a 37ºC por dois dias. A resazurina é um composto capaz de indicar a presença de crescimento bacteriano por uma reação de óxido-redução, ocorrendo à passagem de coloração azul (resazurina) para rosa (resofurina) interpretada como presença de células viáveis, enquanto que nos poços onde a coloração permanece azul interpreta-se como ausência de células viáveis indicando inibição de crescimento celular. O valor da MIC considerado foi a menor concentração de *isoxyl* capaz de inibir visualmente o crescimento bacteriano. A ausência do gene *upp* não afetou a sensibilidade da micobactéria ao *isoxyl*, uma vez que a MIC obtida para as cepas *M. tuberculosis* mutante para o gene *upp,* complementada (pMVHG1::Mt_upp e pNIP40::Ms_upp) e tipo selvagem foi de 12,8 µg/mL.

# Capítulo 5

Considerações Finais

# CONSIDERAÇÕES FINAIS

A TB é uma doença infecto-contagiosa causada principalmente pelo *M. tuberculosis*. Apesar da disponibilidade do tratamento padrão (DOTS) preconizado pela OMS e da existência da vacina BCG, a TB continua sendo um problema global devido a grande incidência de novos casos a cada ano. Isto tem ocorrido devido ao surgimento de cepas resistentes a drogas (TB-MDR, TB-XDR e TB-TDR) e à co-infecção com o HIV que dificultam as possibilidades de tratamento e resultam em uma alta taxa de mortalidade. Assim, há a necessidade urgente de novas estratégias terapêuticas para controlar a TB no mundo. O desenvolvimento de novos agentes quimioterápicos mais eficientes e menos tóxicos levaria a redução da duração do tratamento da TB e a otimização do tratamento da TB-MDR, TB-XDR, TB-TDR, de indivíduos co-infectados com HIV e da TB latente impedindo o desenvolvimento da forma ativa da doença. Além disso, o desenvolvimento de uma nova vacina que previna o estabelecimento da TB latente ou a reativação da TB pulmonar em adultos é fundamental para diminuir a incidência global da TB. As enzimas envolvidas na biossíntese de nucleotídeos pirimídicos são consideradas alvos moleculares promissores para o desenvolvimento de novos agentes quimioterápicos e vacinas contra a TB.

A UPRT parece ter um papel importante na rota de salvamento das pirimidinas, uma vez que o produto (UMP) da reação catalisada por esta enzima é o precursor comum de todos os nucleotídeos pirimídicos. O gene *upp* foi amplificado a partir do DNA gênomico de *M. tuberculosis* H37Rv, clonado em vetor pET23a(+), e o sequenciamento automático de DNA confirmou a identidade e integridade do gene,

mostrando que nenhuma mutação ocorreu na etapa de amplificação. A proteína recombinante *Mt*UPRT foi expressa em células de *E. coli* BL21(DE3) e foi purificada utilizando três etapas cromatográficas. O protocolo de purificação desenvolvido apresentou rendimento de 20 mg de proteína *Mt*UPRT homogênea a partir de 2 g de células úmidas. O ensaio de atividade espectrofotométrico confirmou que a cadeia polipeptídica possui atividade de UPRT pois a conversão de uracil e PRPP a UMP e $PP_i$ pode ser detectada. A enzima não utiliza as bases pirimídicas timina e citosina como substrato, sendo específica para uracil o que também foi demonstrado para a UPRT de outros organismos (57, 58). A *Mt*UPRT homogênea possui uma boa estabilidade, podendo ser armazenada a -80 ºC por pelo menos 1 ano sem perda aparente de atividade. Além disso, análises de espectrometria de massas e sequenciamento N-terminal confirmaram a identidade da proteína *Mt*UPRT.

A massa molecular da *Mt*UPRT nativa foi determinada por ultracentrifugação analítica (AUC) e seguiu o modelo de associação monômero-tetrâmero. Os dados de cinética no estado pré-estacionário para a análise da interação da enzima livre com o substrato PRPP por fluorescência indicou que a *Mt*UPRT existe em duas formas em solução, das quais apenas uma liga ao PRPP. Este resultado corrobora com o modelo de associação monômero-tetrâmero obtido por AUC. No entanto, a forma tetramérica da *Mt*UPRT parece ser a forma mais abundante uma vez que este foi o único estado oligomérico detectado por cromatografia de exclusão por tamanho.

As constantes cinéticas aparentes para a reação catalisada pela *Mt*UPRT foram determinadas na ausência e na presença de GTP. O GTP foi descrito como um ativador alósterico para as UPRTs de alguns organismos, causando um aumento na atividade,

alterando os parâmetros cinéticos e o estado oligomérico de algumas enzimas (41-43, 57-59). A *Mt*UPRT não apresentou uma regulação pronunciada por GTP pois este nucleotídeo não afetou os parâmetros cinéticos da enzima e a sua ligação não foi detectada por calorimetria de titulação isotérmica (ITC). A atividade da enzima UPRT de *S. solfataricus* é altamente dependente de GTP e esta dependência foi comprovada ser devido a presença de um resíduo de glicina no final da sua sequência de aminoácidos, já que quando dois resíduos de aminoácidos foram adicionados na glicina C-terminal, a enzima mostrou-se endogenamente ativada e independente de GTP (38). Como mostrado na **Figura 6** – **Capítulo 1**, a UPRT de *M. tuberculosis*, assim como a enzima de *B. caldolyticus* (60) possuem dois resíduos de aminoácidos após a glicina conservada, assim, esta talvez seja a razão pela qual a atividade destas enzimas é independente de GTP. Os nucleotídeos ATP, UTP e CTP também foram avaliados como efetores alostéricos da enzima *Mt*UPRT, no entanto, a enzima não foi significativamente ativada ou inibida por nenhum dos nucleotídeos testados.

A determinação das constantes cinéticas verdadeiras para a reação catalisada pela *Mt*UPRT forneceu dados para a obtenção do gráfico duplo-recíproco e o padrão de intersecção de retas indicou um mecanismo de reação de formação de um complexo ternário, no qual há uma ordem na sequência de ligação dos substratos (61). Neste tipo de mecanismo, a catálise ocorre apenas quando o segundo substrato liga subsequente à ligação do primeiro substrato (62). A técnica de ITC foi empregada para avaliar a interação de ligantes com a enzima livre e para elucidar o mecanismo cinético da *Mt*UPRT. A interação da enzima livre pode ser detectada apenas com o substrato PRPP e com o produto UMP, sugerindo que o substrato uracil e o produto $PP_i$ não

ligam na enzima livre. Os resultados de ITC também mostraram que a ligação de PRPP e UMP é um processo termodinamicamente favorável. O gráfico duplo-recíproco e os estudos de ITC sugerem que a catálise ocorre por um mecanismo sequencial ordenado, no qual o PRPP liga primeiro, seguido pela ligação de uracil, e $PP_i$ é o primeiro produto a ser liberado, seguido pelo UMP.

A dependência do pH nos parâmetros cinéticos foi avaliada para analisar a catálise ácido-base no modo de ação da *Mt*UPRT. O perfil de pH indicou que grupamentos com valores de pK de 5,7 e 8,1 são importantes para a atividade catalítica enquanto que um grupo com valor de pK de 9,45 está envolvido na ligação do PRPP. O alinhamento da sequência de aminoácidos da UPRT de *M. tuberculosis* com enzimas homólogas que possuem a estrutura terciária e quaternária depositada no PDB (**Figura 6** – **Capítulo 1**), mostrou que os resíduos envolvidos na catálise e ligação de substratos e produtos estão conservados entre as UPRTs. Assim, analisando os resultados obtidos com o experimento de perfil de pH e os dados do alinhamento de sequências, há evidências de que os aminoácidos Asp198 e Arg102 da *Mt*UPRT estejam envolvidos na catálise enquanto que possivelmente Arg77 ou Arg102 da *Mt*UPRT seja importante para a ligação de PRPP. Estes resíduos estão conservados entre as UPRTs de *T. gondii*, *B caldolyticus* e *E. coli*, como descrito anteriormente (40).

A cinética do estado pré-estacionário mostra as mudanças que ocorrem na molécula da enzima e permite o esclarecimento de passos elementares da reação enzimática. Os dados de cinética no estado pré-estacionário obtidos para a reação catalisada pela *Mt*UPRT sugeriram que a liberação de produto não é a etapa limitante da reação catalisada pela enzima. Medidas de variação de absorbância em

milisegundos para a reação catalisada pela *Mt*UPRT também foram realizadas na presença de GTP e a redução observada na constante catalítica foi de apenas 1,6 vezes comparado com a reação na ausência deste nucleotídeo. Esta diminuição na constante catalítica talvez seja apenas um artefato experimental, uma vez que, como mencionado anteriormente, a presença de GTP não altera os parâmetros cinéticos da enzima e a sua ligação não foi detectada por ITC. Assim, o controle do balanço da síntese de nucleosídeos trifosfato de purinas versus pirimidinas em *M. tuberculosis* é fornecido pela próxima enzima da via de biossíntese de pirimidinas, a UMP kinase, descrita como sendo uma enzima alostérica, ativada por GTP e inibida por UTP (63).

Estes resultados possibilitaram a caracterização da enzima UPRT de *M. tuberculosis* codificada pelo gene *upp* e a validação do seu papel bioquímico. Além disso, os dados apresentados podem auxiliar no desenvolvimento de estratégias profiláticas eficientes para reduzir a incidência global da TB. Os resultados obtidos com os estudos bioquímicos da *Mt*UPRT, apresentados no **Capítulo 3**, foram reunidos em um manuscrito que será submetido para a revista internacional *Molecular BioSystems* que possui um fator de impacto de 4,02.

Visando analisar a importância da enzima UPRT na rota de salvamento das pirimidinas e no metabolismo do *M. tuberculosis,* o nocaute do gene *upp* em *M. tuberculosis* H37Rv foi realizado, onde a substituição do alelo tipo selvagem do gene pelo alelo mutado foi obtida por recombinação homóloga. A recombinação homóloga em *M. tuberculosis* ocorre em frequência baixa o que dificulta a obtenção de mutantes definidos nessa micobactéria (48). Portanto, o sucesso no isolamento de mutantes em *M. tuberculosis* é dependente da habilidade de técnicas genéticas e protocolos

utilizados para compensar pela baixa eficiência de transformação e possibilitar a detecção eficiente ou seleção de mutantes de troca alélica entre a população total de transformantes (47). O pPR27*xylE* consiste em um vetor replicativo e integrativo que devido as suas propriedades seletivas evita os problemas decorrentes da baixa eficiência de transformação, é eficientemente perdido em determinadas condições e permite a eliminação de clones que ainda contenham o vetor, possibilitando assim a detecção de eventos genéticos muito raros (19). O protocolo empregado na obtenção do nocaute do gene *upp* utilizando o vetor pPR27*xylE* apresentou eficiência de 100 %, ou seja, todos os clones que foram verificados quanto à inserção do cassete contendo o gene de resistência a canamicina no gene *upp* realmente o possuíam, sendo todos os clones mutantes para o gene *upp* (DCO). Assim, o gene *upp* não é essencial para o crescimento do *M. tuberculosis* H37Rv nas condições empregadas no experimento que estão descritas no **Capítulo 4**. Além disso, a ausência do gene *upp* não alterou o crescimento do *M. tuberculosis* H37Rv quando comparado com a cepa tipo selvagem e com a cepa mutante complementada com uma cópia extra do gene em questão.

A expressão da proteína UPRT foi analisada em diferentes condições de crescimento de *M. tuberculosis* H37Ra. Condições de altas e baixas concentrações de oxigênio (modelo de Wayne e crescimento em película de superfície) utilizando meio de cultura mínimo (Sauton com tyloxapol) e complexo (Middlebrook 7H9), adição de bases púricas (adenina e guanina) e pirimídicas (uracil, timina e citosina) e coleta em diferentes tempos de crescimento foram as condições utilizadas no experimento. A proteína UPRT é expressa tanto em altas como em baixas concentrações de oxigênio. O crescimento das células em meio de cultura mínimo ou complexo e a adição de

bases púricas ou pirimídicas não alteram a expressão da proteína. Além disso, a expressão da UPRT parece não alterar nas diferentes fases de crescimento micobacteriano, como a fase logarítmica e estacionária. O modelo de Wayne é um modelo *in vitro* que simula as condições encontradas em granulomas quando a TB latente está sendo estabelecida, onde ocorre uma depleção gradual de oxigênio (49). A expressão da UPRT foi analisada em quatro diferentes tempos iniciando a coleta das células 1 semana após a depleção de oxigênio e finalizando após 4 semanas. O modelo de Wayne também foi realizado tanto em meio mínimo como complexo. No entanto, a expressão da UPRT na ausência de oxigênio não alterou quando comparada com o controle (presença de oxigênio). Além disso, não houve diferença na expressão da proteína nos diferentes tempos de latência e meios de cultura utilizados. Resultado semelhante foi obtido quando as células foram crescidas em película de superfície. Assim, a expressão da UPRT em *M. tuberculosis* H37Ra foi detectada em todas as condições analisadas e as diferentes condições de crescimento não afetaram a expressão basal da proteína.

O *isoxyl* é um derivado tiouréia que foi descrito como sendo um inibidor da síntese de ácidos oléico e micólico em *M. tuberculosis* (50). Este composto é uma pró-droga ativada por reações de oxidação no grupamento tiocarbonil, catalisadas pela proteína EthA, para expressar sua atividade antimicobacteriana. Experimentos de análise da incorporação de bases e nucleosídeos marcados com trítio em culturas de *M. tuberculosis* H37Ra demonstraram que quando as células eram tratadas com *isoxyl* ocorria uma redução na incorporação de uracil. Havia uma hipótese de que a diminuição na incorporação da base uracil fosse devido a inibição da RNA polimerase

por algum metabólito ativo do *isoxyl*. No entanto, esta suposição foi descartada pelo experimento onde culturas de *M. tuberculosis* H37Ra tratadas com uridina marcada com trítio, *isoxyl* e rifampicina mostraram que a rifampicina inibiu a incorporação de uridina enquanto que nas culturas tratadas com *isoxyl* nenhuma inibição significativa foi observada quando comparado com o controle. Assim, a adição da reação de ativação do *isoxyl* na reação da UPRT, onde a formação do produto UMP é monitorada a 280 nm utilizando espectrofotômetro, mostrou que a diminuição na incorporação de uracil era devido a inibição da UPRT de *M. tuberculosis* por espécies reativas derivadas do *isoxyl*. Experimentos de análise da incorporação das bases guanina e adenina marcadas com trítio em culturas de *M. tuberculosis* H37Ra também foram realizados e demonstraram que quando as células foram tratadas com *isoxyl* não houve redução na incorporação destas bases, o que fornece indícios de que os metabólitos ativos do *isoxyl* não inibem as fosforribosil transferases HGPRT e APRT.

A MIC de *isoxyl* foi determinada para as cepas de *M. tuberculosis* H37Rv mutante para o gene *upp*, complementada com uma cópia extra do gene *upp* e tipo selvagem. O valor de MIC considerado foi a menor concentração de *isoxyl* capaz de inibir visualmente o crescimento bacteriano. A ausência do gene *upp* não afetou a sensibilidade da micobactéria ao *isoxyl*, uma vez que a MIC obtida para as cepas *M. tuberculosis* mutante para o gene *upp,* complementada e tipo selvagem foi de 12,8 µg/mL.

Os resultados obtidos proporcionaram um maior entendimento sobre o metabolismo de nucleotídeos em *M. tuberculosis* H37Rv, demonstraram o papel biológico e bioquímico do gene *upp* nesta micobactéria. Experimentos envolvendo a

infecção de camundongos com as cepas de *M. tuberculosis* H37Rv mutante para o gene *upp*, mutante e complementada com uma cópia extra do gene *upp* e tipo selvagem serão realizados para analisar a importância deste gene na virulência do *M. tuberculosis* H37Rv. Este experimento que investigará a possível virulência fornecerá informações fundamentais quanto à importância do desenvolvimento de cepas atenuadas utilizando o gene *upp* como alvo para o desenvolvimento de uma nova vacina.

# Referências

1.	World Health Organization, Global Tuberculosis Control: Report. 2011.

2.	Young D, Stark J, Kirschner D. Systems biology of persistent infection: tuberculosis as a case study. Nat Rev Microbiol. 2008;6(7):520-8.

3.	Pieters J. *Mycobacterium tuberculosis* and the macrophage: maintaining a balance. Cell Host Microbe. 2008;3(6):399-407.

4.	Stewart GR, Robertson BD, Young DB. Tuberculosis: a problem with persistence. Nat Rev Microbiol. 2003;1(2):97-105.

5.	Basso LA, da Silva LH, Fett-Neto AG, de Azevedo WF, Moreira IeS, Palma MS, et al. The use of biodiversity as source of new chemical entities against defined molecular targets for treatment of malaria, tuberculosis, and T-cell mediated diseases--a review. Mem Inst Oswaldo Cruz. 2005;100(6):475-506.

6.	Dye C, Scheele S, Dolin P, Pathania V, Raviglione MC. Consensus statement. Global burden of tuberculosis: estimated incidence, prevalence, and mortality by country. WHO Global Surveillance and Monitoring Project. JAMA. 1999;282(7):677-86.

7.	Hoft DF. Tuberculosis vaccine development: goals, immunological design, and evaluation. Lancet. 2008;372(9633):164-75.

8.	Corbett EL, Watt CJ, Walker N, Maher D, Williams BG, Raviglione MC, et al. The growing burden of tuberculosis: global trends and interactions with the HIV epidemic. Arch Intern Med. 2003;163(9):1009-21.

9.	Ducati RG, Ruffino-Netto A, Basso LA, Santos DS. The resumption of consumption -- a review on tuberculosis. Mem Inst Oswaldo Cruz. 2006;101(7):697-714.

10.	Jain A, Mondal R. Extensively drug-resistant tuberculosis: current challenges and threats. FEMS Immunol Med Microbiol. 2008;53(2):145-50.

11.	(CDC) CfDCaP. Emergence of *Mycobacterium tuberculosis* with extensive resistance to second-line drugs--worldwide, 2000-2004. MMWR Morb Mortal Wkly Rep. 2006;55(11):301-5.

12.	Velayati AA, Farnia P, Masjedi MR, Ibrahim TA, Tabarsi P, Haroun RZ, et al. Totally drug-resistant tuberculosis strains: evidence of adaptation at the cellular level. Eur Respir J. 2009;34(5):1202-3.

13.	Andersen P. Tuberculosis vaccines - an update. Nat Rev Microbiol. 2007;5(7):484-7.

14.     Sambandamurthy VK, Jacobs WR. Live attenuated mutants of *Mycobacterium tuberculosis* as candidate vaccines against tuberculosis. Microbes Infect. 2005;7(5-6):955-61.

15.     Kamath AT, Fruth U, Brennan MJ, Dobbelaer R, Hubrechts P, Ho MM, et al. New live mycobacterial vaccines: the Geneva consensus on essential steps towards clinical development. Vaccine. 2005;23(29):3753-61.

16.     Barker LF, Brennan MJ, Rosenstein PK, Sadoff JC. Tuberculosis vaccine research: the impact of immunology. Curr Opin Immunol. 2009;21(3):331-8.

17.     Skeiky YA, Sadoff JC. Advances in tuberculosis vaccine strategies. Nat Rev Microbiol. 2006;4(6):469-76.

18.     Brennan MJ, Fruth U, Milstien J, Tiernan R, de Andrade Nishioka S, Chocarro L, et al. Development of new tuberculosis vaccines: a global perspective on regulatory issues. PLoS Med. 2007;4(8):e252.

19.     Pelicic V, Jackson M, Reyrat JM, Jacobs WR, Gicquel B, Guilhot C. Efficient allelic exchange and transposon mutagenesis in *Mycobacterium tuberculosis*. Proc Natl Acad Sci U S A. 1997;94(20):10955-60.

20.     Pelicic V, Reyrat JM, Gicquel B. Genetic advances for studying *Mycobacterium tuberculosis* pathogenicity. Mol Microbiol. 1998;28(3):413-20.

21.     Cole ST, Brosch R, Parkhill J, Garnier T, Churcher C, Harris D, et al. Deciphering the biology of *Mycobacterium tuberculosis* from the complete genome sequence. Nature. 1998;393(6685):537-44.

22.     Voet D, Voet J. Biochemistry. New Jersey: John Wiley & Sons; 2004.

23.     Campbel NA, Reece JB. Biology. 8th ed: Pearson Education,Inc.; 2008.

24.     Berg JM, Tymoczko JL, Stryer L. Biochemistry. 5th ed. New York: W H Freeman; 2002.

25.     Xu Y, Johansson M, Karlsson A. Human UMP-CMP kinase 2, a novel nucleoside monophosphate kinase localized in mitochondria. J Biol Chem. 2008;283(3):1563-71.

26.     Moffatt B, Ashihara H. Purine and pyrimidine nucleotide synthesis and metabolism. Rockville, MD, Online publication: American Society of Plant Biologists; 2002.

27.     Touroutoglou N, Pazdur R. Thymidylate synthase inhibitors. Clin Cancer Res. 1996;2(2):227-43.

28.     Ducati RG, Breda A, Basso LA, Santos DS. Purine Salvage Pathway in *Mycobacterium tuberculosis*. Curr Med Chem. 2011;18(9):1258-75.

29.     Villela AD, Sanchez-Quitian ZA, Ducati RG, Santos DS, Basso LA. Pyrimidine salvage pathway in *Mycobacterium tuberculosis*.  Curr Med Chem. Netherlands 2011. p. 1286-98.

30.     Neuhard J, Kelln RA. Biosynthesis and conversion of pyrimidines. 2nd ed. Washington, D.C: American Society for Microbiology; 1996.

31.     Islam MR, Kim H, Kang SW, Kim JS, Jeong YM, Hwang HJ, et al. Functional characterization of a gene encoding a dual domain for uridine kinase and uracil phosphoribosyltransferase in Arabidopsis thaliana. Plant Mol Biol. 2007;63(4):465-77.

32.     Evans DR, Guy HI. Mammalian pyrimidine biosynthesis: fresh insights into an ancient pathway. J Biol Chem. 2004;279(32):33035-8.

33.     Fox BA, Bzik DJ. *De novo* pyrimidine biosynthesis is required for virulence of *Toxoplasma gondii*. Nature. 2002;415(6874):926-9.

34.     O'Donovan GA, Neuhard J. Pyrimidine metabolism in microorganisms. Bacteriol Rev. 1970;34(3):278-343.

35.     Kantardjieff KA, Vasquez C, Castro P, Warfel NM, Rho BS, Lekin T, et al. Structure of pyrR (Rv1379) from *Mycobacterium tuberculosis*: a persistence gene and protein drug target. Acta Crystallogr D Biol Crystallogr. 2005;61(Pt 4):355-64.

36.     Kadziola A, Neuhard J, Larsen S. Structure of product-bound *Bacillus caldolyticus* uracil phosphoribosyltransferase confirms ordered sequential substrate binding. Acta Crystallogr D Biol Crystallogr. 2002;58(Pt 6 Pt 2):936-45.

37.     Kukimoto-Niino M, Shibata R, Murayama K, Hamana H, Nishimoto M, Bessho Y, et al. Crystal structure of a predicted phosphoribosyltransferase (TT1426) from *Thermus thermophilus* HB8 at 2.01 A resolution. Protein Sci. 2005;14(3):823-7.

38.     Christoffersen S, Kadziola A, Johansson E, Rasmussen M, Willemoës M, Jensen KF. Structural and kinetic studies of the allosteric transition in *Sulfolobus solfataricus* uracil phosphoribosyltransferase: Permanent activation by engineering of the C-terminus. J Mol Biol. 2009;393(2):464-77.

39.     Arent S, Harris P, Jensen KF, Larsen S. Allosteric regulation and communication between subunits in uracil phosphoribosyltransferase from *Sulfolobus solfataricus*. Biochemistry. 2005;44(3):883-92.

40.     Schumacher MA, Carter D, Scott DM, Roos DS, Ullman B, Brennan RG. Crystal structures of *Toxoplasma gondii* uracil phosphoribosyltransferase reveal the atomic basis of pyrimidine discrimination and prodrug binding. EMBO J. 1998;17(12):3219-32.

41.     Schumacher MA, Bashor CJ, Song MH, Otsu K, Zhu S, Parry RJ, et al. The structural mechanism of GTP stabilized oligomerization and catalytic activation of the *Toxoplasma gondii* uracil phosphoribosyltransferase. Proc Natl Acad Sci U S A. 2002;99(1):78-83.

42.     Dai YP, Lee CS, O'Sullivan WJ. Properties of uracil phosphoribosyltransferase from *Giardia intestinalis*. Int J Parasitol. 1995;25(2):207-14.

43.     Jensen KF, Mygind B. Different oligomeric states are involved in the allosteric behavior of uracil phosphoribosyltransferase from *Escherichia coli*. Eur J Biochem. 1996;240(3):637-45.

44.     Donald RG, Roos DS. Insertional mutagenesis and marker rescue in a protozoan parasite: cloning of the uracil phosphoribosyltransferase locus from *Toxoplasma gondii*. Proc Natl Acad Sci U S A. 1995;92(12):5749-53.

45.     Sassetti CM, Rubin EJ. Genetic requirements for mycobacterial survival during infection. Proc Natl Acad Sci U S A. 2003;100(22):12989-94.

46.     Li J, Huang S, Chen J, Yang Z, Fei X, Zheng M, et al. Identification and characterization of human uracil phosphoribosyltransferase (UPRTase). J Hum Genet. 2007;52(5):415-22.

47.     Jackson M, Camacho LR, Gicquel B, Guilhot C. *Mycobacterium tuberculosis* Protocols. Totowa, NJ: Humana Press Inc.; 2001.

48.     McFadden J. Recombination in mycobacteria. Mol Microbiol. 1996;21(2):205-11.

49.     Wayne LG, Hayes LG. An in vitro model for sequential study of shiftdown of *Mycobacterium tuberculosis* through two stages of nonreplicating persistence. Infect Immun. 1996;64(6):2062-9.

50.     Korduláková J, Janin YL, Liav A, Barilone N, Dos Vultos T, Rauzier J, et al. Isoxyl activation is required for bacteriostatic activity against *Mycobacterium tuberculosis*. Antimicrob Agents Chemother. 2007;51(11):3824-9.

51.     Phetsuksiri B, Baulard AR, Cooper AM, Minnikin DE, Douglas JD, Besra GS, et al. Antimycobacterial activities of isoxyl and new derivatives through the inhibition of mycolic acid synthesis. Antimicrob Agents Chemother. 1999;43(5):1042-51.

52.     Engohang-Ndong J, Baillat D, Aumercier M, Bellefontaine F, Besra GS, Locht C, et al. EthR, a repressor of the TetR/CamR family implicated in ethionamide resistance in

mycobacteria, octamerizes cooperatively on its operator. Mol Microbiol. 2004;51(1):175-88.

53.     Willand N, Dirié B, Carette X, Bifani P, Singhal A, Desroses M, et al. Synthetic EthR inhibitors boost antituberculous activity of ethionamide. Nat Med. 2009;15(5):537-44.

54.     Phetsuksiri B, Jackson M, Scherman H, McNeil M, Besra GS, Baulard AR, et al. Unique mechanism of action of the thiourea drug isoxyl on *Mycobacterium tuberculosis*. J Biol Chem. 2003;278(52):53123-30.

55.     Dover LG, Alahari A, Gratraud P, Gomes JM, Bhowruth V, Reynolds RC, et al. EthA, a common activator of thiocarbamide-containing drugs acting on different mycobacterial targets. Antimicrob Agents Chemother. 2007;51(3):1055-63.

56.     Natalini P, Ruggieri S, Santarelli I, Vita A, Magni G. Baker's yeast UMP:pyrophosphate phosphoribosyltransferase. Purification, enzymatic and kinetic properties. J Biol Chem. 1979;254(5):1558-63.

57.     Linde L, Jensen KF. Uracil phosphoribosyltransferase from the extreme thermoacidophilic archaebacterium *Sulfolobus shibatae* is an allosteric enzyme, activated by GTP and inhibited by CTP. Biochim Biophys Acta. 1996;1296(1):16-22.
58.     Rasmussen UB, Mygind B, Nygaard P. Purification and some properties of uracil phosphoribosyltransferase from *Escherichia coli* K12. Biochim Biophys Acta. 1986;881(2):268-75.

59.     Jensen KF, Arent S, Larsen S, Schack L. Allosteric properties of the GTP activated and CTP inhibited uracil phosphoribosyltransferase from the thermoacidophilic archaeon *Sulfolobus solfataricus*. FEBS J. 2005;272(6):1440-53.

60.     Jensen HK, Mikkelsen N, Neuhard J. Recombinant uracil phosphoribosyltransferase from the thermophile *Bacillus caldolyticus*: expression, purification, and partial characterization. Protein Expr Purif. 1997;10(3):356-64.

61.     Segel IH. Enzyme kinetics, behavior and analysis of rapid equilibrium and steady-state enzyme systems. New York: John Wiley and Sons, Inc.; 1975.

62.     Copeland RA. Evaluation of enzyme inhibitors in drug discovery, a guide for medicinal chemists and pharmacologists. New Jersey: John Wiley and Sons, Inc.; 2005.

63.     Rostirolla DC, Breda A, Rosado LA, Palma MS, Basso LA, Santos DS. UMP kinase from *Mycobacterium tuberculosis*: Mode of action and allosteric interactions, and their likely role in pyrimidine metabolism regulation. Arch Biochem Biophys. 2011;505(2):202-12.

# Anexo

Carta de submissão ao periódico *Molecular Biosystems*

**RSC** Publishing   **Molecular BioSystems**

SCHOLARONE™
Manuscripts

Main Menu → Author Dashboard → Submission Confirmation

You are logged in as Luiz Basso

## Submission Confirmation

Thank you for submitting your manuscript to *Molecular BioSystems*.

|  |  |
|---|---|
| Manuscript ID: | MB-ART-12-2011-005489 |
| Title: | Biochemical characterization of uracil phosphoribosyltransferase from Mycobacterium tuberculosis |
| Authors: | Villela, Anne<br>Ducati, Rodrigo<br>Rosado, Leonardo<br>Bloch Junior, Carlos<br>Prates, Maura<br>Ramos, Carlos<br>Basso, Luiz<br>Santos, Diogenes |
| Date Submitted: | 03-Dec-2011 |

🖨 Print    ↺ Return to Dashboard

ScholarOne Manuscripts™ v4.8.0 (patent #7,257,767 and #7,263,655). © ScholarOne, Inc., 2011. All Rights Reserved.
ScholarOne Manuscripts is a trademark of ScholarOne, Inc. ScholarOne is a registered trademark of ScholarOne, Inc.

Follow ScholarOne on Twitter

Terms and Conditions of Use - ScholarOne Privacy Policy - **Get Help Now**